3 1176 00162 7596

NASA CR-159,214

NASA Contractor Report 159214

NASA-CR-159214
1980 0024982

EXPERIMENTAL AND ANALYTICAL STUDIES FOR THE NASA CARBON FIBER RISK ASSESSMENT

THE BIONETICS CORPORATION
18 Research Drive
Hampton, Virginia 23666

NASA Contract NAS1-15238
August 1980

LIBRARY COPY
OCT 9 1980
LANGLEY RESEARCH CENTER
LIBRARY, NASA
HAMPTON, VIRGINIA

NASA
National Aeronautics and Space Administration
Langley Research Center
Hampton, Virginia 23665

CONTENTS

N80-33490 #

INTRODUCTION

In 1978, NASA Langley Research Center undertook a project to assess the risk associated with accidental release of carbon* fibers during fires of commercial aircraft containing carbon-based fiber/epoxy composites. Such fibers were known to be capable of creating electrical malfunctions if ingested into electrical apparatus and electronic controls.

Under Contract NAS1-15238 the Bionetics Corporation supported this effort by conducting analytic investigations of risk in specific areas, developing instrumentation and test facilities, analyzing data from field experiments and by designing and conducting experiments evaluating the vulnerability of electronic apparatus. Many of the results are contained in publications listed in this report and in contributions to NASA status reports covering the efforts over approximately a three-year period. This document describes accomplishments not otherwise reported in detail.

The report represents the combined work of the Bionetics Corporation graphite fibers project staff, including Israel Taback, Ansel J. Butterfield, Seymour Salmirs, Jerome A. Meyers, Cletus J. Vincke, John S. Tanguy, James H. Schrader, Fred W. Phillips, Gregory Schluge, Mark C. Harvey, Paul R. Hodges, Thomas N. Bartron and Herbert F. Hardrath. The contributions of Arthur Newcomb, NASA Technical monitor, whose guidance and suggestions are reflected in much of the work, are also acknowledged.

*Carbon-based fibers are often referred to interchangeably as graphite or carbon fibers. In the strictest sense, graphite is that form of carbon that is highly crystalline in structure. The term "carbon fibers" has been used herein because it is the more general term, and includes graphite and the less graphitic forms commonly used in aircraft structural composites.

Section 1

CARBON FIBER CHARACTERISTICS

The vulnerability of electrical and electronic equipment to carbon fibers is related to the length, electrical resistance and burn-out characteristics of the fibers. Tests have been performed to measure the resistance and burn-out characteristics of several types of fibers. Tests have also been performed to assess the extent of physical breakup of fibers entrained in avionics equipment cooling air during passage through jet engine compressor stages and through avionics cooling air handling equipment. These tests are reported in this section.

1.1 ELECTRICAL RESISTANCE

Carbon fibers produced in an exploratory study by Celanese Research Company were selected for a part of the Bionetics, Incorporated, study on how fiber resistance affected equipment vulnerability. The fibers, designated DG-110, DG-112 and DG-114, which had been developed to have unusually low thermal conductivity, had unusually high electrical resistance. Sample fibers were clamped gently across parallel conductors (spaced 10 mm apart) made of gold or solder. Current was monitored during a test in which 20-Vdc power was applied and the voltage was reduced by 3-Vdc steps. The slopes of the linear portions of the resulting voltage-amperes plots were interpreted as the resistance of the fibers. The curves were non-linear at low voltages because of contact resistance effects. The voltage was subsequently raised gradually until the fibers burned out.

Similar measurements were made on T-300 and GY-70 fibers except that the burn-out amperage was noted after a constant 30-volt power was applied.

The results of these tests are presented in table 1-1. The resistances of the Celanese fibers were as high as 25 times those of T-300 carbon fibers frequently used in structural applications. The voltages at burn-out were also 2 to 3 times those of T-300, but the current capacity was only 1/2 that of T-300. The use of gold or solder conductors had no appreciable effect on results.

1.2 FIBER-BREAKAGE TESTS

The risk of failures in airborne avionic equipment was expected to depend critically on the likelihood of carbon fiber passing intact through the ventilation system into equipment bays and the flight deck. Accordingly, aircraft equipment ventilation systems were reviewed. Typical ventilation systems receive high-pressure air from one of the last stages of the compressor of an auxiliary

power unit or a propulsion engine of the aircraft. The air is cooled and filtered before passing into the ventilation ducts. At its source, this air has passed through the inlet of the engine, a distance of approximately 0.5 meters, and then through 24 to 30 right-angle turns as it passes through successive stages of the compressor at speeds up to 186 m/s. Because of the tortuous path, carbon fibers ingested with the air are quite likely to impact duct walls, compressor rotor and stator blades and filter faces before being released in the avionics bay. These impacts may break fibers if speeds, directions and material properties occur in critical combinations.

Three simple, mathematically tractable, impact configurations were treated analytically to explore whether potentially critical conditions could be anticipated for T-300 fibers passing through a jet engine compressor. To perform the analysis, all kinetic energy in a fiber was assumed to be instantaneously converted to potential energy of deformation in the fiber upon impact. Material properties were assumed as follows:

Density of fiber, ρ - 1760 kg/m^3
Modulus of elasticity, E - 236 GPa (34.2 $\times$ 10^6 psi)
Tensile strength - 2.9 Gpa (423,000 psi)
Compressive strength - 2.9 GPa (423,000 psi)
Stress-strain curve linear to fracture.

The fiber velocity, v, required to produce failure stress, S, for each of the three conditions analyzed was:

Direct Compression

$$v = S \left(\frac{g}{E\,\rho}\right)^{\frac{1}{2}}$$

$$= 112 \text{ m/s}$$

Pure Moment

$$v = 0.82S \left(\frac{g}{E\,\rho}\right)^{\frac{1}{2}}$$

$$= 92 \text{ m/s}$$

Impact at center of beam

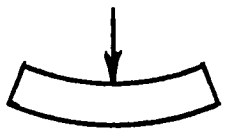

$$v = 0.3S \left(\frac{g}{E\rho}\right)^{\frac{1}{2}}$$

$$= 33 \text{ m/s}$$

These calculations demonstrated that fiber breakage was possible at speeds and configurations encountered in a jet engine. Accordingly, an experimental study was undertaken to simulate and observe the behavior.

Tests had been performed (ref. 1-1) in which fibers were passed through a water separator and an aircleaner that are normally installed in ventilation ducts. The same apparatus was used for the present tests except that the bent tubes shown in figure 1-1 were inserted between the tube into which fibers were injected and the water separator that was used to catch fibers for analysis. The earlier tests had shown that the water separator was an effective filter (passing less than 1% of fibers longer than 3 mm) and that it captured fibers on its felt surface without significant fiber breakage.

The bent tubes were designed to provide a path similar to that followed by fibers passing through a compressor on a jet engine. Three identical tubes having inside diameters of 11.2 mm were mounted in the end wall of the injection tube.

Because air velocity in the injector tube (102 mm diameter) was much lower than in the bent tubes, the fibers were accelerated throughout their traverse of the tubes and exited the tubes at approximately 100 times the entrance velocity. Fiber velocities were calculated (ref. 1-2) to be in the range from 28 to 73 m/s for air speeds of 131 to 312 m/s. The same calculation predicted fiber speeds up to 122 m/s, in the compressor of a jet engine.

Early tests in this series employed virgin fibers chopped to 10-mm lengths. However, these fibers tended to clump and clog the tubes of the simulator. Tests continued with 3-mm-long fibers introduced and these tests were completed without clumping. Fiber length varied somewhat because of difficulties with producing chopped fibers of precisely uniform length and with cleaning the test facility of the previously used 10-mm-long fibers. The length distribution for one typical sample was:

Fiber length	Percent
< 1 mm	4.0
1-2 mm	6.7
2-4 mm	86.0
4-6 mm	2.8
> 6 mm	0.5

Adhesive-coated paper was used to collect fibers from the felt bag of the water separator used to trap fibers that had traversed the tubes. Measurements of fragments revealed a very large number shorter than 1 mm long. The numbers of fibers counted with lengths less than 2 and 3 mm for each of five velocities are plotted in figure 1-2. Clearly, more fibers were broken to shorter lengths at the higher velocities. No fibers longer than 3 mm survived the test in which fibers travelled 73 m/s. Considering that jet engine air velocities are considerably higher than simulated in these tests, that the path through a jet engine entails many more changes in direction and that the water separators and air cleaners normally installed in ventilator systems are excellent filters, the likelihood of ingesting carbon fibers into ventilation and cooling systems is considered remote.

References

1-1 Meyers, Jerome A.: The Transfer of Carbon Fibers Through a Commercial Aircraft Water Separator and Air Cleaner. The Bionetics Corp., NASA CR 159183, No.v 1979.

1-2 Hoerner, Sighard F.: Fluid-Dynamic Drag, 1965 Edition, P. O. Box 342, Bricktown, N. J.

TABLE 1-1 ELECTRICAL PROPERTIES OF SINGLE FIBERS

	DG-110	DG-112	DG-114	T-300	GY-70
Min. Resistance, MΩ/m	16.	1.4	7.5	.43	.22
Max Resistance, MΩ/m	32.	2.0	8.9	.46	.34
Mean Resistance, MΩ/m	20.	1.6	8.0	.44	.26
Mean Voltage at burn-out, Vdc	73	45	63	30(a)	25(a)
Mean Current at burn-out, mAdc	3.85	4.0	4.8	8.57	9.77
Mean Wattage at burn-out, W/m	28.1	18.0	30.2	25.7	24.4

(a) Applied voltages

TABLE 1-2 RESULTS FROM TURBINE SIMULATOR TESTS

Air velocity in tube, m/s	Fiber velocity at second turn, m/s	% Fibers ℓ ≤2 mm	% Fibers ℓ ≤3 mm
131	28	86	93
148	32	65	76
245	56	77	94
278	65	76	98
312	73	99	100

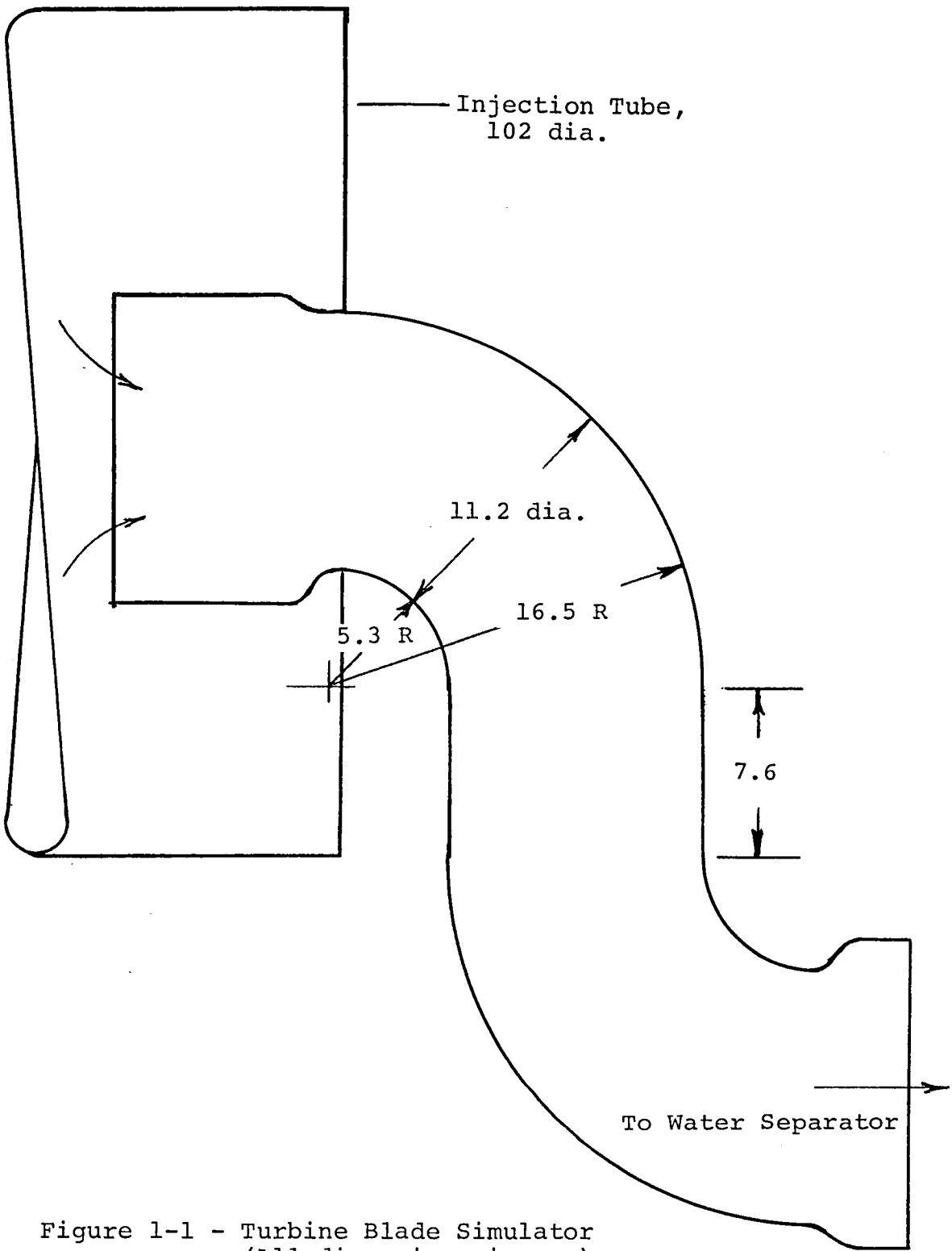

Figure 1-1 - Turbine Blade Simulator
(All dimensions in mm.)

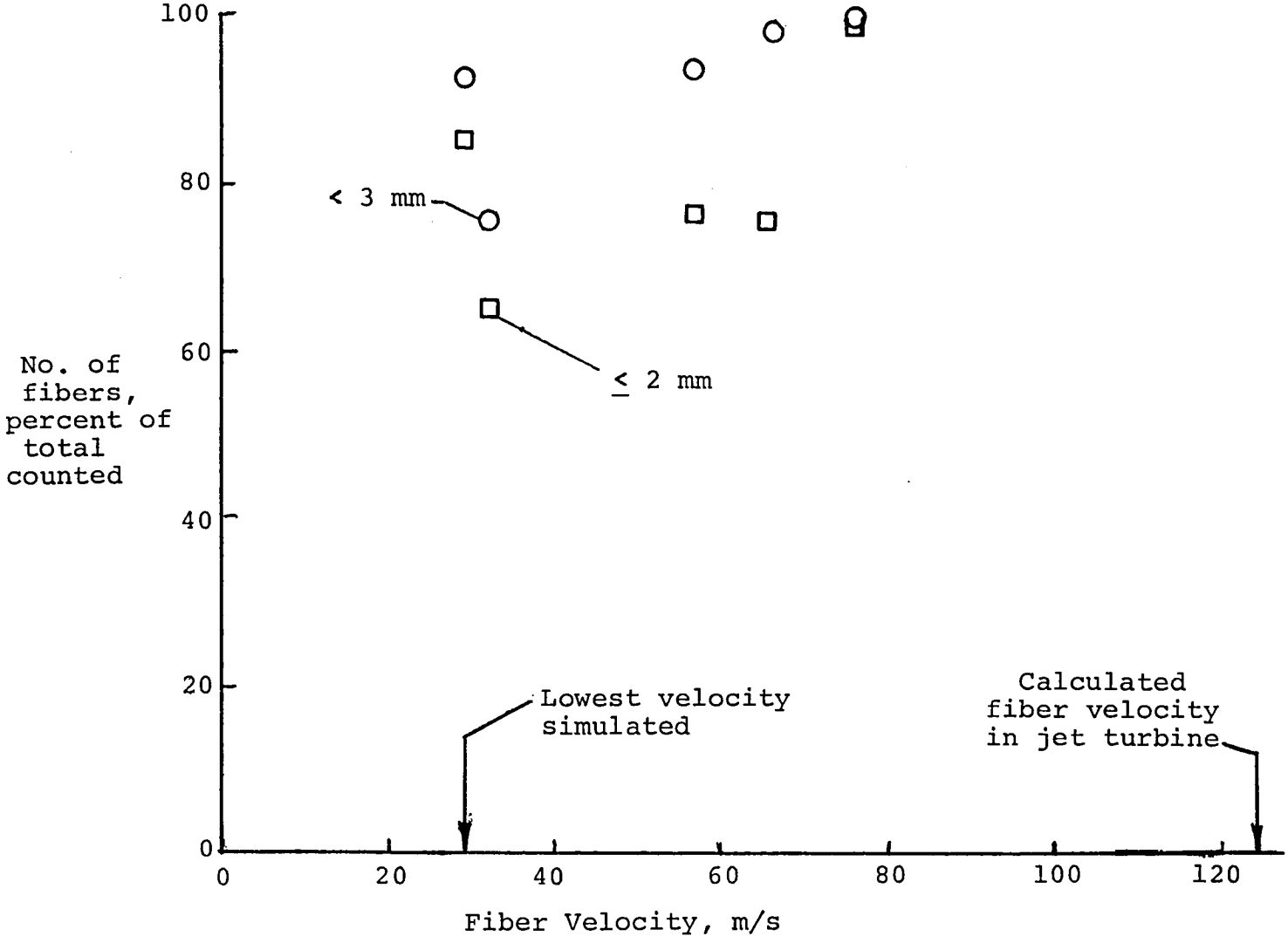

Figure 1-2 - Distribution of fiber lengths after passing through turbine simulator

Section 2

INSTRUMENTATION AND CALIBRATION TECHNIQUES

This section describes carbon fiber detection instrumentation which was modified, developed and/or calibrated by the Bionetics Corporation for use in (1) the NASA, Langley Research Center carbon fiber vulnerability exposure test facility (ref. 2-1), (2) the fire-released fiber tests at the Naval Surface Weapons Center shock tube facility (ref. 2-2), and (3) the large-scale outdoor fire-released fiber tests at Dugway Proving Grounds (ref. 2-3).

A ball detector developed at the Ballistics Research Laboratory, BRL, (ref. 2-4) was used extensively in tests in the NASA carbon fiber exposure test facility (ref. 2-1). The sensitivity of the detector system was improved, the electronic circuitry was modified and the ball was operated at lower voltage to eliminate spurious noise. A procedure was developed to use the detector for measuring fiber length spectra and the detector was recalibrated for exposure measurements at the lower charge voltage. A more sensitive sensor using a wire rather than a ball detector was also developed and calibrated.

The passive, sticky cylinder sampler (ref. 2-4) was also calibrated and used extensively for exposure measurement in the NASA test facility (ref. 2-1) and in the Dahlgren shock tube tests (ref. 2-2).

An active detector system was developed for counting and measuring the resistance of fibers released from burning composites. This detector, which employs a comb-type arrangement of alternately charged wires was used in the Dahlgren shock tube tests (ref. 2-2), and the large scale tests at Dugway Proving Ground (ref. 2-3). Results from calibration tests and fire-released fiber tests are presented.

2.1 MODIFICATION OF THE BRL BALL DETECTOR

In order to adapt the BRL brass ball detector (ref. 2-4) for use in the NASA vulnerability test facility (ref. 2-1) a threefold investigation was conducted in the following areas;

1. Noise reduction in the system.
2. Fiber length correlation.
3. Calibration of the ball for exposure measurements.

Noise reduction. - The basic element of the detector is a 38-mm diameter metallic ball charged to 1500 volts. Voltage pulses are generated when conducting fibers strike the ball and remove a small amount of surface charge. The number and amplitude of these pulses is sensed and recorded to indicate the number and lengths

of fibers detected. Figure 2.1-1 is a photograph of the ball detector. Figure 2.1-2 is a schematic of the ball detector system.

In order to use the ball for length spectrum measurements, the system had to be free of spurious noise pulses. If, during an exposure, noise pulses of only a few millivolts occurred, they would have been interpreted as short (2 to 3 mm) fibers. Eliminating such small noise pulses was a difficult and frustrating job.

Several sources of spurious noise pulses were identified. High-voltage cables and connectors were a prime source, particularly if high-voltage signal lines and ground wires were closely spaced. Any sharply pointed object, such as a poorly dressed connection which had high voltage on it, could produce spurious noise pulses. Excessive crimping of connectors could result in both sharp edges and critically close spacings. Solder connections were found to be preferable. The presence of dust or dirt in high-voltage connectors or in the high-voltage section of the preamplifier also created problems. An air blast was very effective in cleaning high-voltage areas.

Another type of noise, a nonspurious type, was associated with fibers which became lodged against the ball and were not repelled. This usually took place around the ball's nylon mount and was easily recognized by the fairly constant amplitude and frequency of the pulses. This type of noise also occurred if a fiber lodged in the high-voltage section of the preamplifier. The only cure was cleaning before each exposure.

As used by BRL, the ball was charged with 2000 volts. In an attempt to lessen noise problems, several different ball voltages were investigated. Lowering the charge to 1500 volts decreased noise problems and resulted in a good tradeoff between performance degradation and noise reduction. Lowering the voltage any further would have reduced the ball's sampling effectiveness (see ref. 2-4) noticeably in the fiber free-fall velocity range. All testing was done at 1500 volts.

Fiber length correlation.- One of the initial objectives of this work was to determine the ability of the ball to measure length spectra. A simple relationship between fiber length and pulse amplitude was developed to approximate predictions by Bucher's equation (ref. 2-5). Also investigated was the presence of low voltage pulses which occurred during fiber exposures.

The relationship (ref. 2-5) describing the charge transfer, Q, when a fiber strikes a high-voltage ball is,

$$Q = \frac{3\pi\varepsilon_o V_o L^2 \left[1 - \frac{\ell n\ (1 - \alpha)}{\alpha}\right]}{2a\left(\frac{3}{2} + \alpha\right)^2 \left[\ell n\ \left(\frac{2L}{R}\right) - 1\right]}\ , \qquad (1)$$

where a = Ball radius, m (19 mm for the ball used)
L = Fiber length, m
V_o = Ball potential, V (1500 volts used)
$\alpha = L/a$
ε_o = Permittivity of free space, 8.85×10^{-12} F/m
R = Fiber diameter, m (8 μ m for Thornel 300 fibers)

This relationship is cumbersome and involves many parameters which were constant. Since the only variable using these fibers was fiber lengths, the pulse amplitude resulting from charge transfer was expressed in a simple power relationship,

$$V_P = K\ L^x \qquad (2)$$

where V_P = Voltage pulse amplitude, mV
K = System constant
L = Fiber length, m
x = Appropriate exponent

In figure 2.1-3, the feasibility of using this approximation is demonstrated. The symbols represent predictions by Bucher's equation arbitrarily normalized to a value of 0.001 volt at L = 1 mm. The straight line represents equation 2 and is a good fit for the form of Bucher's equation. The exponent required, over the range from 1 to 20 mm is 2.34. Therefore, equation 2, adjusted to this case, is

$$V_P = K\ L^{2.34} \qquad (3)$$

Experiments were conducted to determine the voltages corresponding to impacts of fibers with known lengths. Typical values are given in the following table:

Fiber length mm	Pulse amplitude mV
4	50
8	310
12	800

Equation 2 fits these data best when K = 1.53 and x = 2.52 giving

$$V_P = 1.53\ L^{2.52} \qquad (4)$$

This equation was used to convert voltage pulses to fiber lengths for exposure tests. The value of K for a given system depended on both the type of preamplifier and the cables used. However, by making several calibration runs using known fiber lengths, the proper constant for each system was determined.

Equation (4) was used to convert the observed spectrum of voltage pulses to a fiber-length spectrum. However, spurious noise caused problems at the low-voltage end of the pulse spectrum. An example of this is shown in figure 2.1-4. The very high numbers of counts at low voltages were not consistent with the expected number of short fibers, but they occurred only during fiber exposure. These low-voltage pulses usually occurred at levels equivalent to those caused by fibers at least 2 or 3 mm long. This put a lower bound on the lengths of fibers that could be measured accurately. Another problem was the broad range of the voltage pulses that needed to be measured. From the foregoing data one can see that if both 4 and 12 mm fibers were present in an exposure, the expected pulses would be concentrated at 50 and 800 mV. At gain settings suitable for 800 mV, resolution of 50-mV pulses was poor. Also, the low-voltage noise was large enough to distort and sometimes totally swamp the 50-mV pulses of the 4-mm fibers, if present.

Accordingly, the ball detector was considered to be an acceptable instrument for measuring fiber length spectra, but only for fiber lengths greater than 4 mm.

Calibration. - Fiber samplers inherently count the number of fibers passing through their effective frontal area in some prescribed time interval. The number of fibers counted is obviously dependent upon the effective area of the sampler, the concentration of fibers in the fiber stream, the velocity of the stream, and electromagnetic forces that modify the particle trajectory.

The calibration standard used in this investigation was "bridal veil." This is a nylon mesh fabric having approximately hexagonal apertures measuring about 1.5 mm between parallel sides. The veil was coated with a tacky substance to capture fibers that came into contact with the mesh. The device was assumed to capture all fibers longer than 4 mm (see reference 2-6 for mesh calibration data) and to have no significant sensitivity to velocity of the stream or electromagnetic effects. Fibers captured by the veil were counted manually after exposure.

The BRL ball detector required an independent calibration because the charging voltage was different than that used by BRL (1500 volts vs. 2000 volts) and because trajectories of the fibers around the ball were expected to be sensitive to both velocity and electric charge on the ball. The calibration device shown

in figure 2.1-5 was used to calibrate the ball detector. A motor-driven fan controlled the downward velocity through a vertical duct and assured reasonably uniform flow past the detector. Fibers of known lengths were introduced at the top of the duct. The ball detector was mounted above the bridal veil sampler on a support that pierced the veil at its center. Fibers that impinged on the ball were assumed to be repelled without modifying the distribution in the airstream.

The number of fibers deposited on the veil were directly related to counts of voltage pulses on the ball sampler because the environments for the two devices were identical.

Typical results are portrayed in figure 2.1-6 for two experiments in which fibers either 4 mm or 8 mm long were introduced into the calibration chamber and the velocity of the airstream was varied systematically. The calibration constant, K, for each step of the experiment is plotted against the velocity of the airstream. The calibration constant relates the pulses detected by the ball, x_b, to the exposure, E, by the simple equation:

$$E = K\, x_b \qquad (5)$$

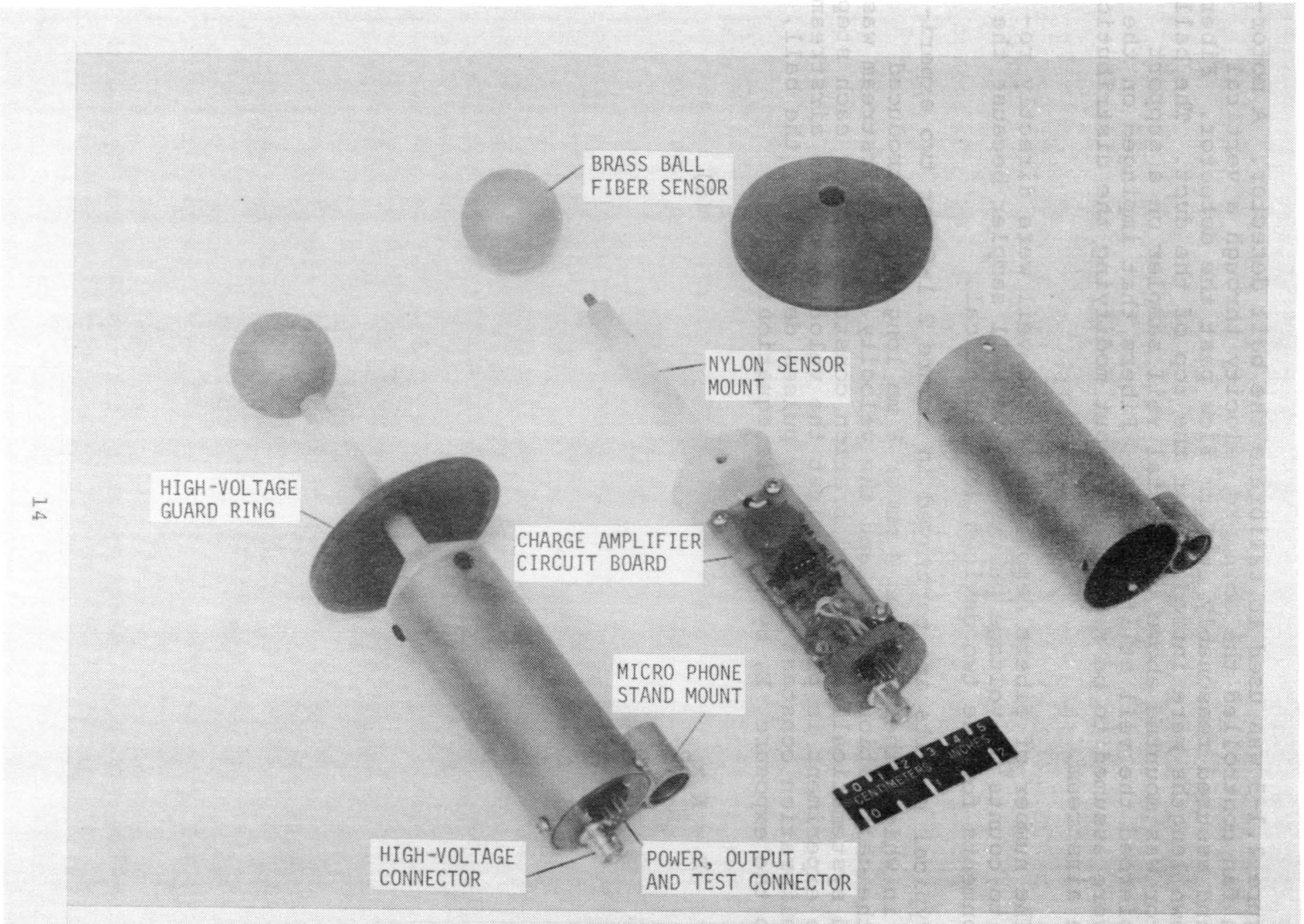

Figure 2.1-1 - Ball Detector

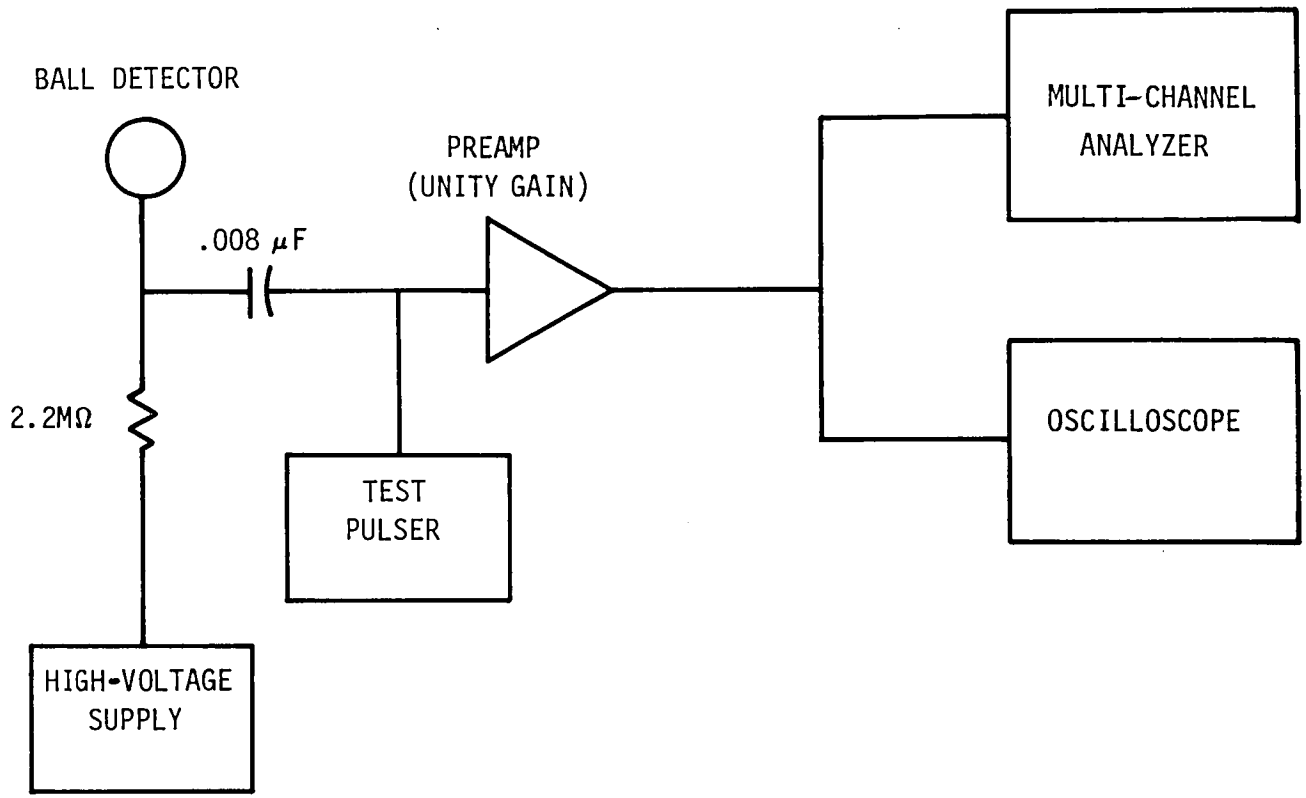

Figure 2.1-2. - Ball detector system

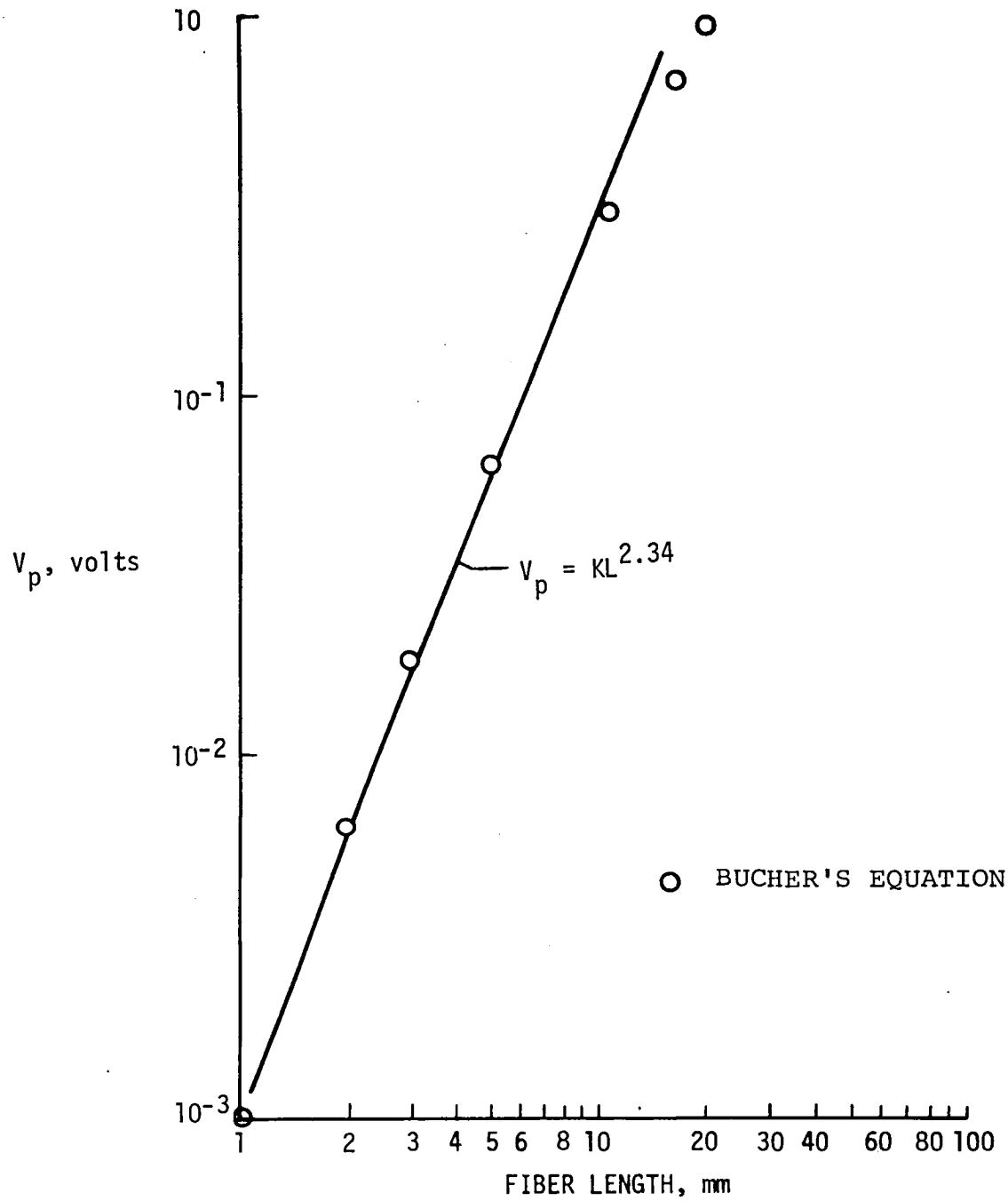

Figure 2.1-3. - Fiber length vs. charge pulse amplitude

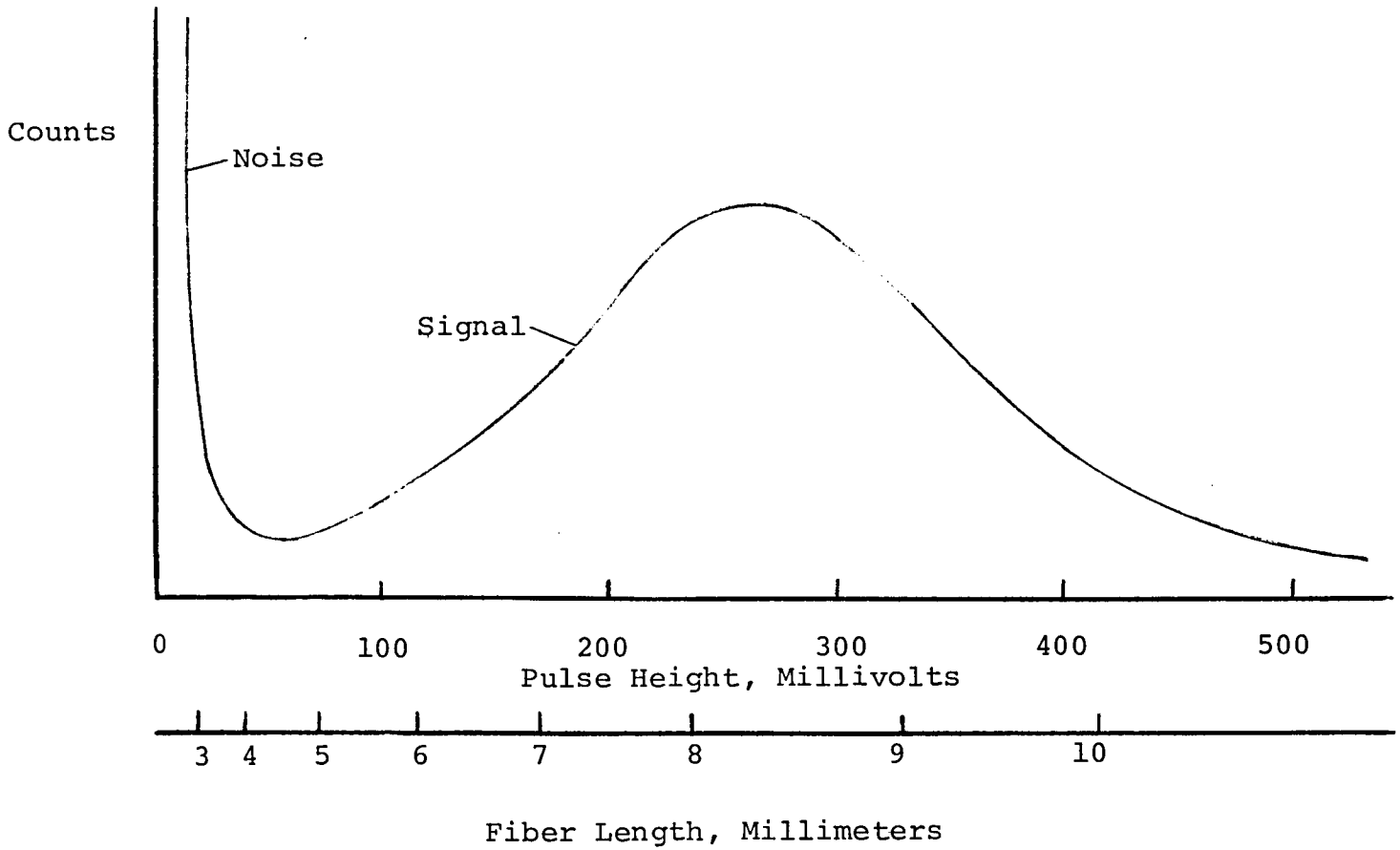

Figure 2.1-4. - Typical Spectrum

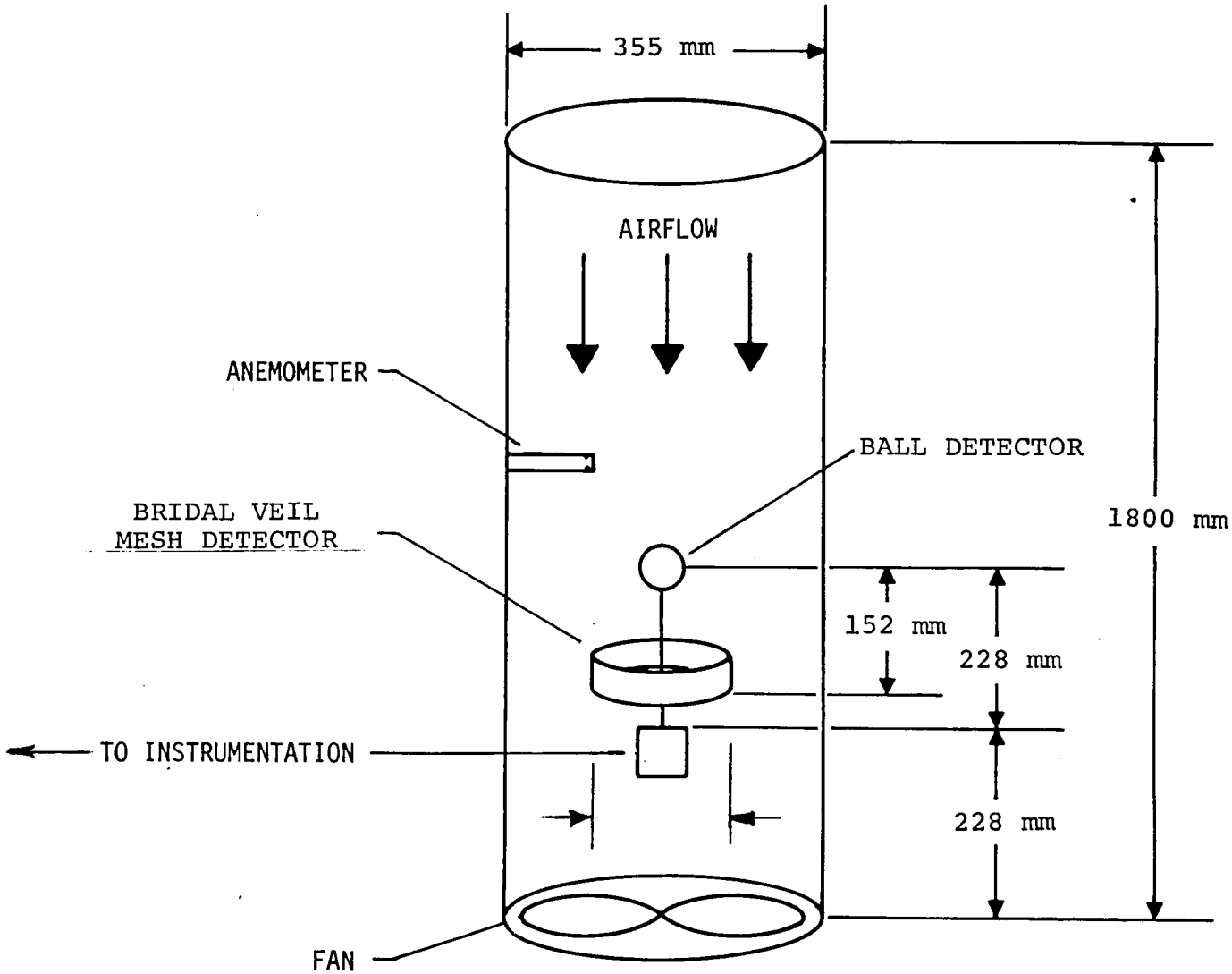

Figure 2.1-5. - Ball calibration chamber

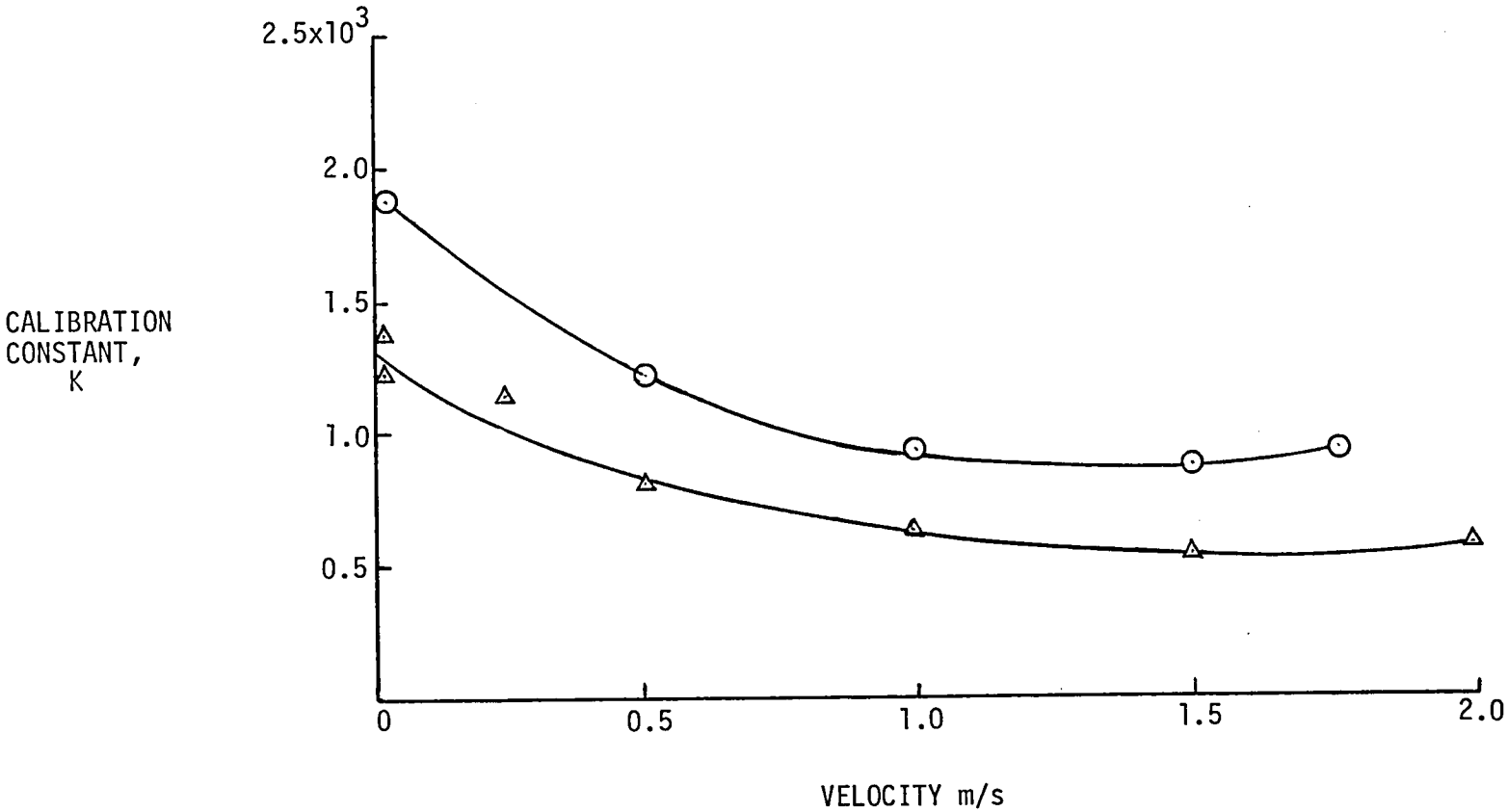

Figure 2.1-6. - Ball Detector Calibration

2.2 CHARGED WIRE DETECTOR

The charged ball detector discussed in section 2.1 is not suitable for sensing short (1 mm) fibers because of insufficient signal-to-noise margin. A wire sensor was conceived and developed to replace the charged ball sensor in the ball detector system. The wire sensor consists of a straight tinned copper wire 153 mm long, and 0.51 mm in diameter. The longitudinal axis of the wire was mounted normal to the fiber flow direction. The wire sensor was interchangeable with the ball sensor on the ball sensor attachment base. No modifications were required in the ball detector electronics system when the wire detector was used. A photograph of the charged wire detector is shown in figure 2.2-1.

The relative sensitivity of the wire and ball detector in the 1-to 3-mm fiber-length range is shown in the following tabulation of detector system output voltage levels.

	Output Voltage, mV	
Fiber Length	Ball Sensor	Wire Sensor
1 mm	1.25	40
2 mm	7.2	100
3 mm	20.0	171

The wire detector was initially calibrated for 1- and 2-mm-long fibers and subsequently for 3-mm-long fibers. Although the calibrations were all referenced to fiber deposition measurements, a different deposition measurement technique was used for the 3-mm calibration. Therefore, the calibration for 1- and 2-mm-long fibers is discussed separately from the calibration for the 3-mm-long fibers.

The wire detector was calibrated for 1- and 2-mm fiber lengths in a fiber free-fall environment using sticky paper deposition samplers as a reference. Each test run used two wire detectors and three 50 mm by 50 mm sticky paper samplers. Because a large number of fibers were deposited in the tests, only portions of each sticky paper were counted for fibers. The exposure measured by the sticky papers was calculated based on a 25 mm/s fiber free-fall velocity and the following relationship,

$$E = \frac{D}{v} = \frac{N}{Av} \qquad (1)$$

where E = Exposure, fiber-sec/m^3
D = Deposition, fibers/m^2
v = Fall velocity, m/sec, (.025 m/s)
N = Fiber count
A = Area counted, m^2, (2.83×10^{-4} m^2)

$$\text{thus } E = \frac{N}{2.83 \times 10^{-4} \times .025} = 1.414 \times 10^5 \, N, \text{ fiber-sec/m}^3$$

By relating the exposure determined by the sticky paper deposition samplers and the wire detector pulse count indications, the wire detector calibration constant, K_w, as contained in the following expression, was determined.

$$E = K_w \, N_w \qquad (2)$$

where E = Exposure, fiber-sec/m^3
K_w = Exposure calibration constant
N_w = Fiber counts indicated by detector system

Letting $K_w \, N_w = \frac{N}{Av}$, from (1)

$$K_w = \frac{N}{N_w \, Av} = \frac{1.414 \times 10^5 N}{N_w}$$

Test data and resulting values of K_w for each test are shown in table 2.2-1.

The average K_w for 1-mm-long fibers was 6.7×10^3 sec/m^3 and for 2-mm-long fibers was 5.26×10^3 sec/m^3.

A typical pulse amplitude spectrum resulting from the wire detector tests for 1-mm-long fiber is shown below. The variation in pulse amplitude is attributed primarily to variations in orientation of fibers hitting the wire detector and to small variations in fiber length produced by the fiber chopper used in the NASA vulnerability exposure test facility (see ref. 2-1). For the tests with 1-mm-long fibers, in table 2.2-1, only pulse amplitudes greater than 20 mV were counted, and all were assumed to be caused by 1-mm fibers.

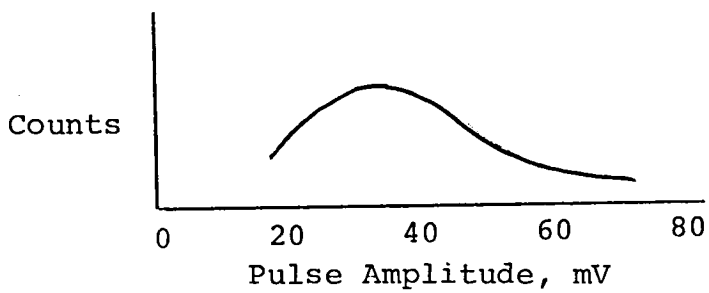

The wire detector was subsequently calibrated for 3-mm-long fibers using bridal veil mesh deposition samplers as a reference rather than sticky paper deposition samplers. The bridal veil mesh was similar to that described in section 2.1. Four open-ended, hollow cylinders, 115 mm in diameter by 160 mm long with bridal veil mesh covering one end were placed mesh end down on a table around the wire detector.

Due to the large number of fibers deposited on the mesh samplers, the line intersection counting technique discussed on pages 32 and 33 of reference 2-6 was employed. A single line 10 mm long was chosen and the average of 5 repetitive countings was used to determine the number of intersections, I, for a given sampler. The estimate of fibers deposited in a unit area was then determined in accordance with reference 2-6 to be,

$$\frac{N_T}{A_T} = \frac{I\,\pi}{2\,\ell\,L} \qquad (3)$$

where N_T = Total number of fibers in area A_T
A_T = Area, m^2
I = Number of fiber intersections
ℓ = Fiber length, m
L = Length of line on which intersections are counted, m

Since $\frac{N_T}{A_T}$ is also fiber deposition, D, and from (1), exposure, $E = \frac{D}{v}$, then

$$E = \frac{I}{2\,\ell\,L\,v}$$

$$= \frac{I}{2 \times .003 \times .1 \times .025}$$

$$= 2.09 \times 10^5\, I$$

and from (2) $E = K_w N_w$, then

$$K_w N_w = 2.09 \times 10^5\, I, \text{ and}$$

$$K_w = \frac{2.09 \times 10^5\, I}{N_w}$$

Test data and resulting values of K_w for each of the 3-mm-fiber tests are shown in table 2.2-2.

The average K_w for 3-mm-long fibers was 5.9×10^3 sec/m^3.

In addition to calibrating the wire detector for use with 1, 2, and 3 mm virgin fibers, an investigation was conducted to determine the suitability of the detector for use in a soot-laden environment to detect fibers released from burning composites. The detector was found unsuitable for this purpose. Signals generated by soot particles from burning JP-4 fuel were virtually indistinguishable from signals generated by virgin one millimeter carbon fibers. The investigation which led to the above conclusion

is described below.

The wire sensor was placed at the bottom of a metal trash can. An oscilloscope was connected to the sensor electronics output. With the oscilloscope display as a reference, a threshold of twenty millivolts (equivalent to that used for counting 1-mm fibers) was set in the portable ball discriminator.

A rich mixture of JP-4 was burned to produce dense sooty smoke which was directed into the can containing the wire sensor. Counting of particles began almost immediately and within a few seconds reached an average of 270 contacts per second. Simultaneously, short rise-time pulses were seen on the oscilloscope. Raising the discriminator threshold to about twenty-three millivolts eliminated counting. As the sensor with its attached amplifier became covered with soot (after about one minute), the sensor output ceased. Subsequent cleaning of the sensor and its amplifier was sufficient to restore the sensor to operating condition.

Heating effects on the sensor were not considered to be responsible for the output signal observed during the first minute of exposure to the smoke. Temperature in the can was not monitored during the test described above but was monitored in a later similar test. When the smoke was directed into the can, the temperature rose gradually from 300K to a peak of 443K in about six minutes. During the first minute of the sensor test, the temperature in the can was under 323K.

TABLE 2.2-1 WIRE DETECTOR CALIBRATION DATA FOR 1-AND 2-MM FIBERS

Test #	Fiber Length mm	Pulses Counted by Wire Detectors, N_w		Fibers Counted on Sticky Papers, N			Average Calibration Constant, K_w*
		#1	#2	#1	#2	#3	
1	1	124	182	5	13	7	7.4×10^3
2	1	363	386	32	14	23	8.7×10^3
3	1	761	832	23	32	37	5.5×10^3
4	1	697	400	9	21	39	5.9×10^3
5	2	590	400	16	22	30	6.5×10^3
6	2	1100	990	48	47	33	5.8×10^3
7	2	881	780	23	33	16	4.1×10^3
8	2	610	574	11	20	32	5.0×10^3

$$*K_w = \frac{1.414 \times 10^5 \, N}{N_w}$$

TABLE 2.2-2 WIRE DETECTOR CALIBRATION DATA FOR 3-MM FIBERS

Test No.	Pulses Counted by Wire Detector, N_w	Fibers Intersecting 100 mm Line on Bridal Veil, I				Average Calibration Constant, K_w*
		#1	#2	#3	#4	
1	629	14	28.4	28	11	6.8×10^3
2	727	12.8	26.4	26.4	11	5.5×10^3
3	1012	22	34.8	25.8	8.6	4.7×10^3
4	848	32.8	36.8	32.4	15.6	7.2×10^3

$$*K_w = \frac{2.09 \times 10^5 I}{N_w}$$

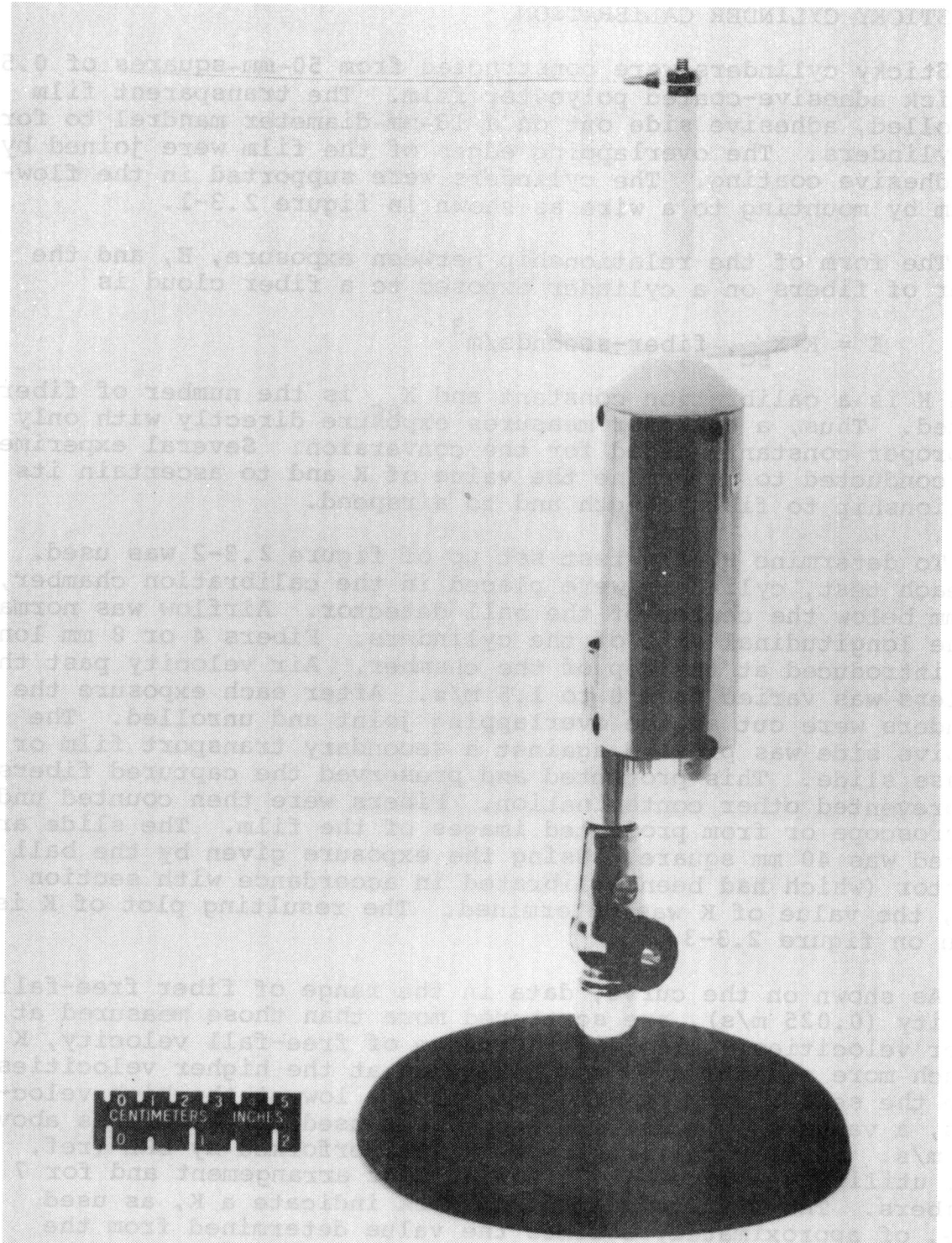

Figure 2.2-1 - Charged-wire detector

2.3 STICKY CYLINDER CALIBRATION

Sticky cylinders were constructed from 50-mm-squares of 0.5-mm-thick adhesive-coated polyester film. The transparent film was rolled, adhesive side out on a 13-mm-diameter mandrel to form the cylinders. The overlapping edges of the film were joined by the adhesive coating. The cylinders were supported in the flow-stream by mounting to a wire as shown in figure 2.3-1.

The form of the relationship between exposure, E, and the number of fibers on a cylinder exposed to a fiber cloud is

$$E = K X_{sc}, \text{ fiber-seconds/m}^3$$

where K is a calibration constant and X_{sc} is the number of fibers counted. Thus, a cylinder measures exposure directly with only the proper constant needed for the conversion. Several experiments were conducted to determine the value of K and to ascertain its relationship to fiber length and to airspeed.

To determine K, the test set up of figure 2.3-2 was used. For each test, cylinders were placed in the calibration chamber, 152 mm below the center of the ball detector. Airflow was normal to the longitudinal axis of the cylinders. Fibers 4 or 8 mm long were introduced at the top of the chamber. Air velocity past the samplers was varied from 0 to 1.5 m/s. After each exposure the cylinders were cut at the overlapping joint and unrolled. The adhesive side was pressed against a secondary transport film or a glass slide. This protected and preserved the captured fibers and prevented other contamination. Fibers were then counted under a microscope or from projected images of the film. The slide area counted was 40 mm square. Using the exposure given by the ball detector (which had been calibrated in accordance with section 2.1), the value of K was determined. The resulting plot of K is shown on figure 2.3-3.

As shown on the curve, data in the range of fiber free-fall velocity (0.025 m/s), are scattered more than those measured at higher velocities. Also, in the range of free-fall velocity, K is much more sensitive to velocity than at the higher velocities. Since the sensitivity of K to velocity is low at the high velocities, a value of $K = 2 \times 10^3$ sec/m^3 was used at velocities above 0.25 m/s. Similar calibration work was performed by BRL (ref. 2-4), utilizing a somewhat different test arrangement and for 7 mm fibers. The results of the BRL work indicate a K, as used above, of approximately 3 times the value determined from the Bionetics tests. This difference may have been caused by the different orientations of the sensors with respect to the fiber flow direction in the two calibrations. The K value derived here was accepted because, in use, it led to higher vulnerability assessments for equipment than would have resulted from use of the BRL calibration.

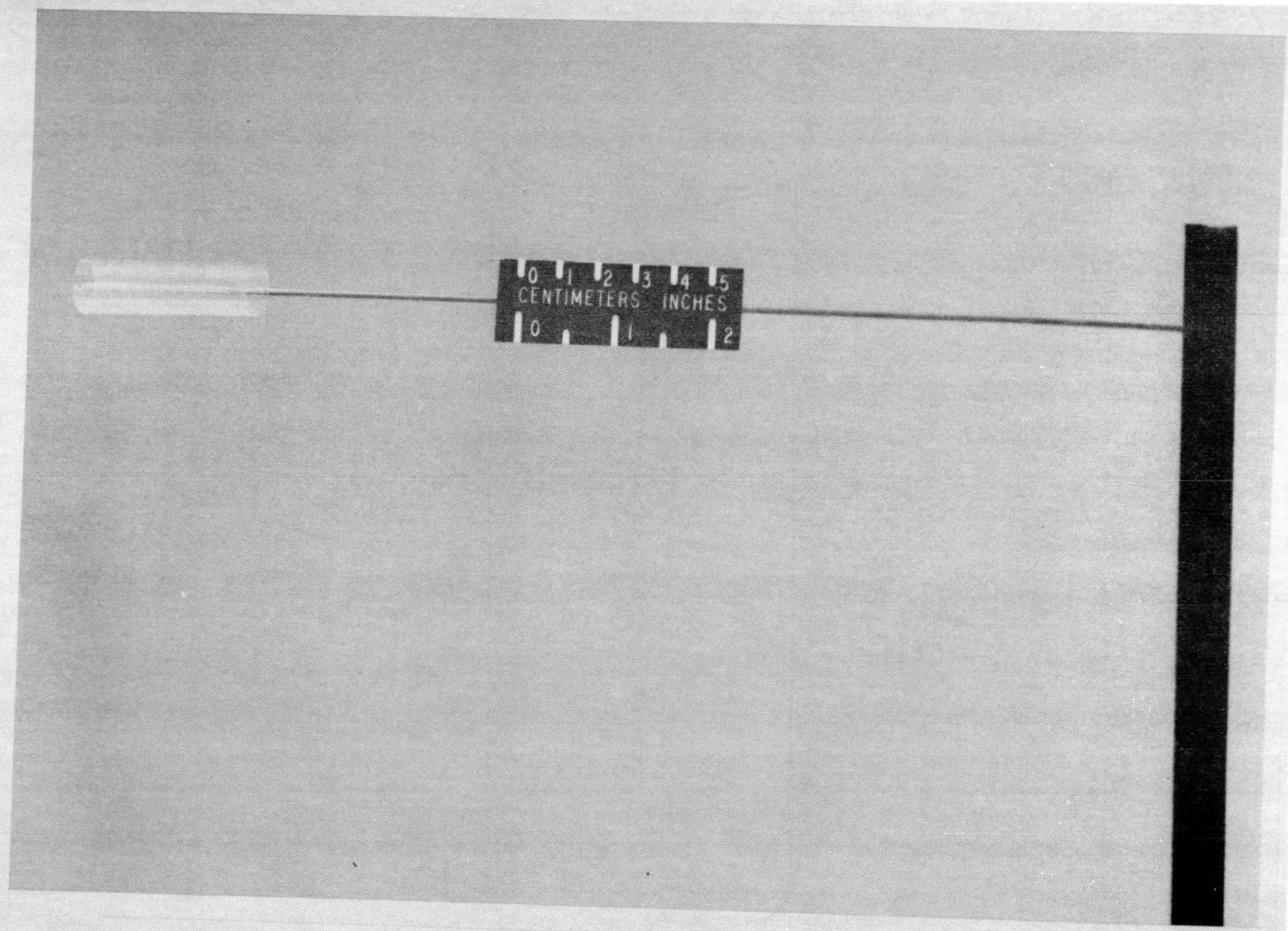

Figure 2.3-1 - Sticky cylinder sampler

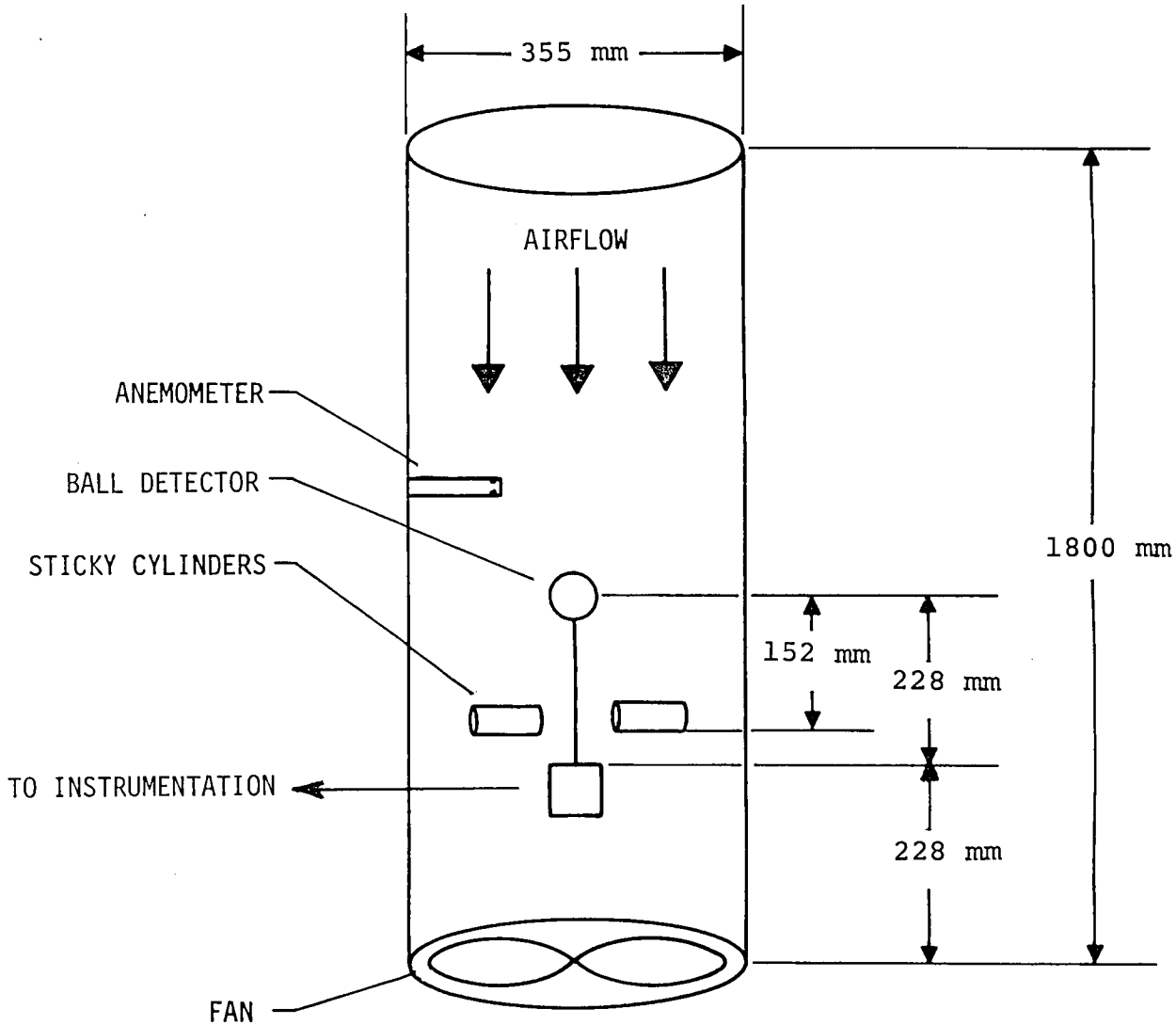

Figure 2.3-2 - Sticky cylinder calibration chamber

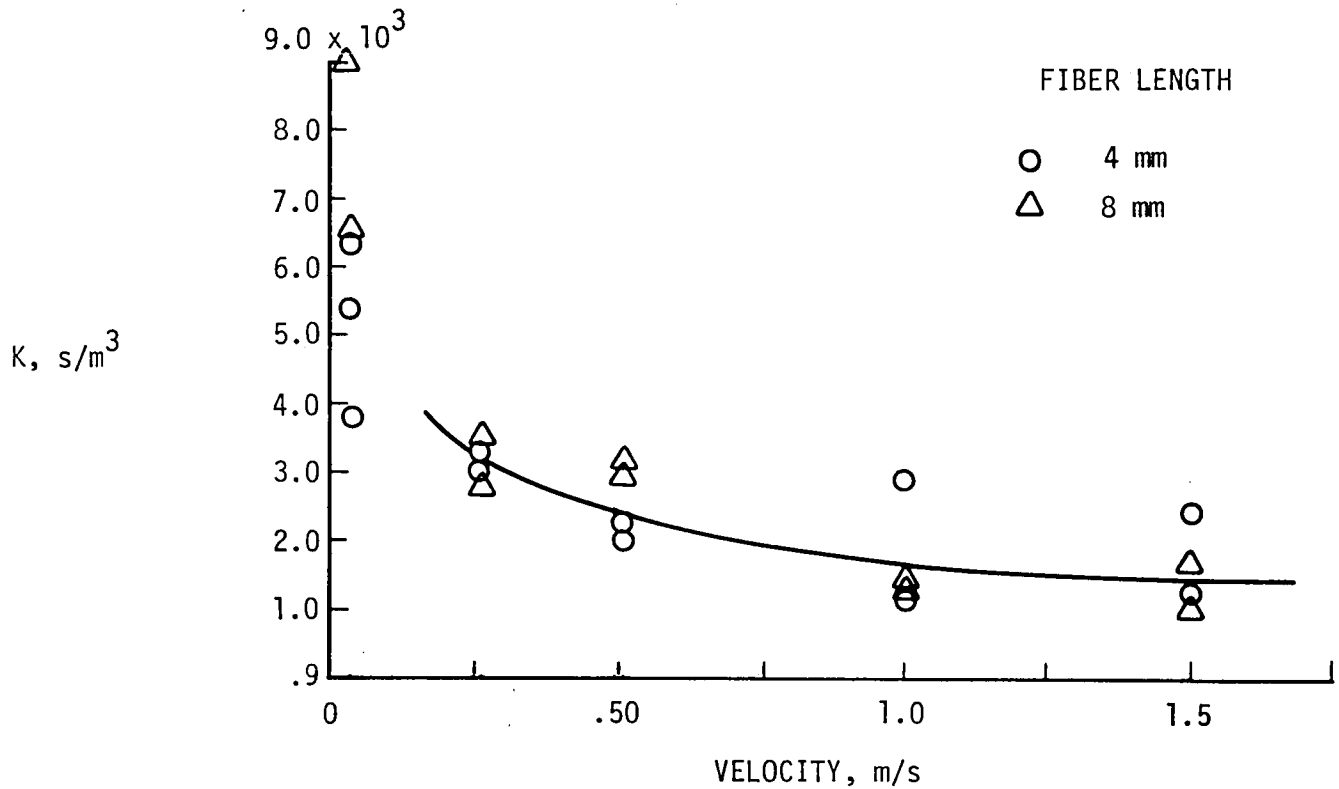

Figure 2.3-3. - Exposure calibration constant for sticky cylinders

2.4 WIRE-GRID FIBER SENSORS

The wire-grid fiber sensor was developed primarily for the purpose of measuring the electrical characteristics of fire-released carbon fibers. However, it was also used to measure the time histories of carbon fiber concentrations and exposures in the plumes of a number of fire tests. The relationship of the electrical characteristics (resistance and burn-out power) of fire-released fibers relative to virgin fibers was required to interpret the results of equipment vulnerability tests using virgin fibers. The electrical characteristics of virgin fibers have been measured for a number of fiber types as reported in section 1.1. However, because of the difficulty of collecting, isolating, and measuring electrical characteristics of individual fire-released fibers, in situ measurement of these characteristics was considered necessary.

Sensor description.- The sensor developed in this effort consisted of a wire comb assembly, shown in figures 2.4-1 and 2.4-2, connected to an electronic assembly, illustrated in figures 2.4-3, 2.4-4, and 2.4-5. The wire comb consisted of a number of parallel steel wires (approximately 0.75 mm dia. and 90 mm length) mounted at their mid-point in a single plane through a printed circuit board with 2 mm center-to-center spacing. The etched pattern on the board was such that when a voltage was applied to the two input electrodes, that voltage would appear between any two adjacent wires. The wire grid (fig. 2.4-1) used in the Dahlgren tests (ref. 2-3) had a total area of approximately .015 m^2 and the grid (fig. 2.4-2) used in the Dugway tests had a total area of .044 m^2. As shown in figure 2.4-3, these wire grids were connected to the grid monitor and switch unit shown in figure 2.4-4. This unit had a separate circuit for each of eight grids which either applied a 250 Vrms, 60 Hz signal to the grid or connected that grid to the scope interface unit (fig. 2.4-5) depending on the position of the manual selector switch for that grid. The 250-Vrms signal was maintained on the grid for the purpose of burning out any fibers which intercepted the grid, and had a 10-ohm resistor in series to provide an output voltage for recording the number of fibers which intercepted the grid. The scope interface unit, in conjunction with the x-y oscilloscope, provided the capability for measuring and recording the voltage-current characteristic during burn-out. This unit maintained a high-voltage (200 Vdc), high-impedance source connected to the grid until a fiber intercepted the grid, at which time the scope sweep circuit was triggered and a ramp voltage was applied to the interface unit increasing the current until the fibers burned out. The monitor outputs were applied to the x and y inputs of the oscilloscope, producing a plot of the voltage-current characteristic to burn-out as shown in figure 2.4-6. Figure 2.4-6a shows a calibration where the grid was replaced with a 500-ohm and a 1000-ohm resistor, and figure 2.4-6b shows the actual characteristic

of a fiber intercepted and burned out during Dugway test D-2 (ref. 2-3).

Calibration. - A series of calibration tests were conducted to determine the efficiency factor as a function of the velocity of the fibers relative to the grid. The data acquired in these tests are given in Table 2.4-1. All tests were conducted in the Langley Research Center fiber chamber (ref. 2-1) with virgin T-300 fibers, cut in 3-mm lengths, injected into the chamber with resulting fiber concentrations of approximately 10^4 fibers/cubic meter.

The static calibrations consisted of a comparison of the number of fibers, N_v, collected on a bridal veil relative to the number of fibers, N_g, burned out on a grid mounted directly adjacent to the bridal veil, over the period of the test (approximately 1000 sec.). The number of fibers, N_g', expected to pass through an area equal to the area of the grid, based on the fiber deposition on the bridal veil, was determined as follows:

$$N_g' = N_v \frac{A_g}{A_v} \qquad \begin{aligned} A_g &= 0.044 \text{ m}^2 \\ A_v &= 0.000955 \text{ m}^2 \end{aligned}$$

where A_v is the area of the bridal veil over which the fibers were counted, and A_g is the area of the wire grid. The collecting efficiency (F) then is simply the ratio of the actual sensor counts, N_g, to the expected sensor counts, N_g', and is approximately 0.7 as shown in table 1.4-1a.

Dynamic tests were performed by installing the grid on a pendulum as illustrated in figure 2.4-7. A fiber count (N_g static) was obtained with the grid oriented horizontally (position 1). The grid was then released and allowed to swing through an arc to position 3 with a measured period and another fiber count (N_g dynamic) was obtained. The radius of swing was 0.846 meter in all cases. Upon release from position 1, the grid almost immediately assumed a position such that the axis of swing lay in or close to the plane of the grid face during the entire swing.

Some problems were encountered in these tests due to the nonuniform distribution of fibers within the chamber. Consequently, a series of tests were conducted to determine the approximate ratio of the average fiber concentration over the path of the grid during the swing to the fiber concentration at position 1. Bridal veil was used to measure the fiber deposition $N_v(1)$, $N_v(2)$, $N_v(3)$ over a period of time at positions 1, 2, and 3 in figure 2.4-7. A chamber correction factor (F_c) was calculated as follows:

$$F_c = \frac{N_v(1) + N_v(2) + N_v(3)}{3\, N_v(1)}$$

The results of these tests are given in table 2.4-1, and yield a correction factor of 1.93.

The results of the dynamic tests are given in table 2.4-1c at three different velocities as indicated. A velocity correction factor (F_v) was determined for each series of tests as follows

$$F_v = \frac{N_g\ (d)\ V_f\ T}{N_g\ (s)\ r\ \theta\ F_c}$$

$T = 200$ sec.
$V_f = 0.025$ m/sec.
$F_c = 1.93$

where N_g (s) was the count over a period of time (T) prior to the swing, N_g (d) was the count during the swing, V_f is the free-fall velocity of the fibers, r is the radius and θ is the arc through which the grid was swung. The radius of the pendulum (0.846 m) and the time, T, were chosen to make the number of counts N_g (s) and N_g (d) equal if no velocity effects were present.

The resultant values of F_v (0.81, 0.96, 0.96) are close enough to unity that, considering the experimental uncertainties involved, the sensor was considered insensitive to relative velocity for velocities of up to 4 meters/second.

In addition to these laboratory tests, one fire test (#54) was conducted at Dahlgren to determine the sensitivity of the instrumentation to particulates, other than carbon fiber, which may be emitted from such a fire. In this test, a sample of material (glass fiber/epoxy matrix) was burned which contained no carbon fiber. During the 105 min. burn, 15 counts were indicated on the sensor. This number of counts is negligible compared to the corrected total count (44,000) obtained from test #53 where graphite/epoxy was burned in a similar test.

Results.- A number of experiments were conducted using these sensors. First, a series of experiments were conducted in the laboratory to measure the electrical characteristics of both G.Y.-70 and T-300 chopped virgin fibers. Second, the sensors were used in a series of fire experiments to determine the fiber concentrations and exposures obtained in these fires. A series of laboratory measurements on fibers from debris collected after the Dugway fire were subsequently conducted to evaluate the electrical characteristics of fire-released fibers.

In conducting the laboratory experiments, fibers were released in a closed chamber containing a grid. They were then distributed within the chamber by a blast of forced air and allowed to fall freely to the chamber floor during which time a

number of fibers intercepted the grid. Figure 2.4-8 shows the distribution of measured resistances of GY-70 and T-300 virgin fibers. These resistances were derived from the voltage and current at fiber burn-out and are for fibers bridging a 2-mm gap. The mean resistance of the GY-70 fibers was 307 ohms, based on 14 samples of data. For the T-300 fibers, the mean resistance was 1590 ohms, based on 54 samples of data.

Measurements were also made on some burned T-300 fibers. Some fibers were burned in a laboratory oven, and some burned fibers were obtained from debris collected after the Dugway fire (test D-2). These fibers were measured in the chamber and inspected microscopically. Figure 2.4-9 shows the distribution of the diameters of these burned fibers. In these distributions, all fibers with diameters greater than 6.5 μm were included in the 6.5 to 7.0 μm bin although some exceeded 7.0 μm diameter. The distributions of resistances were predicted from the diameter distributions on the assumption that resistance was inversely proportional to cross-section area of the fibers. That is:

$$R = 1590\left(\frac{7\times10^{-6}}{d}\right)^2$$

Figure 2.4-10 shows the measured and predicted distributions of resistances for the oven-burned fibers. Microscopic inspection of these fibers revealed they were not typical of fire-released fibers observed in both the Dahlgren and Dugway fires in that they were much more uniform in diameter and length than those obtained from the fires.

Figure 2.4-11 is a histogram of resistances measured by the grid and resistances predicted from optical measurements of fibers taken from Dugway debris. The mean grid-measured resistance was 3924 ohms, based on 145 measurements. Because all fibers found optically to have diameters greater than 6.5 μm were counted in one bin, all fibers with measured resistances less than the resistance of 6.5 μm fibers (1844Ω) should also be placed in one bin, as indicated by the arrow. Measured resistances as low as 600Ω imply diameters as large as 11 μm, an unlikely diameter. During optical measurements, double fibers, adhering firmly to each other, were noted. These were excluded from the optical measurements. The abnormally low grid-measured resistances most probably were the result of the grid encountering a few twin or triplet fibers. The good agreement between the two resistance distributions at higher resistance levels (smaller diameters) supports the assumption that resistance is inversely proportional to cross-section areas, as expected.

A preliminary analysis of earlier data, reported in reference 2-7, suggested that the reduction of diameter produced by burning did not change fiber resistance. Based on the present measurements, fire-released fibers have a higher resistance than was originally reported. Hence, their threat to electrical equipment is also lower than reported earlier.

These sensors were used to measure the fiber concentrations and exposures in Dahlgren test #53 and Dugway tests D-1, D-2, and D-3. In the Dahlgren test, the grid was located 220 m downstream from the fire and approximately in the center of the tube. The air velocity in the tube was 0.67 m/s. Figure 2.4-12 shows the measured rates of fibers intercepting the grid, based on approximately 30-sec. averages, and the calculated fiber concentrations in the airflow as a function of time after ignition. Figure 2.4-13 gives a computed cumulative count and exposure at this location, based on the rates indicated in figure 2.4-12.

Figures 2.4-14 through 2.4-19 provide similar data for Dugway test D-1, grid 2, Dugway test D-2, grids 6 and 8, and Dugway test D-3, grids 4 and 6. The rates shown in these tests were based on approximately 1-minute averages. The location of the grids on the ladder is shown in figure 2.4-20. All grids were active. Data are presented herein on grids which accumulated significant counts. The air velocities and directions used in the calculation of concentration and exposure were as follows; test D-1 - 6.4 m/s at 360°, test D-2 - 5.8 m/s at 289°, and test D-3 - 5.3 m/s at 326°. The fiber concentration (C) and exposure (E) were determined as follows:

$$C = \frac{\dot{N}}{A_g \, F V_a \, \cos \Theta} \qquad \text{and} \qquad E = \frac{N}{A_g \, F V_a \, \cos \Theta}$$

where N is the total fiber count, $\dot{N}$ is the rate of fibers intercepting the grid, A_g is the area of the grid, F is the grid efficiency factor, V_a is the air velocity and Θ is the wind direction relative to the grid. Due to the dimensions of the grids, the concentrations and exposures indicated are for fibers approximately 2 mm and greater in length.

Figure 2.4-6b illustrates a currently unexplained phenomenon which caused the voltage on the grid to drop partially and to recharge with very little current. Experimentation indicated that this was the result of a momentary high-resistance (i.e., 100 kΩ) shunt on the grid. A similar phenomenon occurred in the Dahlgren fire tests, including #54 with no carbon fiber in the composite, but did not occur in the chamber tests involving virgin cut fibers. However, similar results were obtained in laboratory tests using burned fibers containing some unusually high-resistance fibers.

TABLE 2.4-1 WIRE GRID CALIBRATION DATA

a. Static Calibration at Position 1.

Numbers of Fibers

Run	Counted on Veil N_V	Expected Grid Counts N_g'	Counted on Grid N_g	Efficiency F
1	50	2303	853	0.37
2	12	553	403	0.73
3	57	2626	1895	0.72
4	56	2580	1927	0.75
Totals	175	8062	5078	0.63
	125*	5759*	4225*	0.73*

*Excluding Run 1 because result appeared spurious.

b. Chamber Uniformity Calibration

Run	Position 1 $N_V(1)$	Position 2 $N_V(2)$	Position 3 $N_V(3)$	
1	66	75	84	
2	41	111	98	
3	39	102	84	
4	97	327	281	
Totals	243	615	547	1405

$$F_c = \frac{1405}{3(243)} = 1.93$$

TABLE 2.4-1 Continued

c. Dynamic Calibration of Grid

θ	Max. Velocity (m/s)	Run	(static) N_g	(dynamic) N_g	F_v
3.14	4.06	1	628	394	
		2	212	209	
		3	386	419	
		Totals	1226	1022	0.81
2.40	3.24	1	503	259	
		2	514	448	
		3	297	278	
		Totals	1314	985	0.96
1.99	2.73	1	204	322	
		2	623	195	
		3	511	343	
		4	334	130	
		Totals	1672	1040	0.96

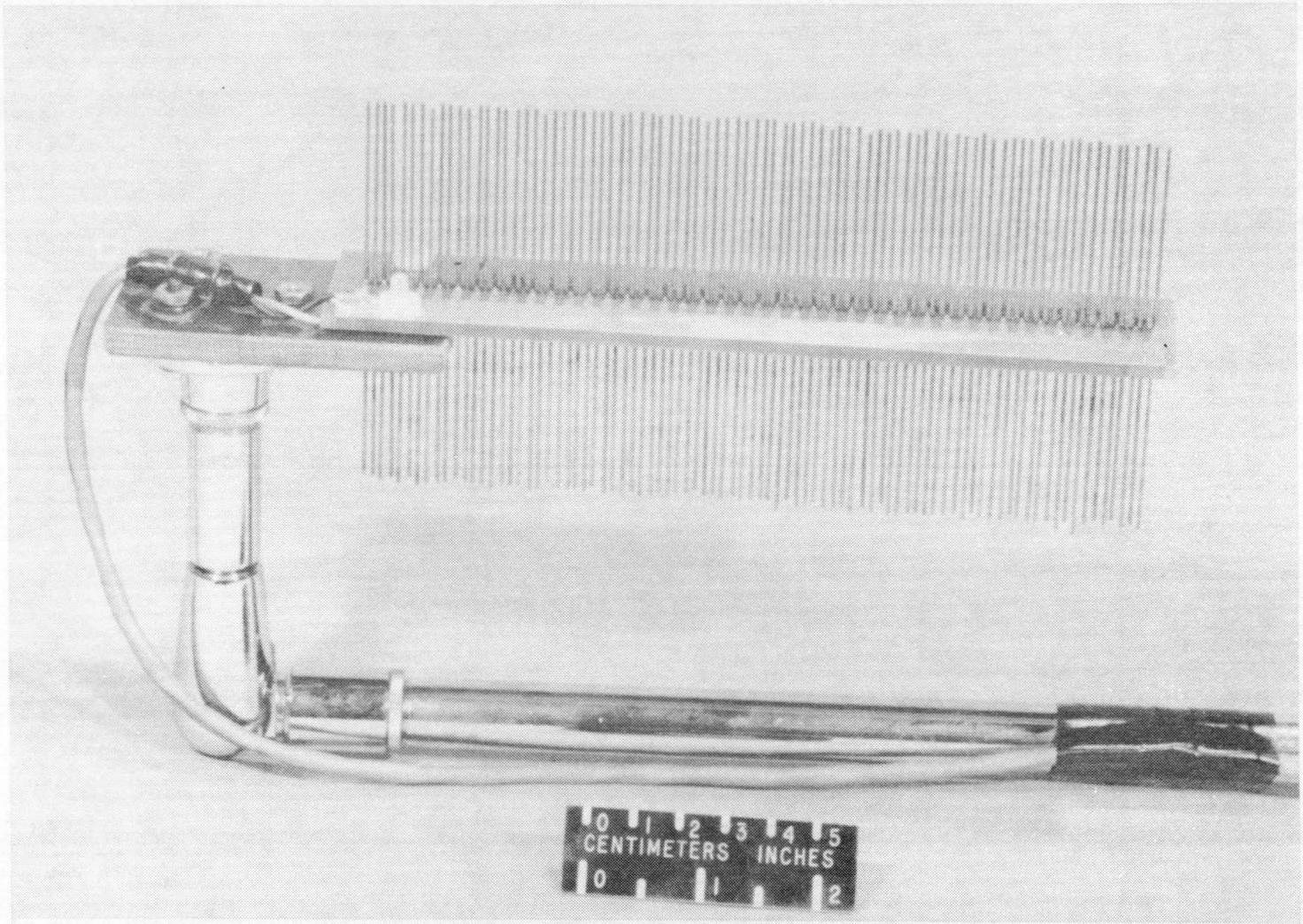

Figure 2.4-1 - Wire grid used in Dahlgren tests

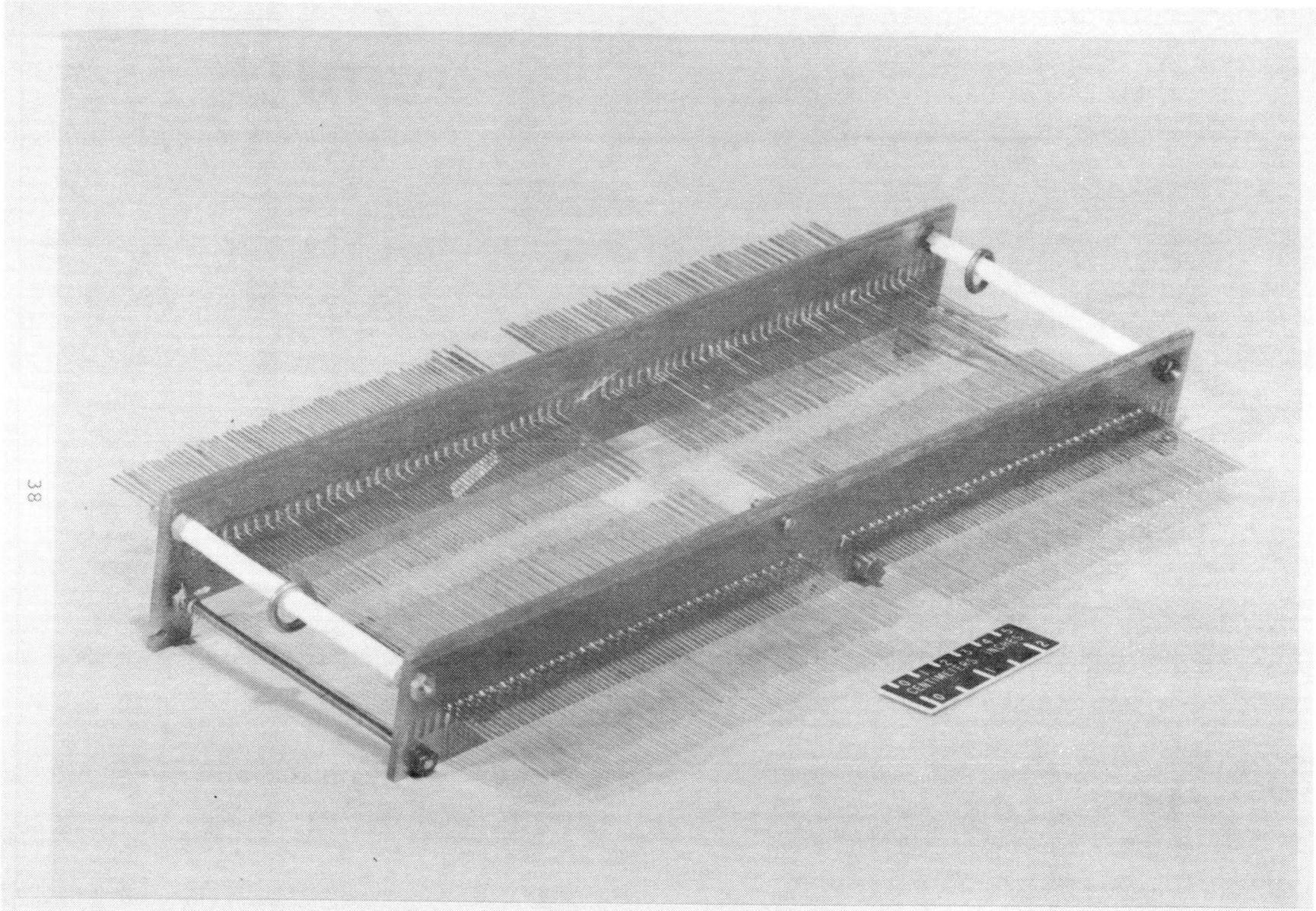

Figure 2.4-2 - Wire grid sensor used in Dugway tests

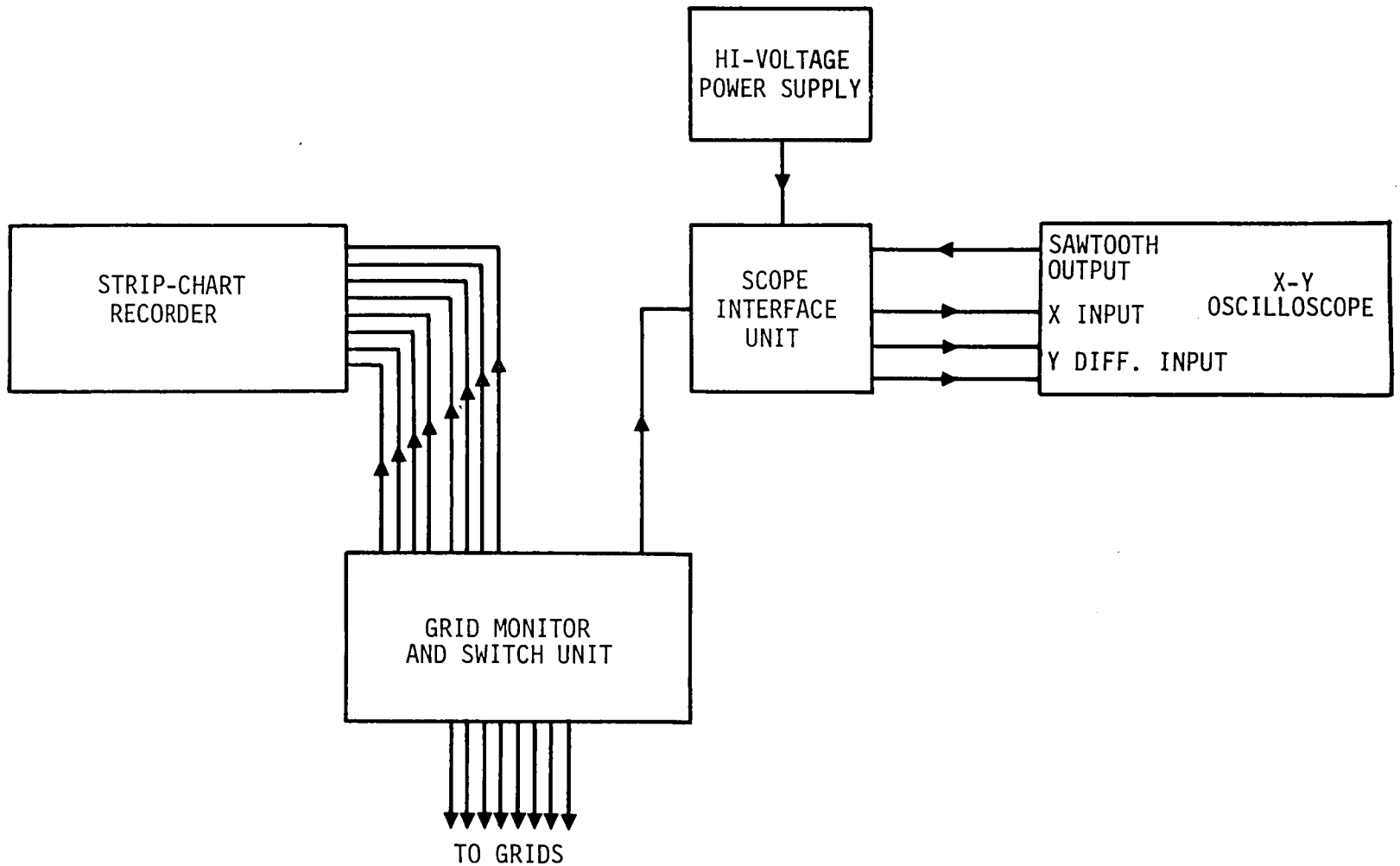

Figure 2.4-3. - Block diagram of instrumentation

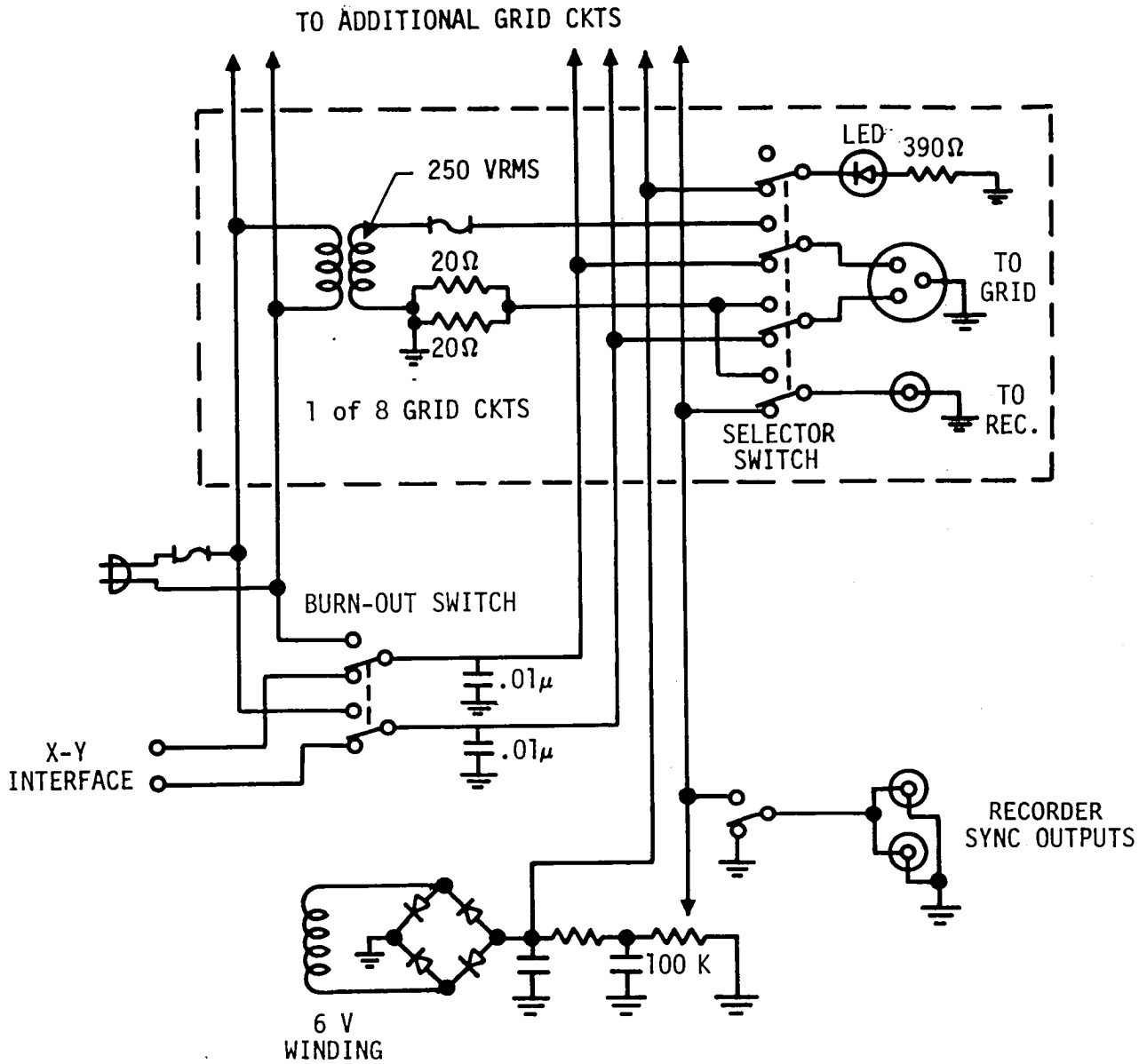

Figure 2.4-4. - Circuit diagram of grid monitor & switch unit

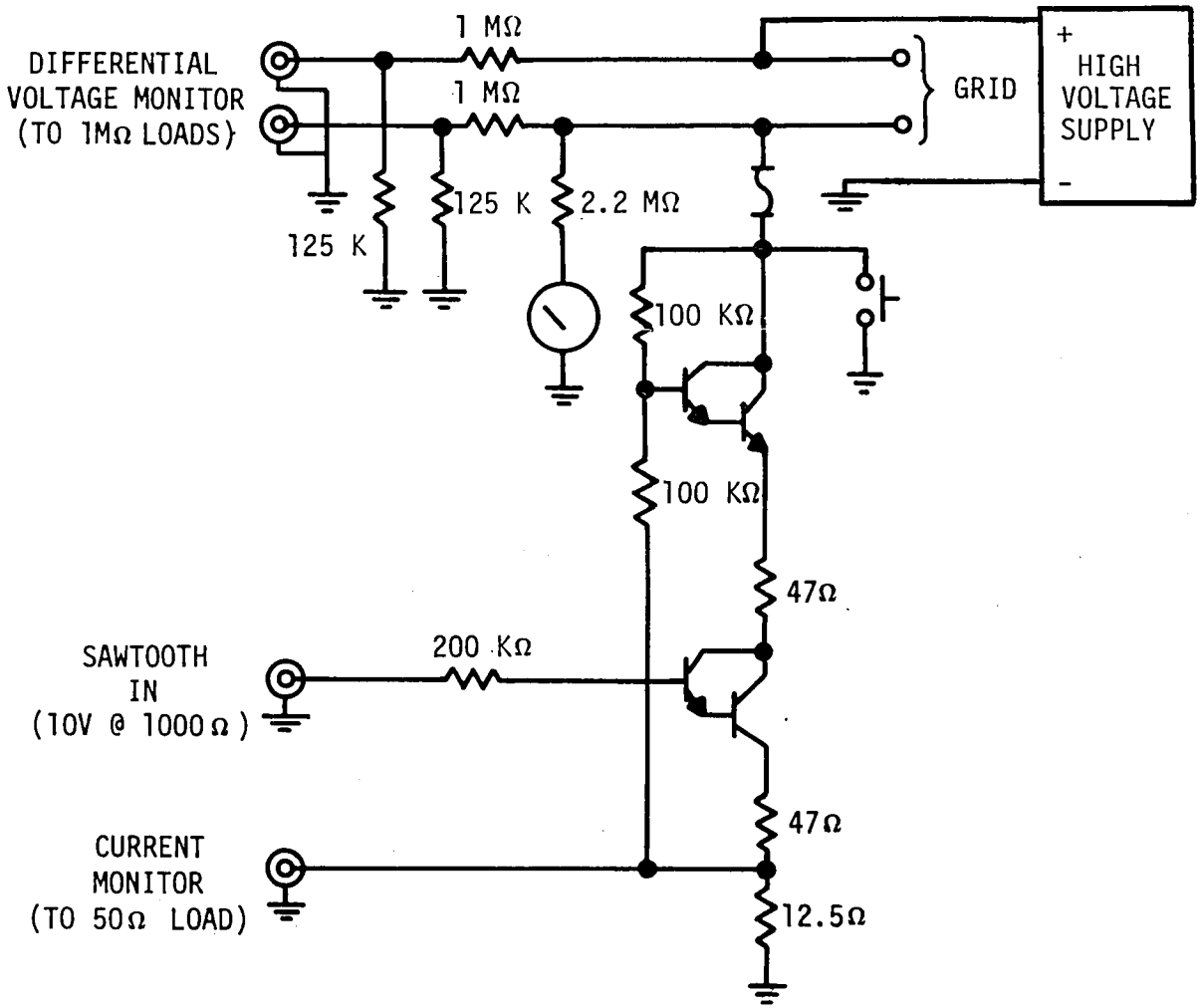

Figure 2.4-5 - Circuit diagram of X-Y scope interface unit

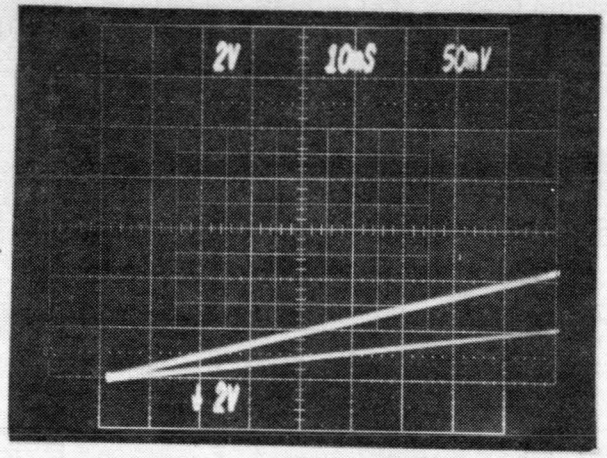

Voltage,
20v/div.

Current, 5 ma/div.

a. Calibration Resistors

500, 1000 ohms

Unexplained Phenomenon

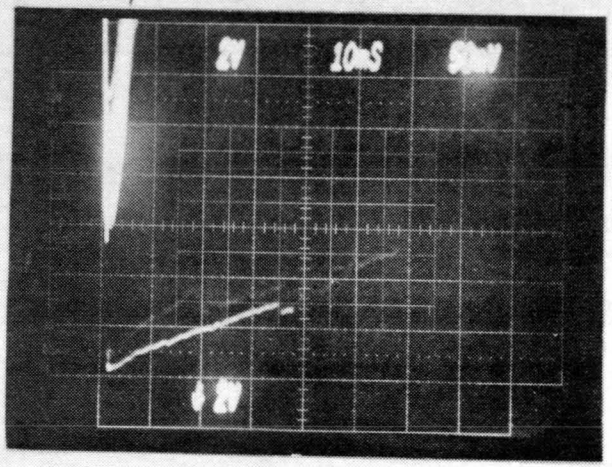

Current, 5 ma/div.

b. Fire-Released Fibers

Figure 2.4-6 - Wire-grid sensor calibration and test data

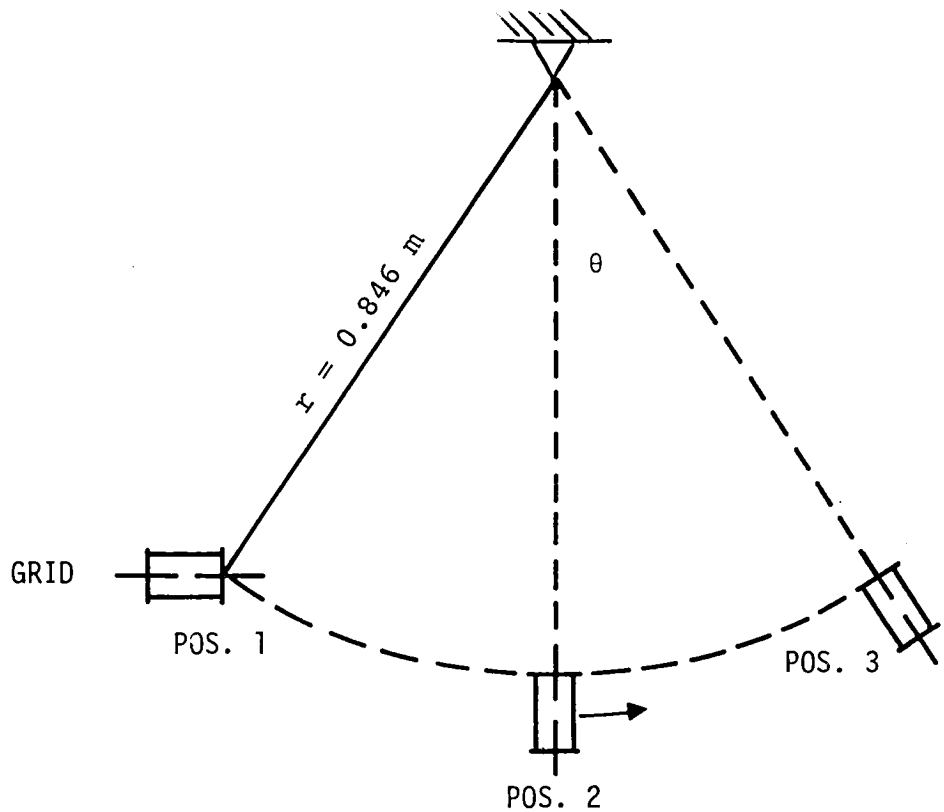

Figure 2.4-7 - Dynamic calibration geometry

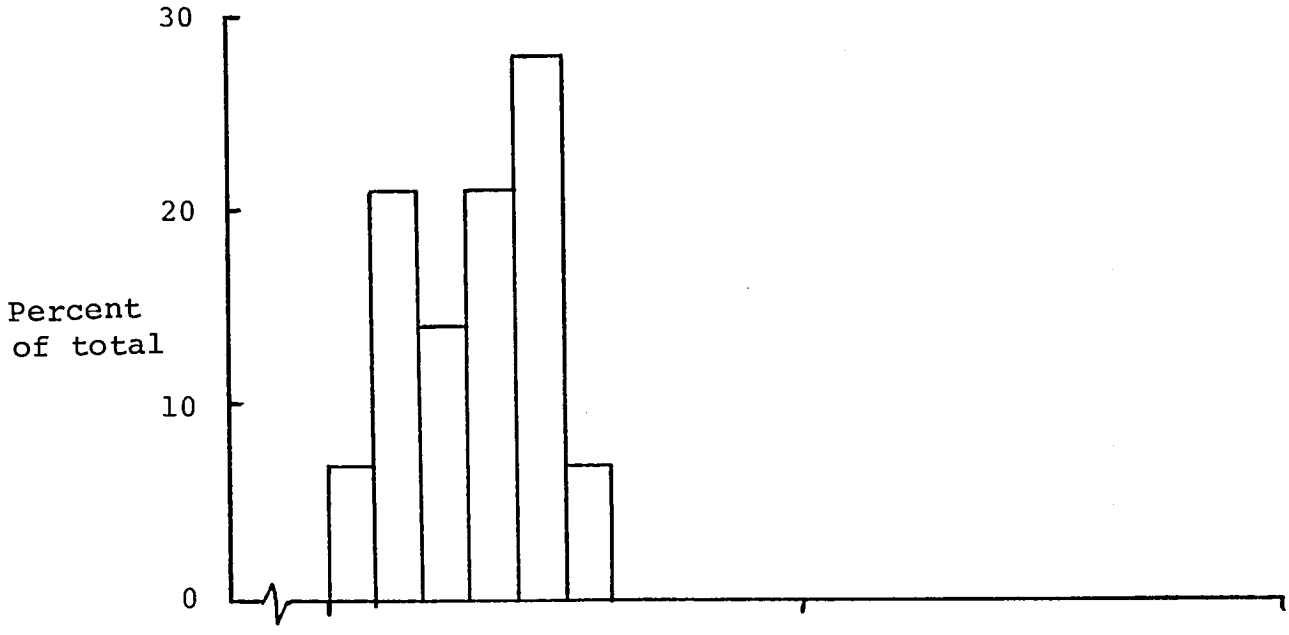

a) Virgin GY-70 fibers

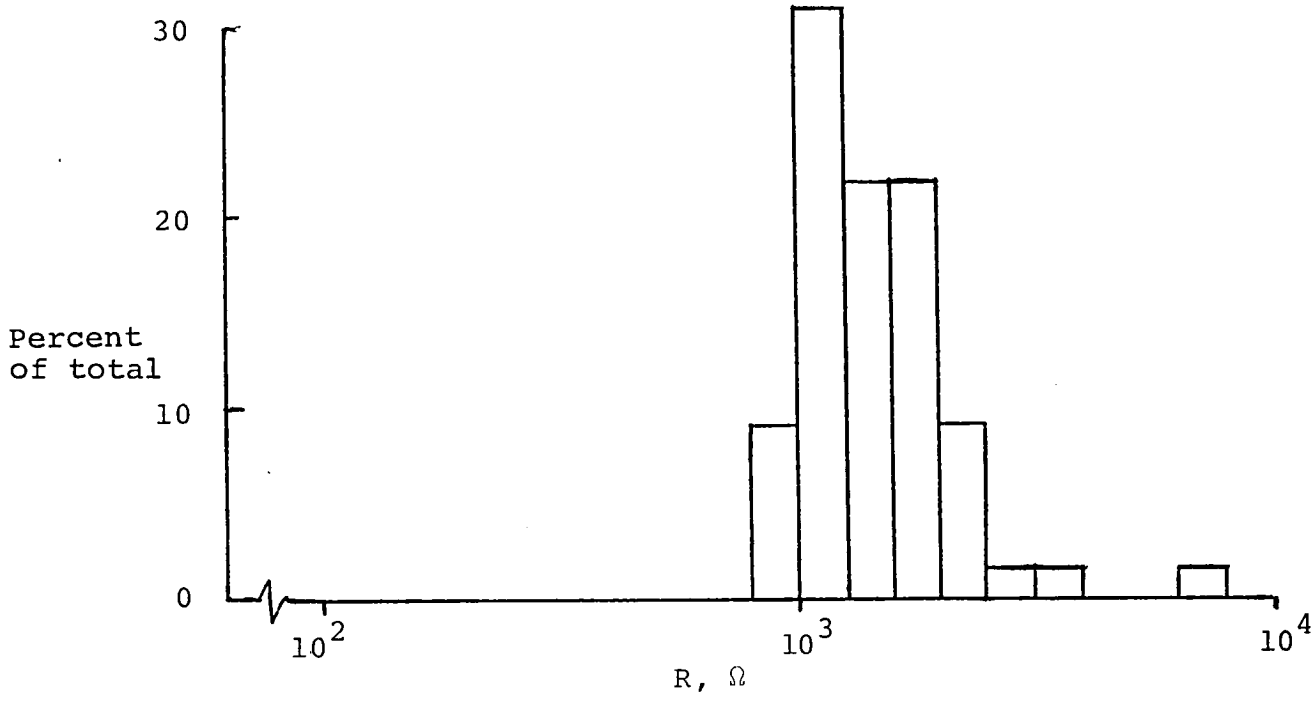

b) Virgin T-300 fibers

Figure 2.4-8 - Resistances of virgin fibers 2 mm long

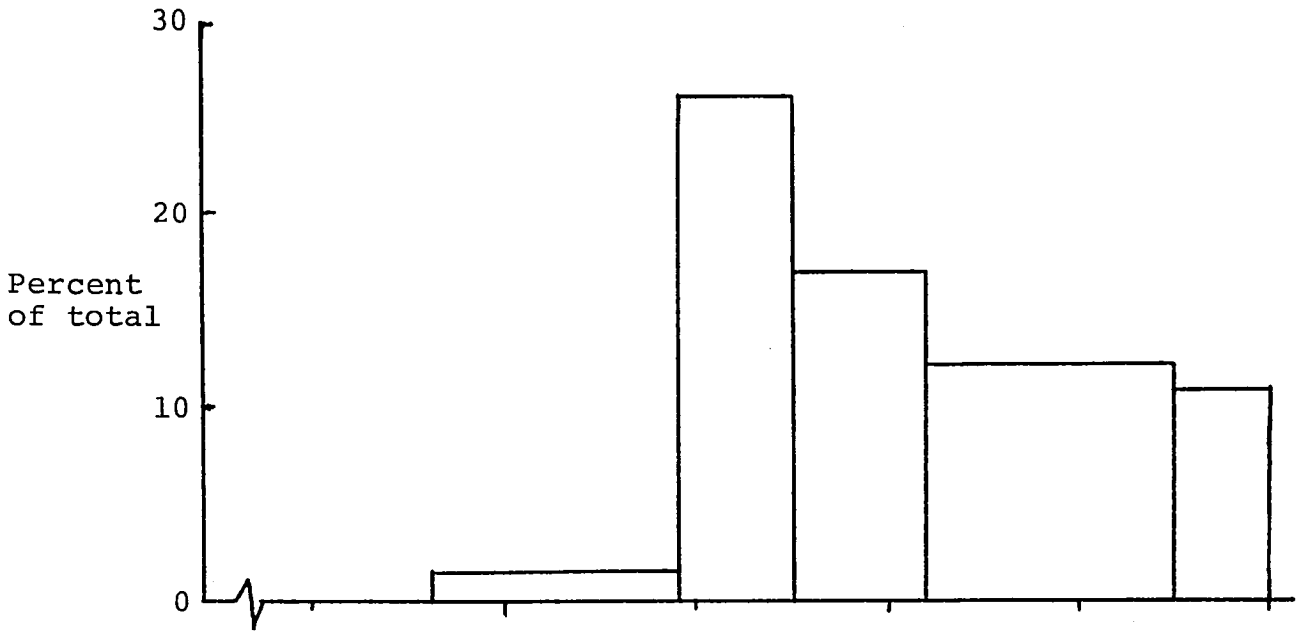

a) Oven-burned fibers

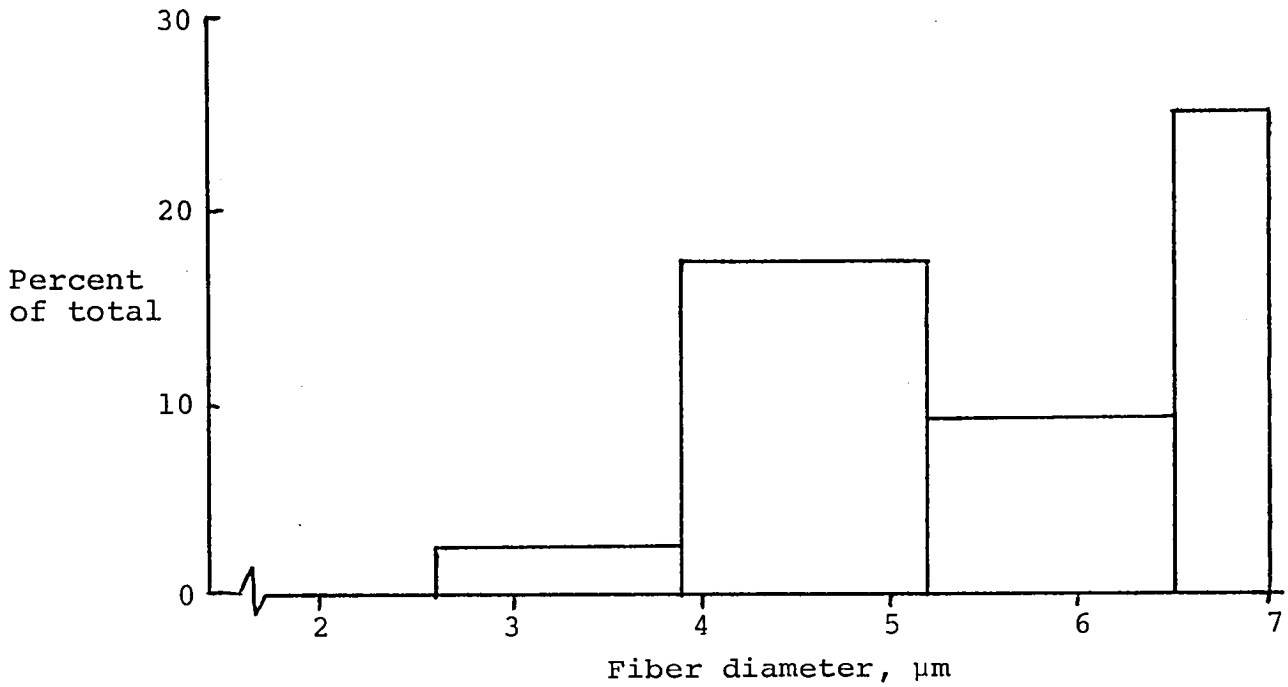

b) Fibers collected after Dugway fire

Figure 2.4-9 - Diameters of burned fibers. (Data were gathered in bin sizes shown, but values have been normalized to 0.5 μm bin size.)

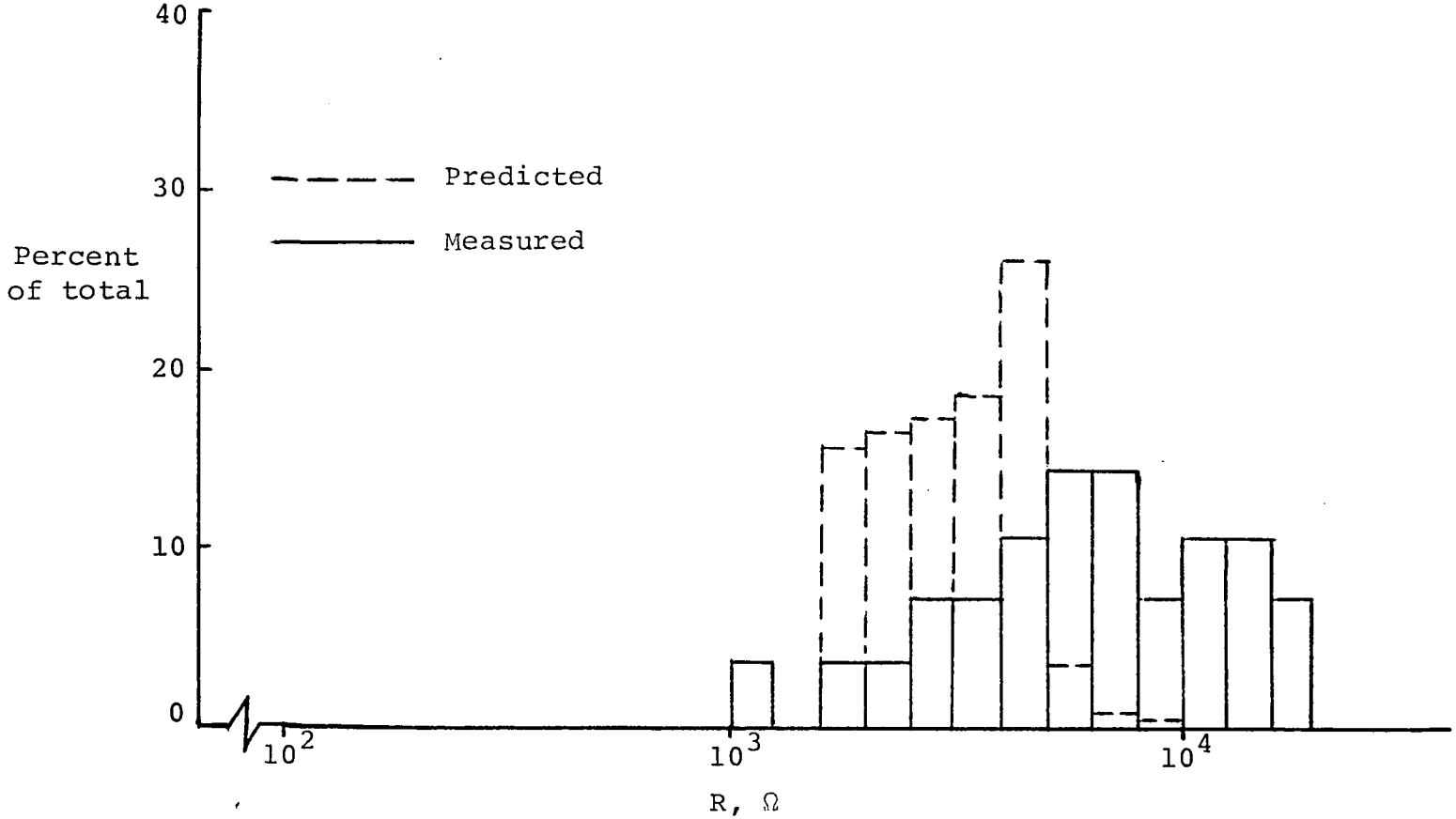

Figure 2.4-10 - Measured and predicted resistances of oven-burned fibers 2 mm long

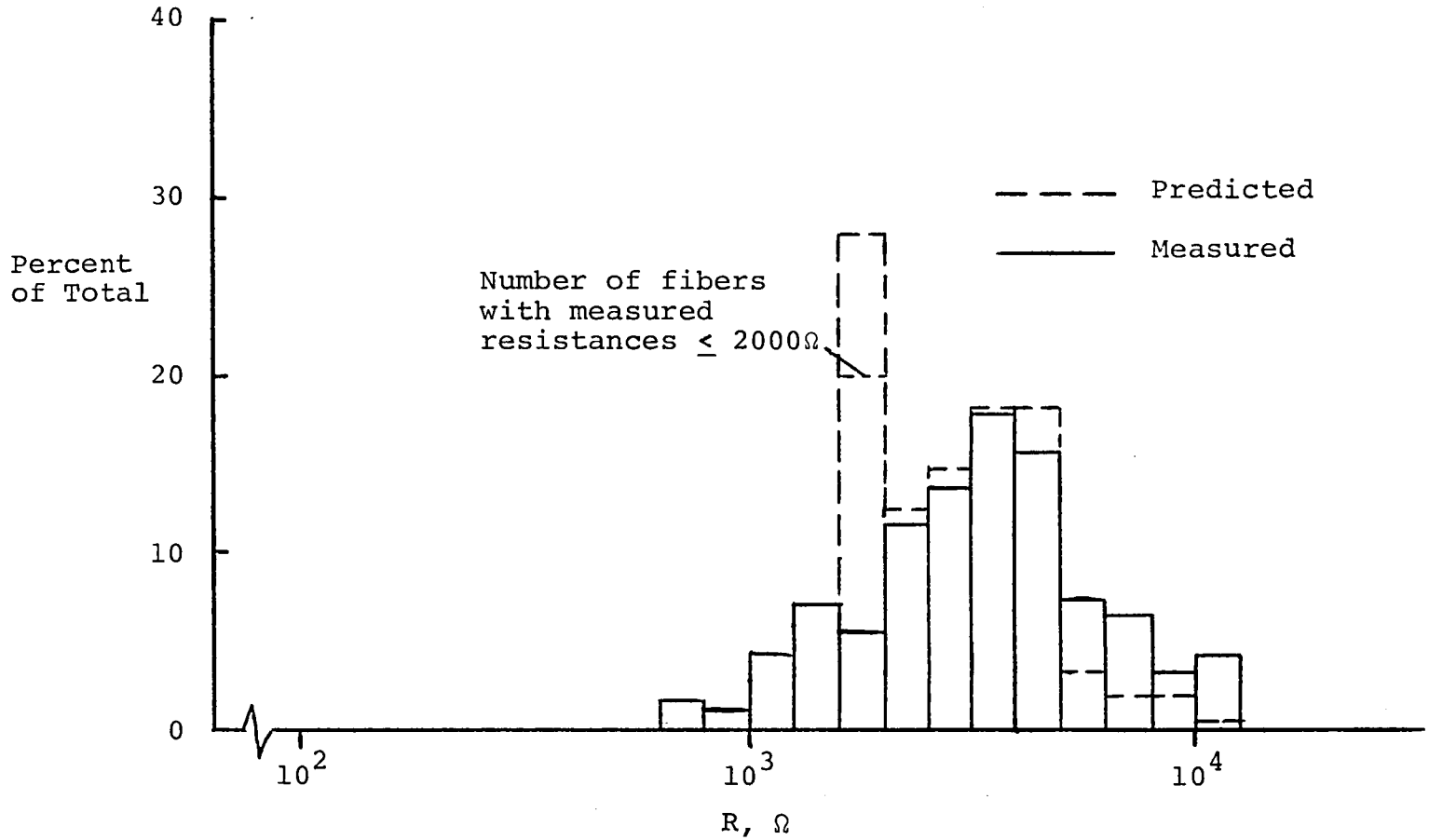

Figure 2.4-11 - Measured and predicted resistances of 2-mm-long fibers collected after Dugway fire

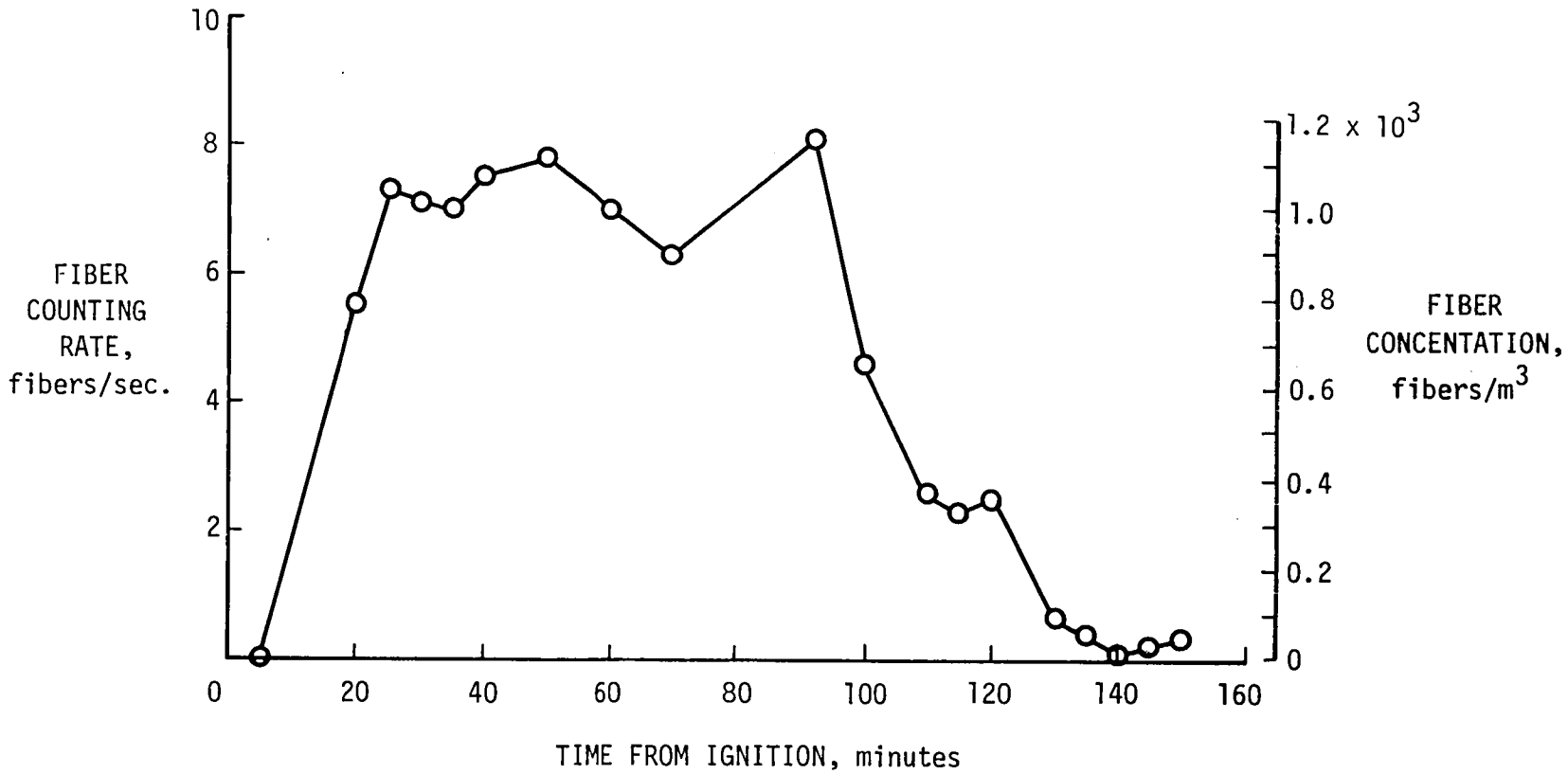

Figure 2.4-12 - Fiber concentration in Dahlgren test #53

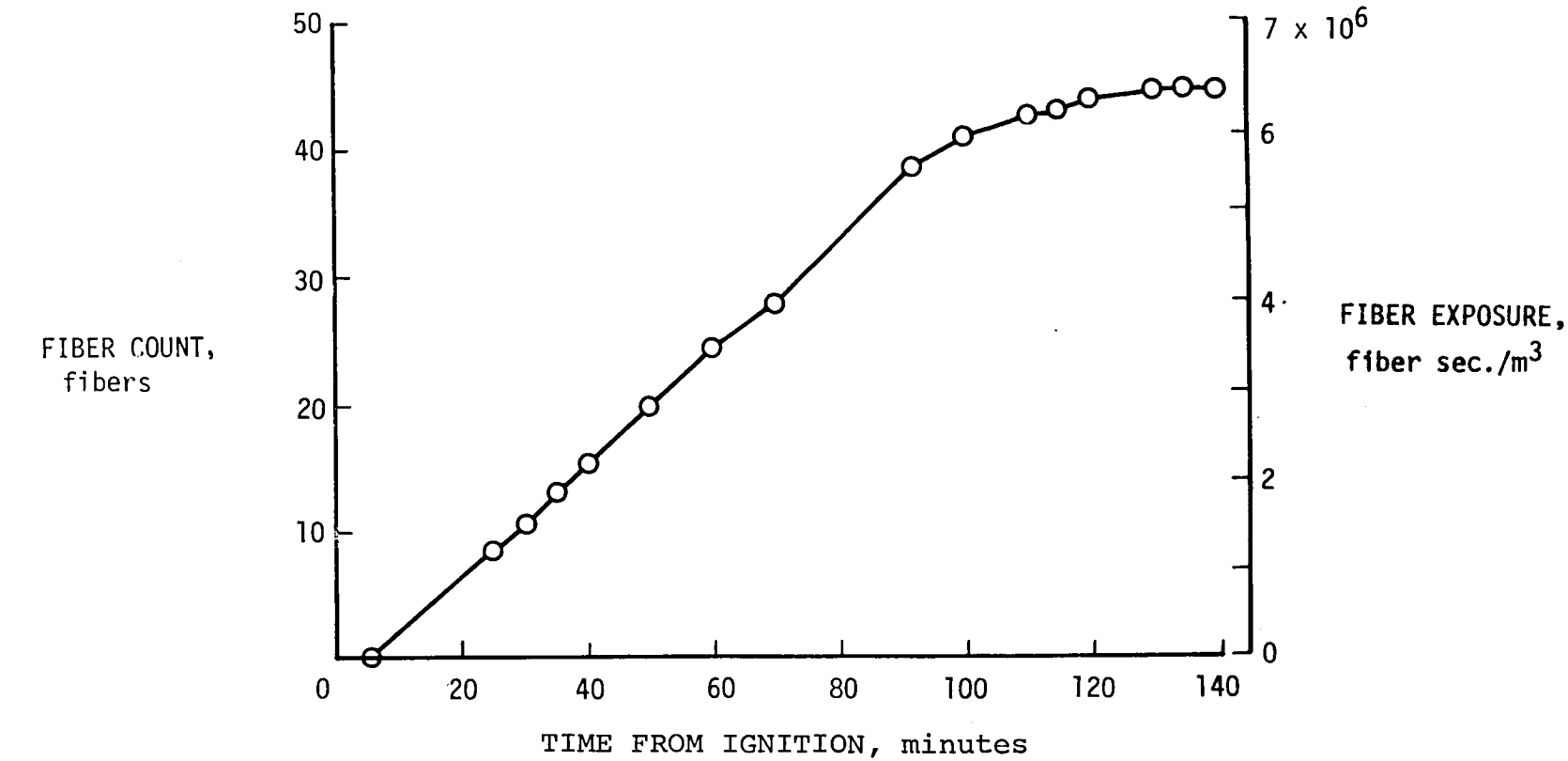

Figure 2.4-13 - Fiber exposure in Dahlgren test #53

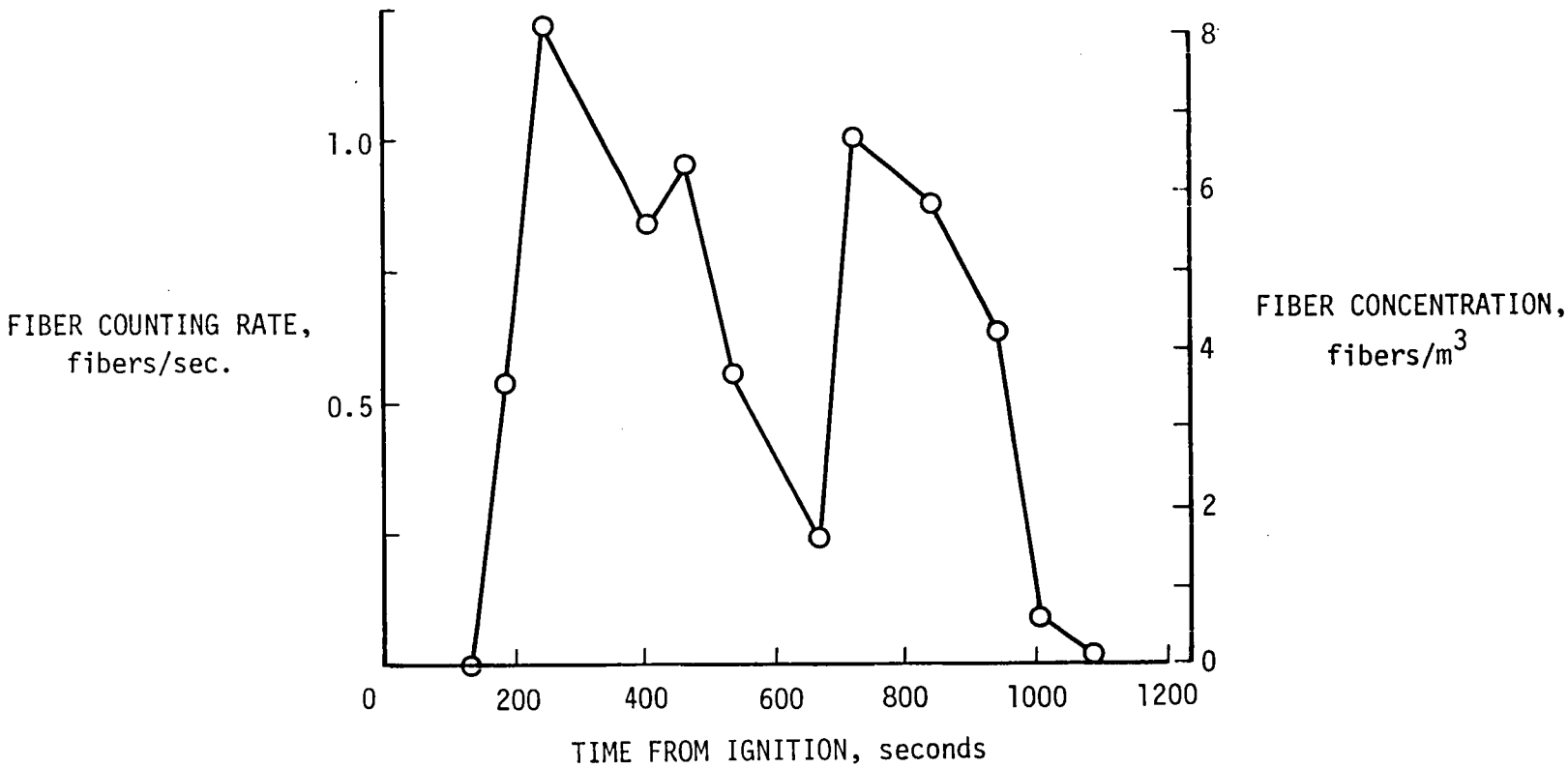

Figure 2.4-14 - Fiber concentration in Dugway test D-1, grid 2

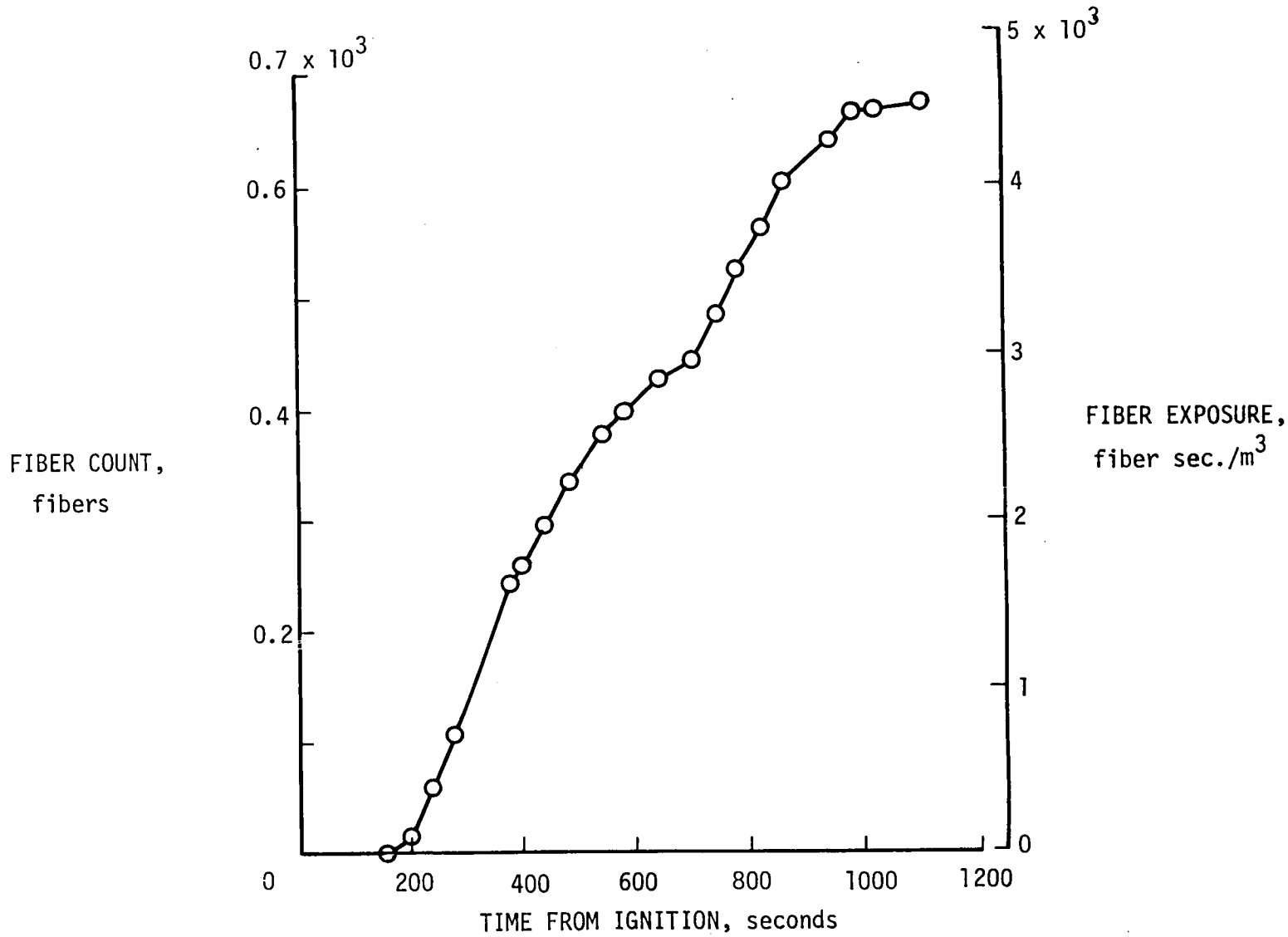

Figure 2.4-15 - Fiber exposure in Dugway test D-1, grid 2

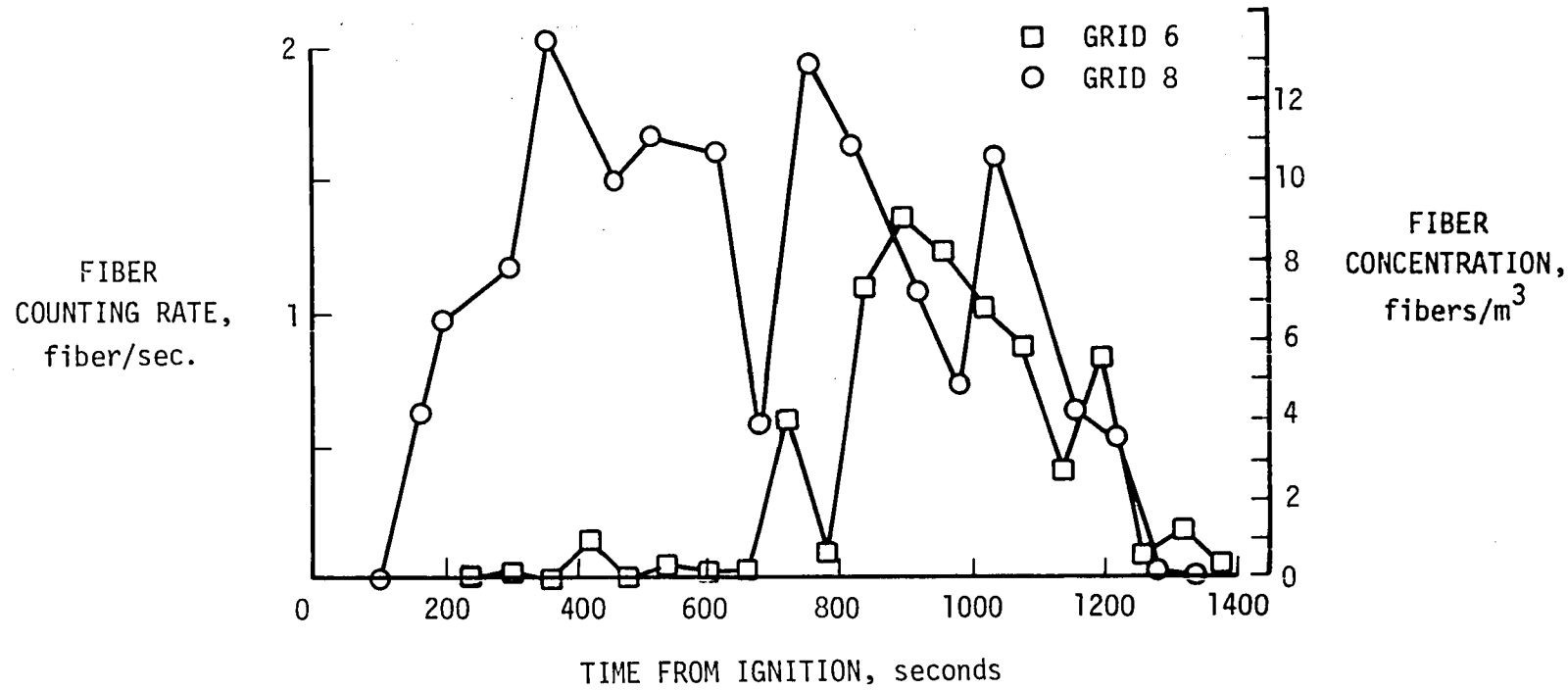

Figure 2.4-16 - Fiber concentration in Dugway test D-2

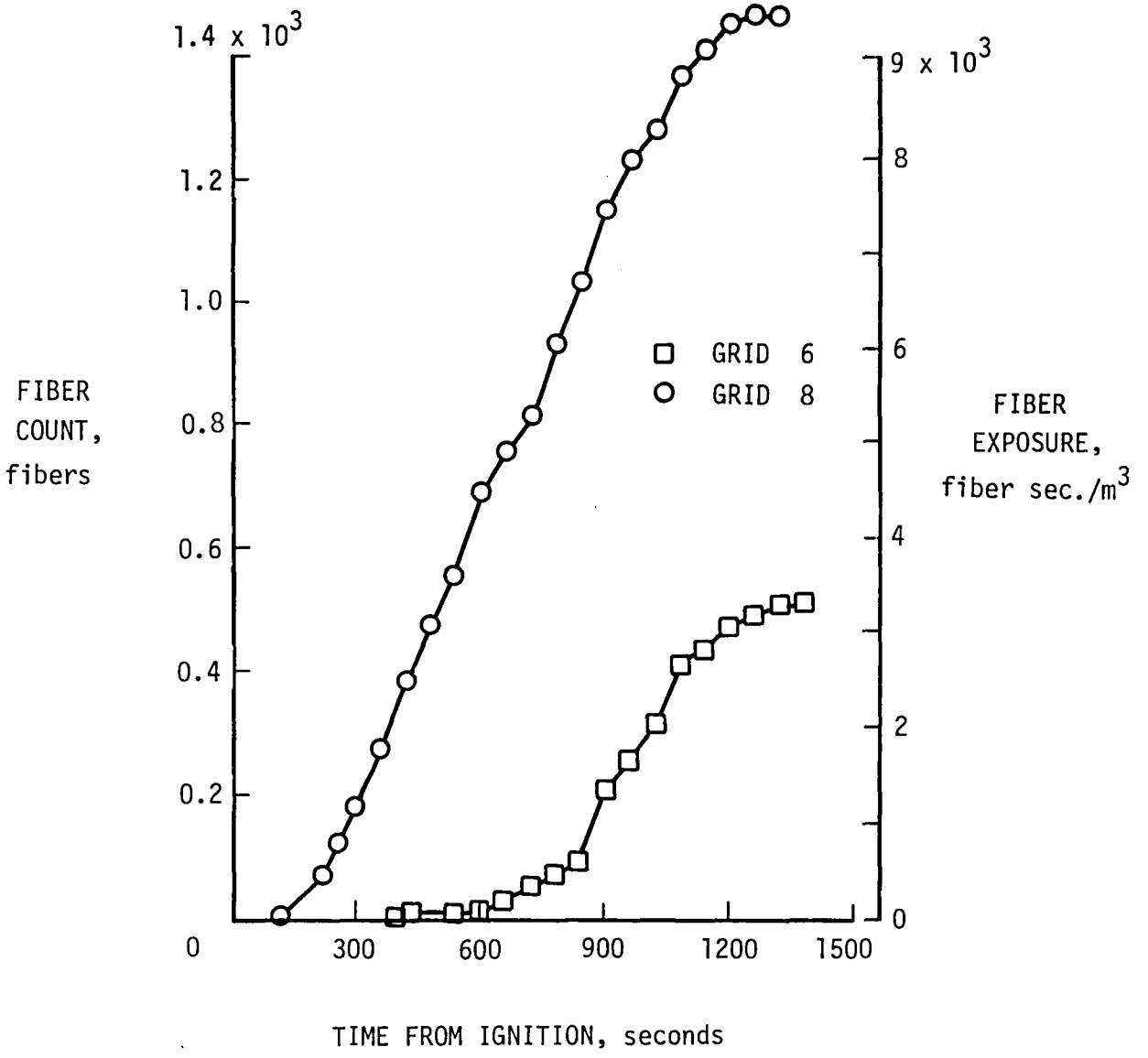

Figure 2.4-17 - Fiber exposure in Dugway test D-2

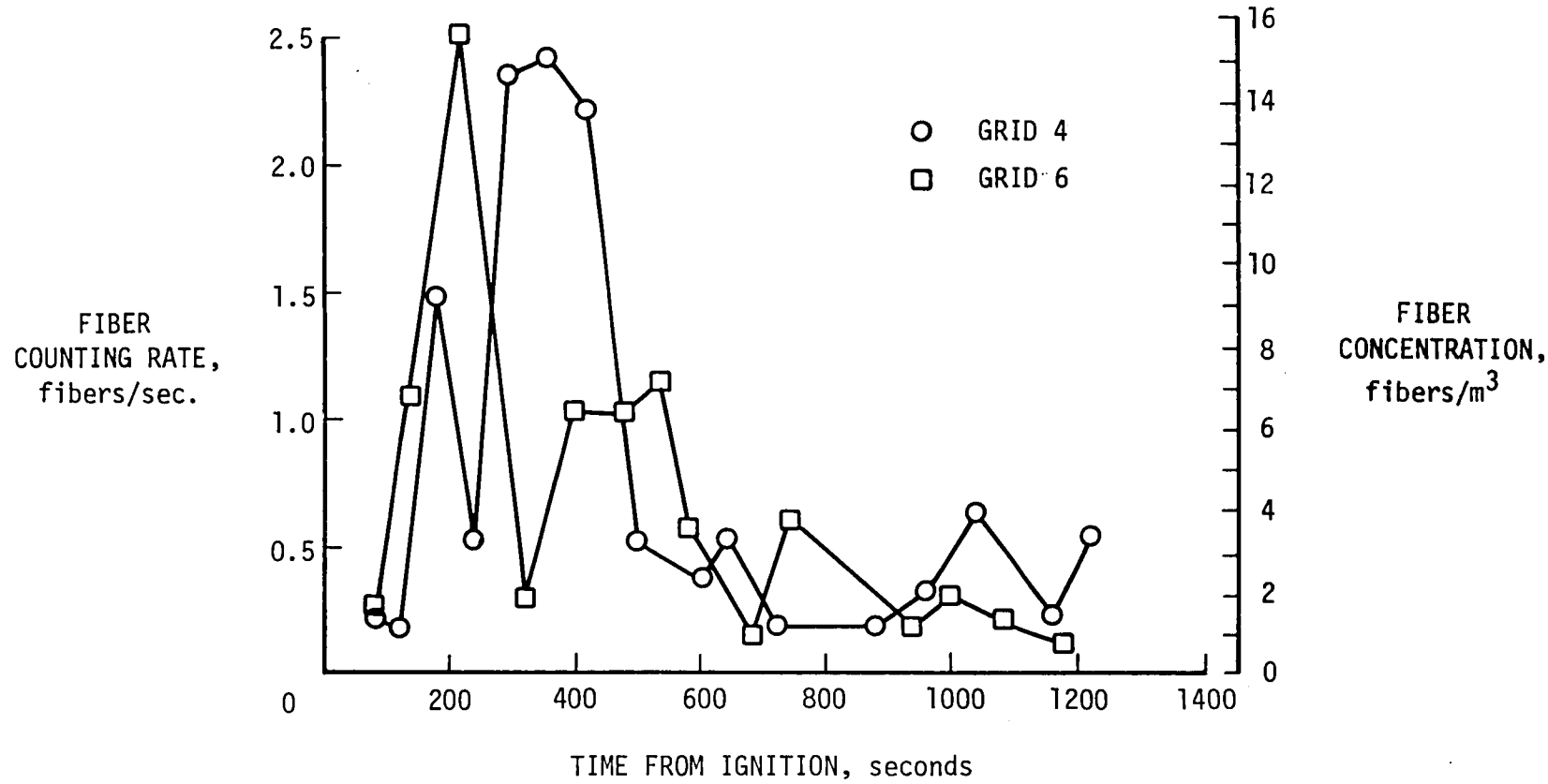

Figure 2.4-18 - Fiber concentration in Dugway test D-3

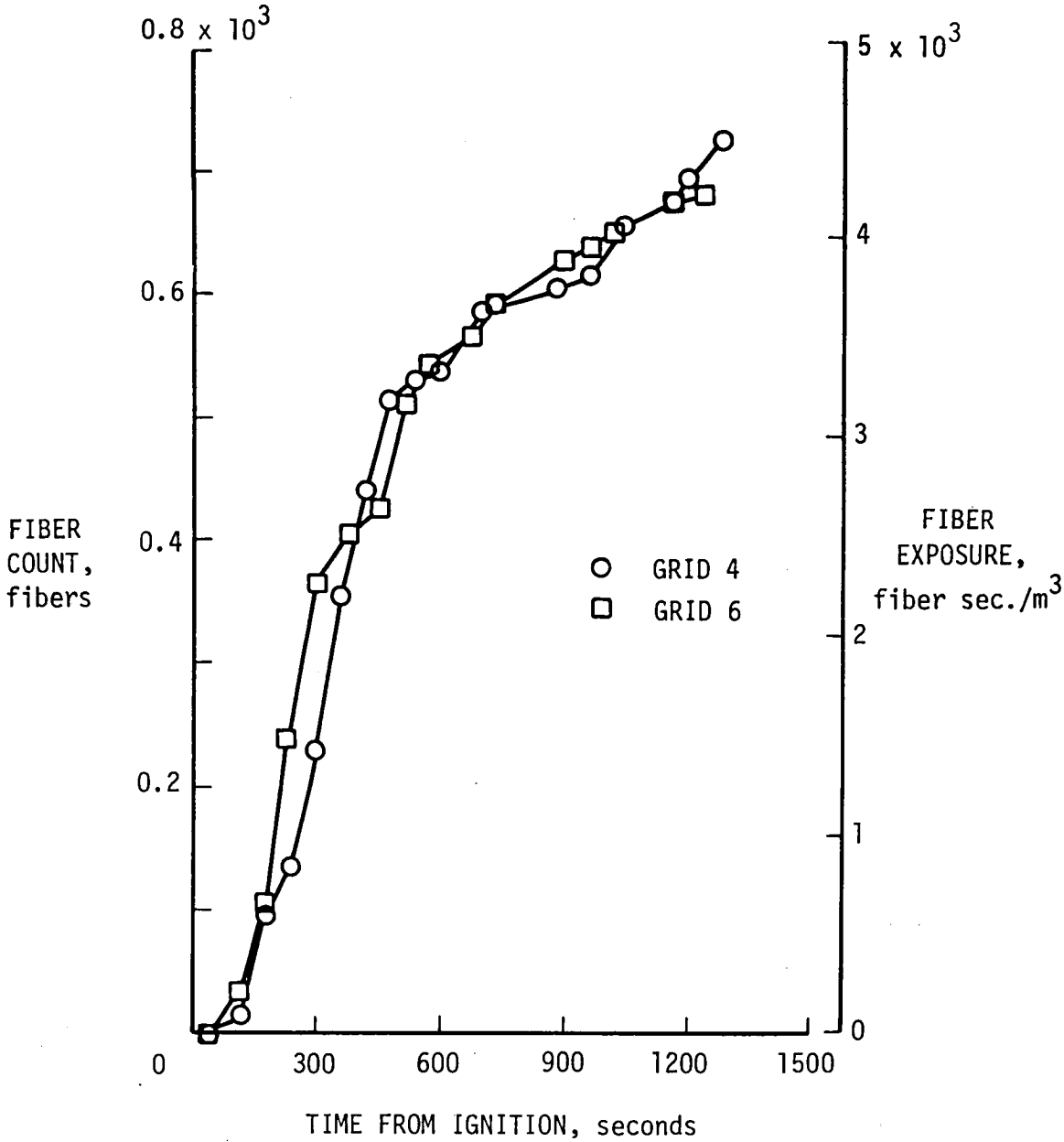

Figure 2.4-19 - Fiber exposure in Dugway test D-3

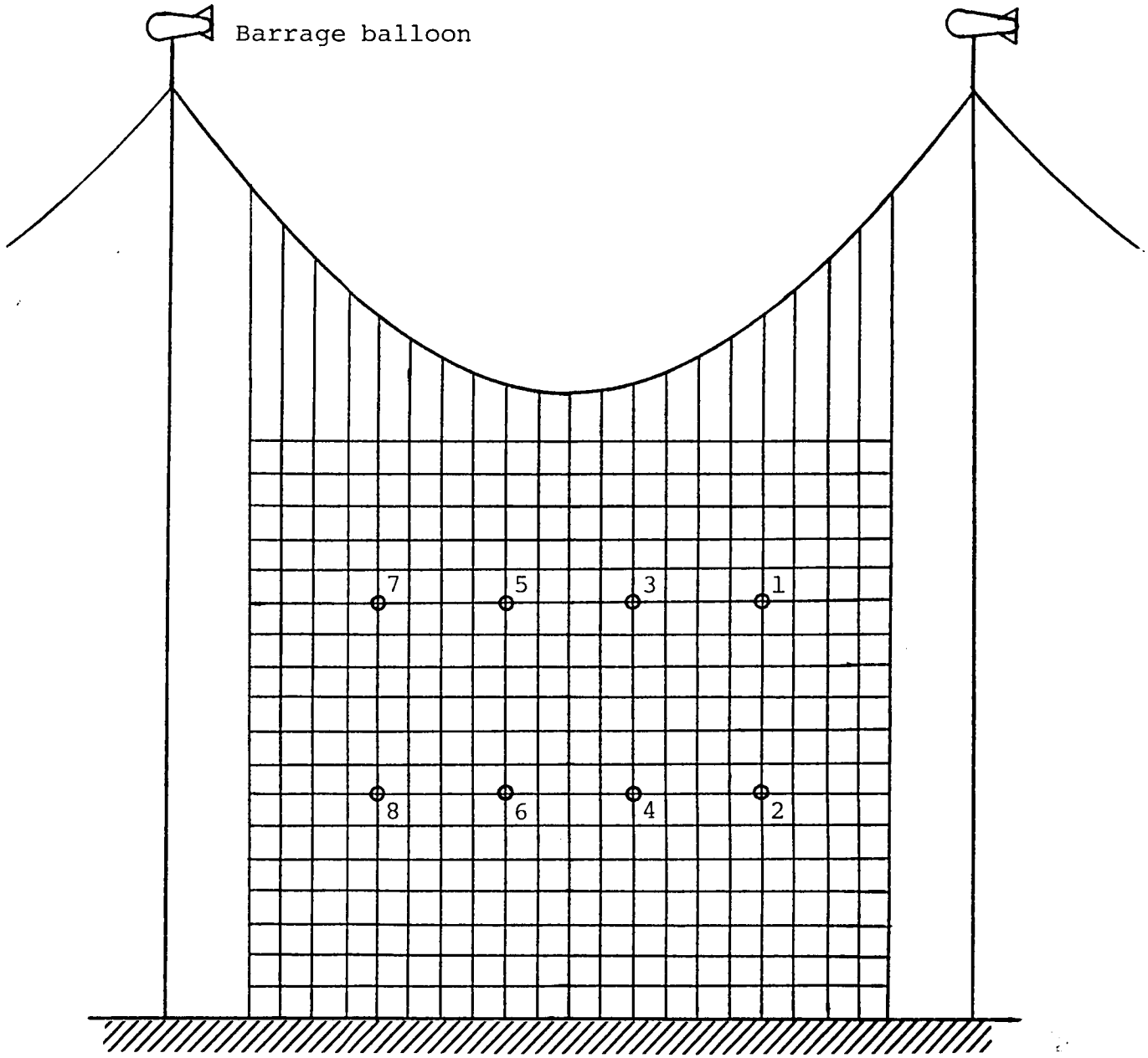

Figure 2.4-20 - Location of Charged Grids on Sampling Net, Dugway Fire Tests

REFERENCES

2-1 Newcomb, Arthur: Carbon Fiber Exposure Test Facility and Instrumentation. NASA TM 80220, 1980.

2-2 Pride, Richard A.; McHatton, Austin D.; Musselman, K.: Electronic Equipment Vulnerability to Fire-Released Carbon Fibers. NASA TM 80219, 1980.

2-3 Pride, Richard A.: Large Scale Carbon Fiber Tests. NASA TM 80218, 1980.

2-4 Morrissey, L. A.; Braunan, W. I.; and Thompson, S. C.: Calibration of BRL Ball and Sticky Cylinder Detector Systems. ARBRL-TR-02079, Ballistics Research Laboratories U. S. Army, June 1978.

2-5 Bucher, W. P.: On the Phenomenon of Current Pulses Generated by Conductors Near Contact in Electric Fields. Ballistics Research Laboratories Report No. 1951, December 1976.

2-6 Solomon, L. L., Trethewey, John D.; Bushnell, Melvin J.: Evaluation of Clouds of Airborne Fibers. U. S. Army, Dugway Proving Ground Army Science Conference Proceedings, Volume III 18-21, June 1974 Defense Documentation Center No. AD 785-672.

2-7 Anon: Assessment of Carbon Fiber Electrical Effects. NASA CP-2119, 1979.

Section 3

FIBER RESISTANCE EFFECTS ON ELECTRONIC EQUIPMENT VULNERABILITY

Tests using a fiber simulator probe (ref. 3-1), were conducted on a number of electronic devices to determine the effect of fiber resistance on the vulnerability of the equipment to damage by carbon fibers and, in particular, to assess their vulnerability to damage by Thornel 300 fibers, which is commonly used in aircraft structural composites. The testing consisted of bridging across adjacent circuit nodes with shunts that simulated each of four fiber resistance levels. After making appropriate resistance corrections for variations in gap distances between nodes, the relationship between fiber resistance and numbers of malfunctions occurring in a device was determined. The fiber simulator probe used in the testing simulated the combined effect of fiber contact and bulk resistances. The resistance was adjustable to simulate different types and lengths of carbon fibers. The fiber simulator provided fiber burnout simulation when a predetermined voltage level for each resistance level was exceeded.

A stereo power amplifier, a television receiver, a microcomputer and several smoke detectors were tested. Except for the smoke detectors, the devices had previously been subjected to carbon fiber exposure tests by the Ballistics Research Laboratory (ref. 3-2). The devices were selected for testing because they were considered representative of generic equipment types. The probe tests are discussed in the following sections.

3.1 STEREO POWER AMPLIFIER

The amplifier was a two-channel fan-cooled audio power amplifier employing silicon semiconductors and conventional printed circuit boards. Figure 3.1-1 is a photograph of the device. A number of these units were also used in the exposure tests covered in section 4.

The amplifier was energized for the tests and provided with a sinusoidal input signal of 1.6 volts at 1 kHz. The output of each of the channels of the amplifier was fed to a 100-watt light bulb. An oscilloscope was used to monitor the output voltages of each channel. Malfunction was considered to have occurred if the output voltage changed by more than 40% from nominal output.

The amplifier was probed with resistances of 10k, 3k, 1k and 0.4k ohms. The only area which caused amplifier malfunctions when probed was the printed circuit board, figure 3.1-2. The printed circuit board for each of the two identical channels of the amplifier contained 181 nodes. Each node in one of the channels was shunted to an adjacent node or circuit trace. The number of malfunctions occurring at the various resistance levels are tabulated

below.

Simulated fiber resistance, ohms	10k	3k	1k	0.4k
Number of shunted node pairs causing malfunctions	19	36	51	54

The data were plotted on semi-log graph paper as the number of shunted node pairs causing malfunction versus shunt resistance, as shown in figure 3.1-3.

For reference, the effective resistance of several materials was calculated. In figure 3.1-3, the labeled horizontal lines show the resistance of the indicated material over the range of fiber length of 3 mm and 7 mm. This range was characteristic of the spacing between nodes or between nodes and circuit traces for this amplifier. The range of resistance for each material is shown on the resistance axis. For multiple fibers bridging a gap in parallel, the minimum and maximum resistance for each material may be divided by the number of fibers to predict the expected number of malfunctions. Table 3.1-1 gives these results in tabular form for single and double fibers.

The results of the fiber simulator probe tests were compared with the results of carbon fiber exposure tests conducted by the Ballistics Research Laboratory using Thornel 300 fibers (ref. 3-2) and with carbon fiber exposure tests using DG-114 fibers. The DG-114 tests were conducted by the Bionetics Corporation for this comparison in the NASA carbon fiber exposure test facility (ref. 3-1). Critical exposure levels for 3-mm fiber lengths were 2.5×10^6 fiber seconds/meter^3 for the low resistance T-300 fiber and 2.48×10^7 fiber seconds/meter^3 for the high resistance DG-114 fibers. The carbon fiber exposure tests therefore confirm the effect indicated by the carbon fiber simulator tests, i.e., the power amplifier is more vulnerable by approximately an order of magnitude to the T-300 fibers than to the DG-114 fibers. This ratio is consistent with the ratio of the number of shunts causing malfunction indicated on figure 3.1-3.

TABLE 3.1-1 POWER AMPLIFIER MALFUNCTIONS CAUSED BY SIMULATED CARBON FIBERS 3 TO 7 MM LONG

Simulated Carbon Fiber Material	Number of Shunts Causing Malfunctions	
	Single-Fiber Shunts	Double-Fiber Shunts
4104	54-55	55
HMS	44-53	52-54
GY-70	41-52	50-54
T-300	30-42	40-51
DG-112	17-29	27-39
DG-114	0-7	5-17
DG-110	0	0-4

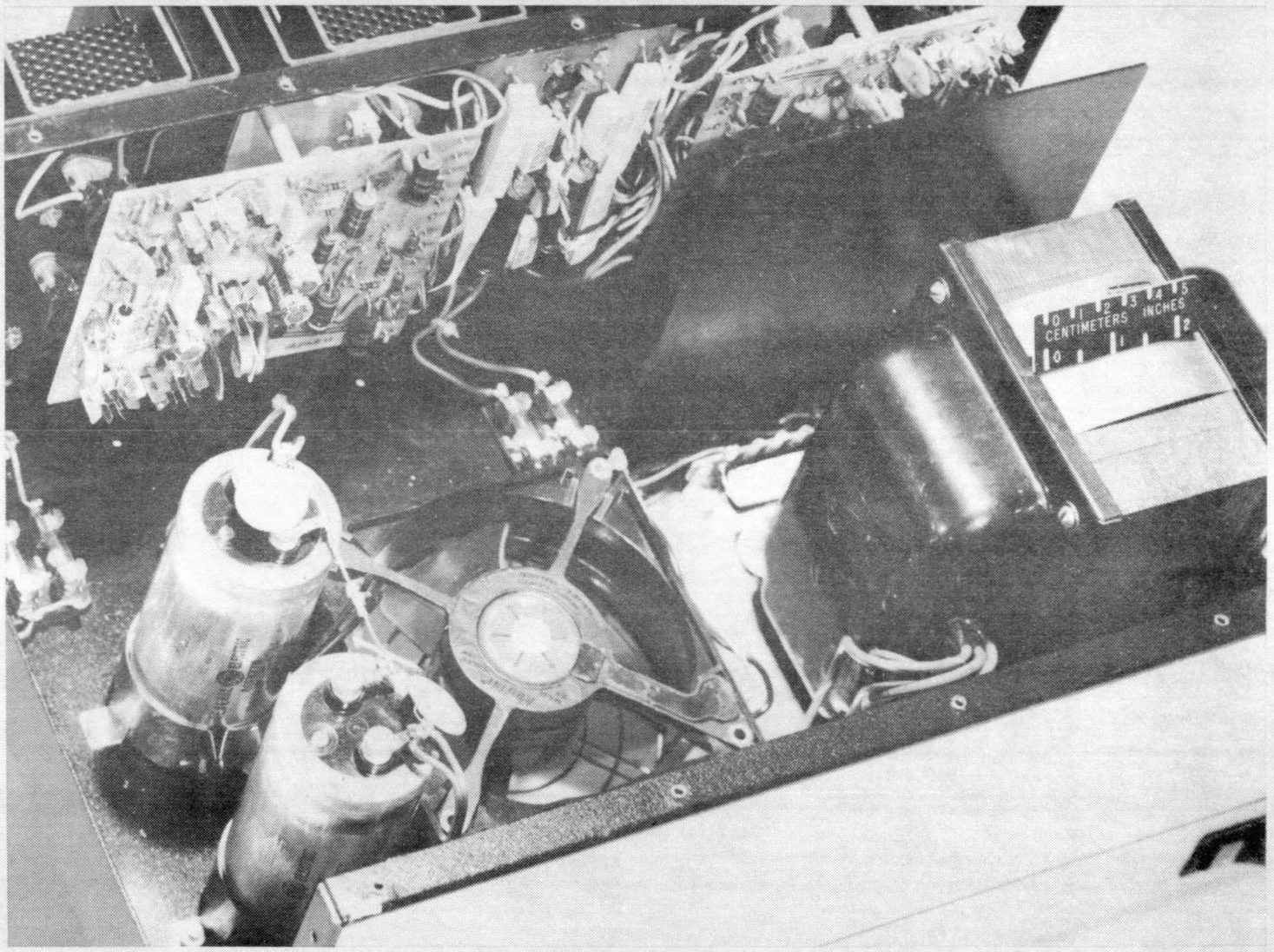

Figure 3.1-1 - Stereo power amplifier, cover removed

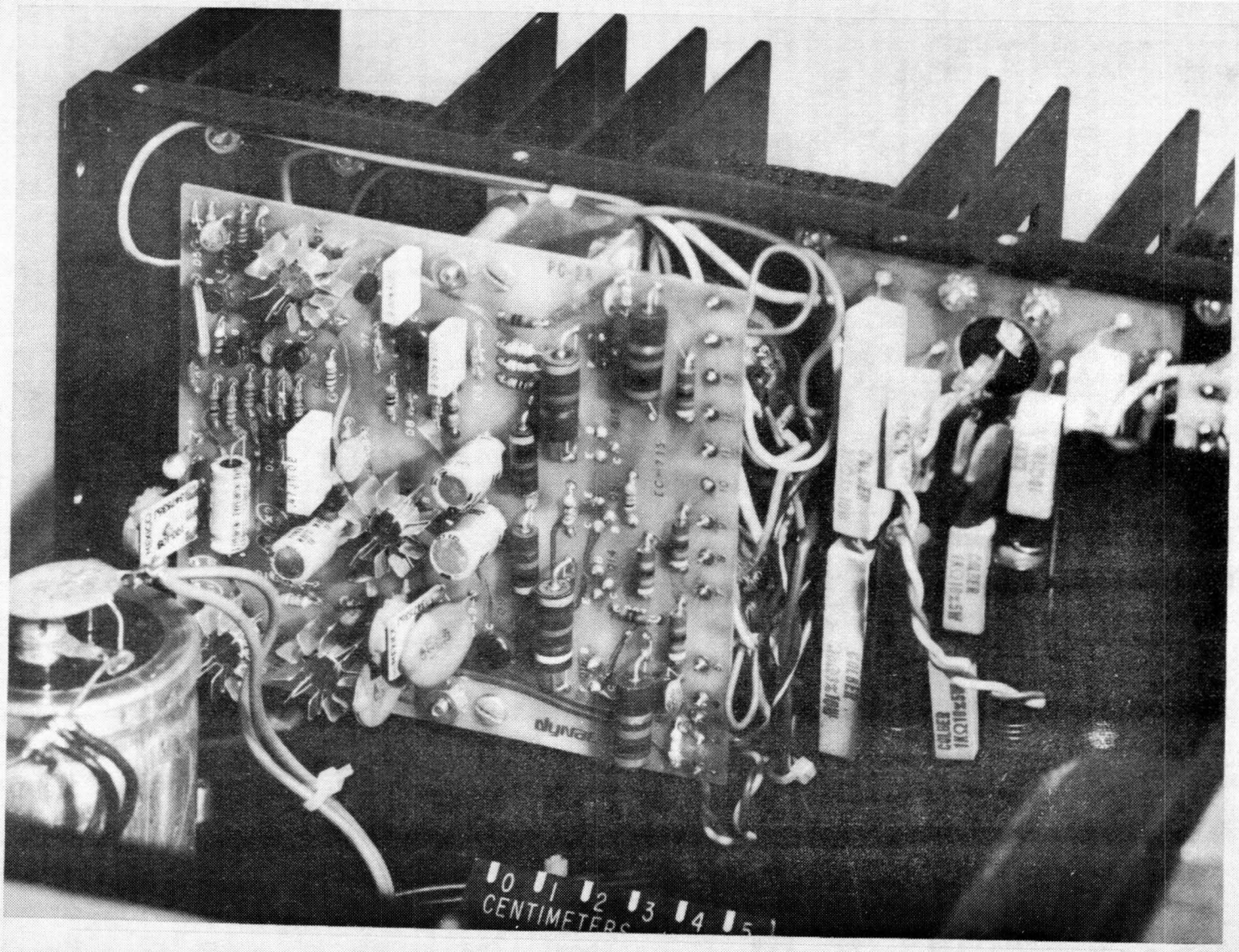

Figure 3.1-2 - Stereo power amplifier circuit board

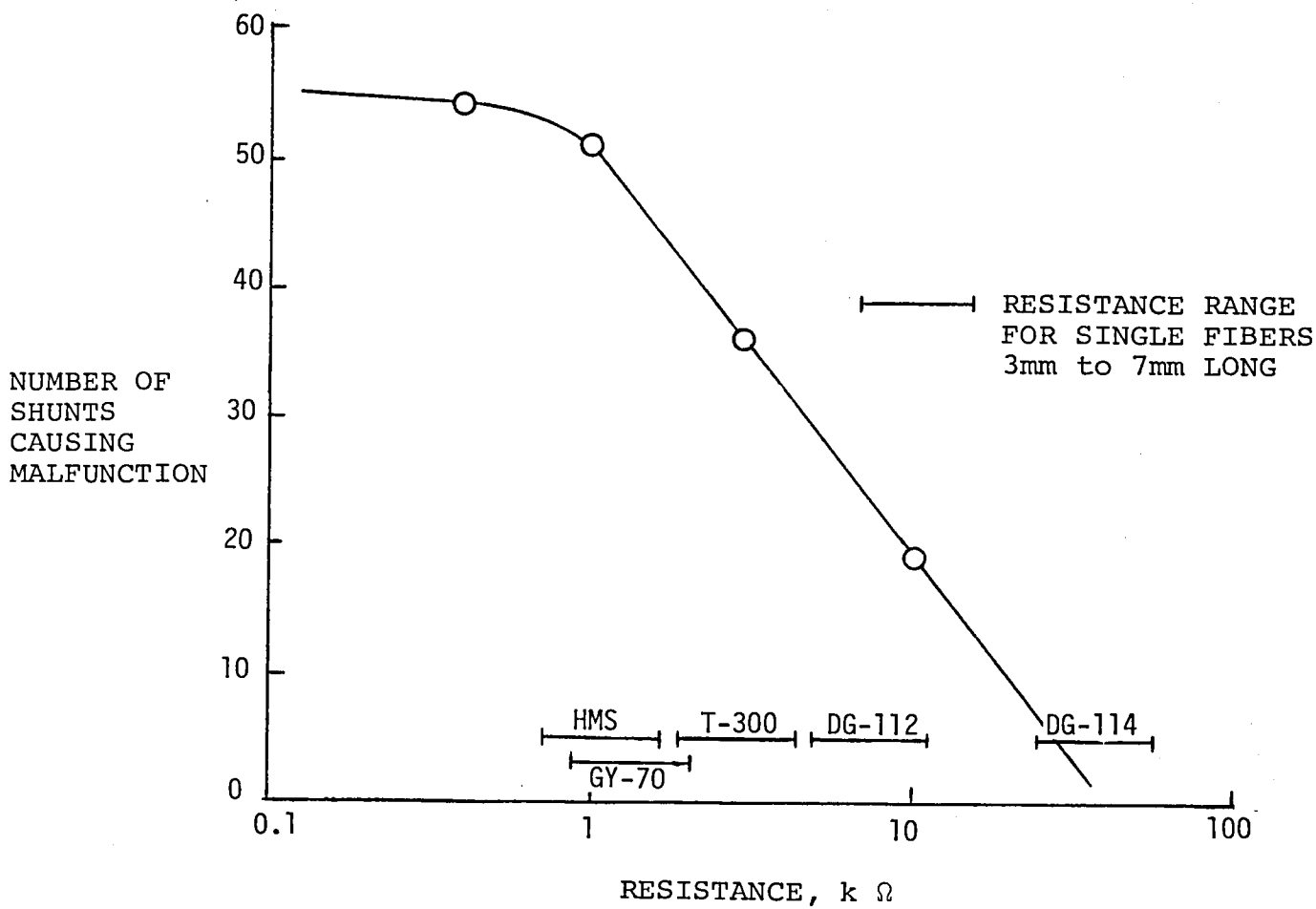

Figure 3.1-3 - Amplifier sensitivity to shunting resistance

3.2 MICROCOMPUTER

A digital computer incorporating microprocessor technology was tested using the fiber simulator probe. Figure 3.2-1 is a photograph of the microcomputer circuit board and keyboard. The following describes elements of the computer.

MPS 6502 Microprocessor Array - This microprocessor is a 40-pin device which contains n-channel, silicon-gate, depletion-type MOSFET's. It is the heart of the microcomputer and incorporates an on-the-chip oscillator and clock driver and provides signals to and connections for an 8-bit bidirectional data bus, a 16-bit address bus, two interrupts and a sync signal.

MPS 6530 Peripheral Interface Adapters (PIA) - The microcomputer utilizes two PIA's. These are 40-pin devices which utilize the same MOSFET technology as the MPS 6502. Each of the PIA's provides the system with an 8-bit bidirectional connection for direct interface from the microprocessor to the peripherals, and 10 bits of the address bus for access to the microprocessor and memory. Each PIA also contains a 1024 × 8 read-only memory (ROM) and a 64 × 8 random access memory (RAM). The ROM's contain the monitor and executive programs.

1K Random Access Memory (RAM) - An additional RAM is used which is comprised of an array of eight 1024 × 1 n-channel, silicon-gate depletion-type MOSFET memory devices. This RAM supplies data and program storage and retrieval for application programs.

The microprocessor, the two PIA's, and the eight memory devices are the basic components of this microcomputer system. They employ the only NMOS-type of devices in the system.

Keyboard and display - The keyboard has 23 keys (16 hexadecimal numbers and 7 control keys) and a slide switch for single-stepping an application program. Six 7-segment digit displays are used. During normal operation, four digits indicate the address and two digits indicate the data stored at that address.

An interval timer is utilized for the generation of time base signals. A 1-MHz crystal oscillator operates with the oscillator circuit in the 6502 microprocessor to provide the basic timing source.

The application software program provides the computer with program execution instructions. The software program is entered via the keyboard in hexadecimal numbers. For the fiber-simulator tests, the microcomputer was programmed to operate as a digital stopwatch. This program utilizes only about half the microcomputer. It was chosen for this test to permit correlation of results with

carbon-fiber exposure tests on the same type of microcomputer conducted by the Ballistics Research Laboratory (ref. 3-2).

Most of the conductive lines on the microcomputer circuit board were arranged in groups or buses as shown on figure 3.2-1. Adjacent conductors in the groups were generally connected to adjacent pins on devices such as the microprocessor, the two PIA's or the eight memory devices. Spacing between adjacent pins on the devices was 1 to 2 mm and was similar to the spacing between adjacent conductors on the circuit board. Spacings between alternate pins on the devices was 3 to 5 mm.

Fiber-simulator tests - Since the conductor and pin spacings were approximately the same and since adjacent conductors generally connected to adjacent pins on the devices, the fiber simulation tests were conducted by shunting at the pins of the devices.

Tests were made at each of four resistance levels by shunting adjacent pins and then shunting alternate pins. Since approximately the same number of malfunctions were caused whether shunting adjacent pins or alternate pins at a given resistance level, no distinction between adjacent and alternate pin shunting was made in reporting the data. Also, where pin shunting at one device was equivalent to pin shunting at another device, such as for many of the address and data bus pins, only one shunting was counted.

The data from the fiber-simulator tests of the NMOS devices (the microprocessor, the two PIA's and the eight memory devices) in which a total of 306 pairs of pins were shunted, are shown in the following table and are plotted in figure 3.2-2.

Simulated fiber resistance, ohms	3.4k	1.1k	0.43k	0.1k
Number of shunted pin pairs causing malfunctions	1	23	31	160
Percent of shunted pin pairs causing malfunctions	.33%	7.5%	10.1%	52.2%

Fiber-simulator probe testing was also done on other devices in the computer. Figure 3.2-3 lists these and the NMOS devices and shows the pin shunting resistance at or below which malfunctions occurred in the computer. For reference, the Thornel 300 fiber length corresponding to the shunt resistance is shown on figure 3.2-3 (contact resistance is not included). As can be seen, few devices would be affected by fibers in the length range (1 to 5 mm) required to bridge the pins or conductor gaps. Adding the effect of contact resistance would reduce the number of devices vulnerable to Thornel 300 fibers.

The results of BRL exposure tests using Thornel 300 fibers (ref. 3-2) indicated that the microcomputer was invulnerable at exposures up to 10^8 fiber-seconds/m^3. This suggests that contact resistance raised the effective fiber resistance above a level where disruptive shunts occur or the fibers were unable to shunt sensitive devices such as the crystal because of the small contact area offered by the devices.

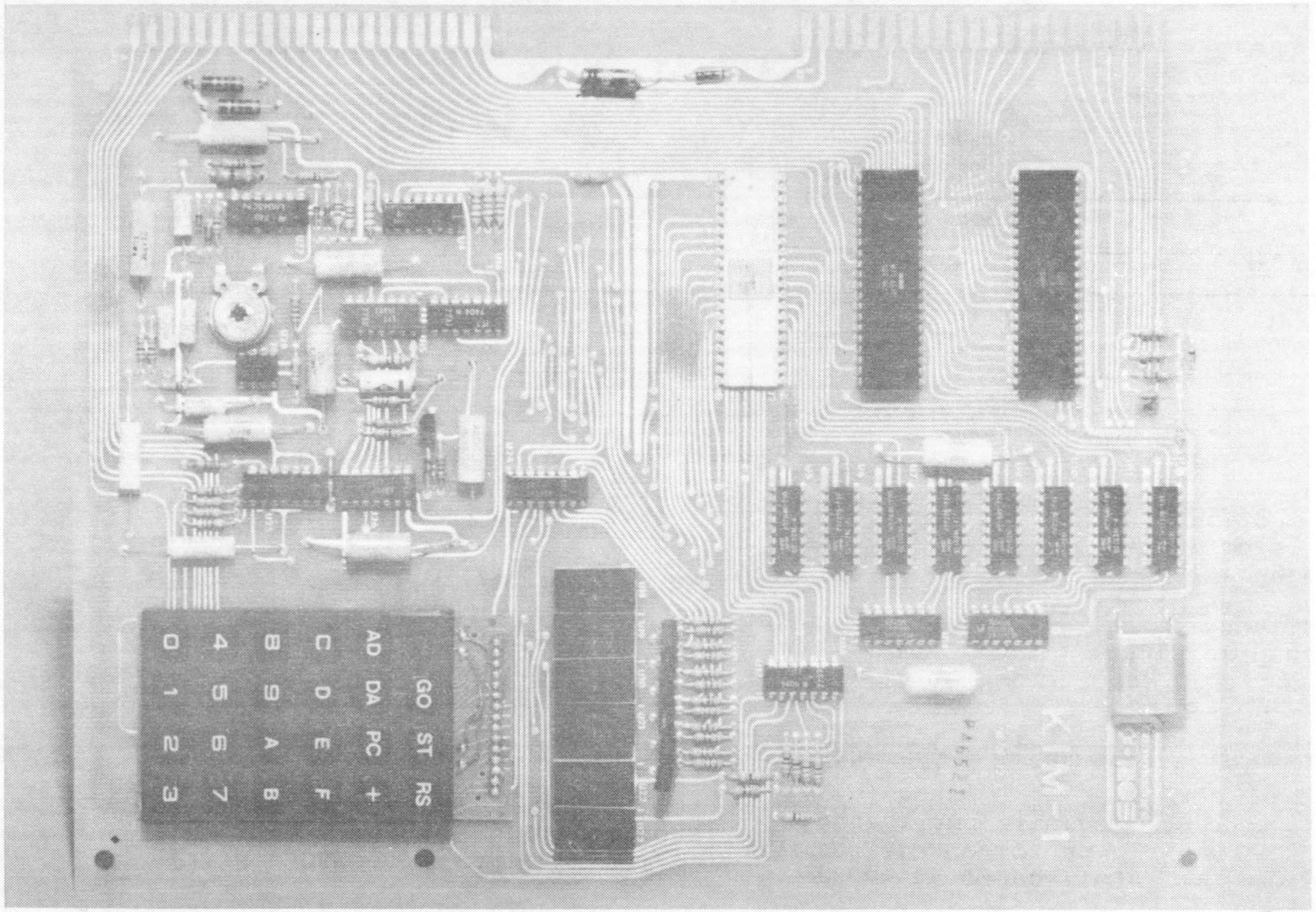

Figure 3.2-1 - Microcomputer circuit and keyboard

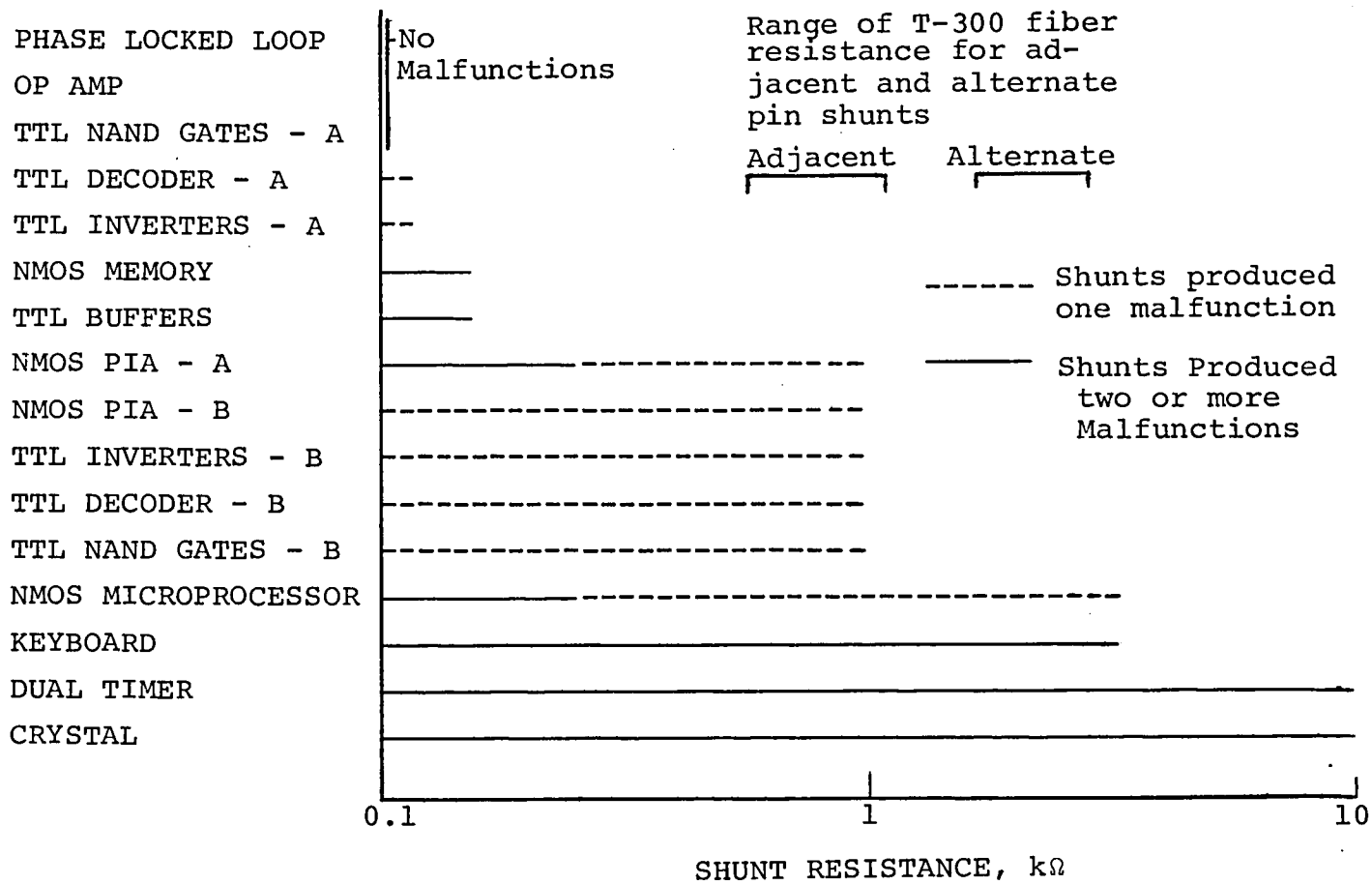

Figure 3.2-2 - Microcomputer NMOS device sensitivity to shunting resistance

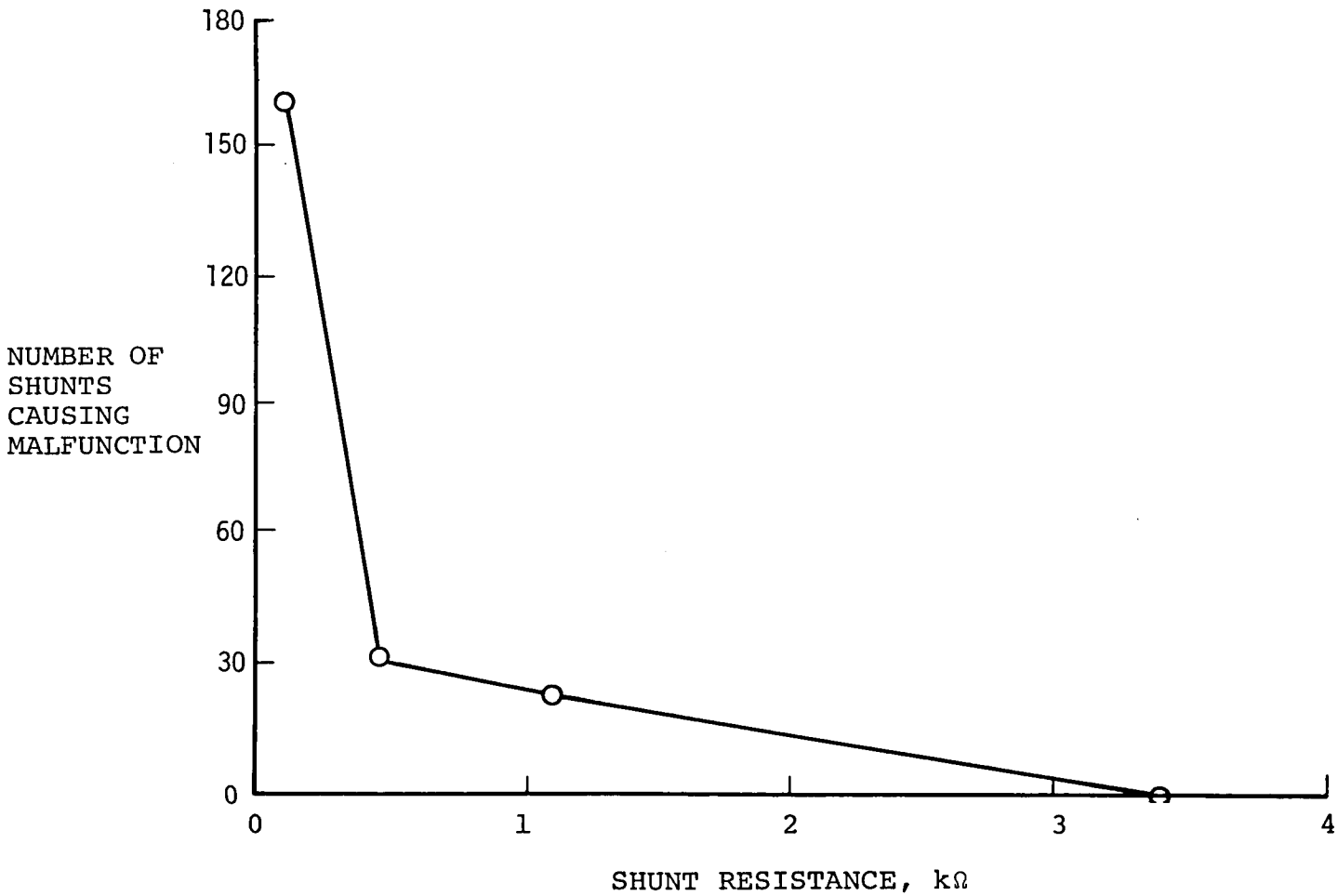

Figure 3.2-3 - Microcomputer component sensitivity to shunt resistance

3.3 TELEVISION RECEIVER

The vertical and video modules of a 19" black and white television receiver were subjected to fiber-simulator probe tests. The vertical module provides the vertical deflection signal for the cathode-ray tube (CRT) in the television receiver. This module is contained on a printed circuit board having component-pin and circuit-trace spacings 3 mm or greater. The board is mounted vertically off the main circuit board and is located directly under the ventilation slots on the back of the television set.

The vertical module was probed with the fiber simulator instrument across 47 pairs of nodes. It failed frequently at higher resistances than would be expected from a Thornel 300 carbon fiber (greater than 5 kΩ/cm). The data from this test are shown below and are plotted on figure 3.3-1.

Simulated fiber resistance, ohms	10k	3.4k	1.1k	0.1k
Number of shunted node pairs causing malfunctions	20	23	28	36
Percent of shunted node pairs causing malfunctions	42.5	48.9	59.6	76.6

The video module takes the RF from the tuner and provides the input for the sound module and the video signal for the CRT. The module is contained on a printed circuit board with component pin and circuit trace spacings 3 mm or greater. The module is mounted vertically off the main circuit board approximately parallel to and two inches from the vertical module. The video module is larger than the vertical module; however, part of the video module is covered by metal plates which shield the RF on the module.

The video module was probed with the fiber-simulator instrument across 34 pairs of nodes. Fewer nodes are accessible on this board because of the areas covered by the RF shielding. The video module had fewer failures at the high resistance than did the vertical module. The data from this test are shown below and are also plotted on figure 3.3-1.

Simulated fiber resistance, ohms	10k	3.4k	1.1k	0.1k
Number of shunted node pairs causing malfunctions	5	11	18	26
Percent of shunted node pairs causing malfunctions	14.7	32.3	53	76.5

Almost half of the shunts on the vertical module caused malfunctions at 10K ohms or less resistance whereas only 15 percent of the shunts on the video module caused malfunctions at this resistance. For the node spacings in this receiver, about 28 node pairs were sensitive in the vertical module compared to 18 node pairs on the video module in the resistance range of Thornel 300 fiber.

BRL exposed this complete television receiver to Thornel 300 virgin carbon fibers (ref. 3-2). The vertical module failed six times out of the nine exposures and the video module failed one time out of nine exposures. No other failures occurred in the receiver. The BRL tests confirm the higher likelihood of vertical-module failures which was indicated by the fiber simulator tests.

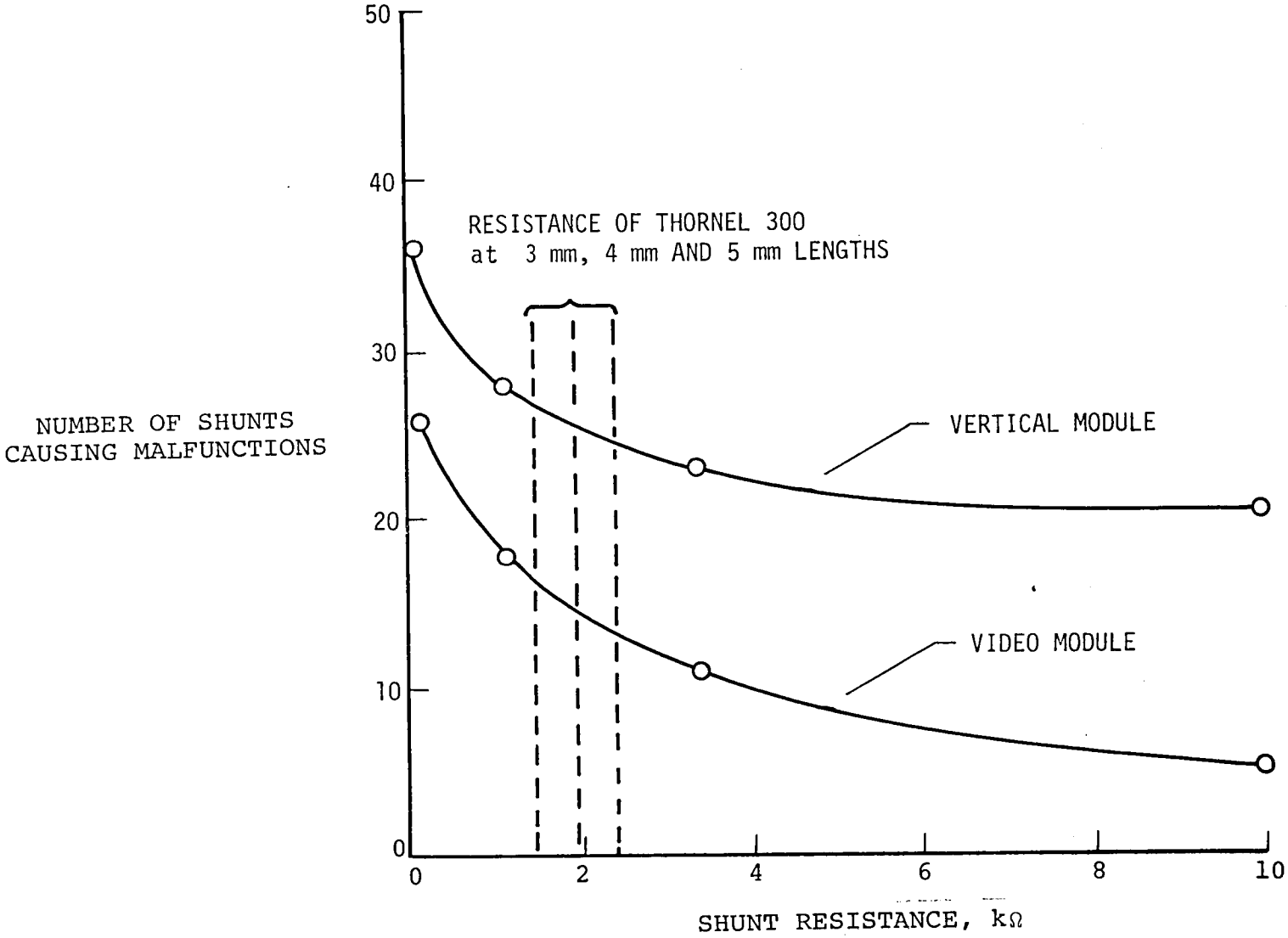

Figure 3.3-1 - Television receiver module sensitivity to shunting resistance

3.4 SMOKE/FIRE DETECTORS

Several ionization-type smoke detectors were tested with the fiber simulator. In addition, a photoelectric-type smoke detector was examined for vulnerability to carbon fibers.

Photoelectric-type smoke detectors contain a light source that sends a beam of light through a light-tight chamber to a collector. A photocell is positioned to see no light as long as the air is clean. When smoke enters the sensing chamber, the light beam is reflected or scattered. Part of the reflected light is sensed by the photocell which triggers the alarm.

Ionization smoke detectors contain a chamber of ionized air which conducts a small electric current. The ionization energy source is usually 2 to 4 microcuries of Americium 241. A voltage applied across two electrodes in the sensing chamber causes a small current to flow through the ionized air. When smoke enters the sensing chamber, the ions attach themselves to the smoke particles instead of the air particles. The ionized smoke particles move much more slowly than ionized air particles, decreasing the current flowing through the chamber. The decrease in current is sensed to trigger the alarm.

Although most smoke/fire detectors work by one of these principles, each manufacturer provides unique design features.

The arrangement of the electronics in the detectors acquired for this test program was similar. The components were mounted on the front side of a printed circuit board with conductive lines on the back side of the board. Minimum spacings between neighboring nodes were generally 3 mm. The enclosures of the electronics depended on the type of detector. The ionization-type of detectors were essentially open, permitting ready entry for almost any fiber length. The photoelectric-type of detector was very well sealed with the electronics in a chamber having a filtered air passage.

The following describes the fiber simulator tests performed on each detector. Failure of a detector to alarm in the presence of smoke while indicating an "ON" mode of operation was considered a failure of the test.

Detector "A" - This was a 9-volt battery-operated smoke and fire detector that operated on the ionization principle described previously.

All of the electronics within the detector were mounted on a single printed circuit board. This board had conductive lines on the back side and the components on the front side. The components were separated with a minimum spacing between any two

nodes of approximately 4 mm.

The data collected from this test are shown in the following table. Of 44 pairs of nodes shunted, 8 produced failures for all values of the shunt resistance.

Simulated fiber resistance, ohms	10k	3.4k	1.1k	0.1k
Number of shunted node pairs causing failure	8	8	8	8
Percent of shunted node pairs causing failure	18.2%	18.2%	18.2%	18.2%

Detector "B" - This detector operated on the ionization principle and is available in 120-volt ac or 9-volt battery-operated models. Both models were tested with the fiber simulator.

The battery-operated model was the simpler of the two models. Only two capacitors were visible on the circuit board. No failures were recorded with any value of shunting resistance down to 100 ohms.

The 120-volt AC model also had very few components, but more than the battery operated model. It, too, did not fail in these tests.

Detector "C" - This was a 9-volt battery-operated smoke and fire detector that operated on the ionization principle.

The construction of this detector was similar to that of detector "A". All of the components were mounted on the front side of a printed circuit board with the conductive lines on the back side of the circuit board. The minimum spacing between nodes was approximately 3 mm.

The data collected from this test are shown in the following table. Of the total of 51 pairs of nodes shunted, only five caused failure.

Simulated fiber resistance, ohms	10k	3.4k	1.1k	0.1k
Number of shunted node pairs causing failure	1	1	4	5
Percent of shunted node pairs causing failure	2%	2%	7.8%	9.8%

Detector "D" - This was a 120-volt ac operated detector that operated on the photoelectric principle described previously.

The construction of this smoke detector was somewhat different than for the other detectors tested. Because of the operating principle, all of the electronics were encased in a light-tight chamber. When the cover is removed while the detector is "ON", the alarm sounds and will not stop until the cover is replaced. For this reason, this detector could not be tested with the fiber simulator. Nevertheless, special note was taken of its enclosure.

The electronics were sealed very well with a filter over the portion in which the air flows. Fibers larger than 2 mm are unlikely to pass through this filter, and such short fibers would be unable to shunt any two nodes in the system without coupling multiple fibers in a single shunt. The minimum spacing between two nodes was approximately 4 mm. Thus, this unit was regarded invulnerable, and was not tested.

The shunting resistance at which failures were caused in two of the four ionization type smoke detectors tested was in the range of resistance of Thornel 300 fibers (approximately 200 ohms for 3-to 4-mm fibers).

REFERENCES

3-1 Newcomb, Arthur L., Jr.: Carbon Fiber Exposure Test Facility and Instrumentation, NASA TM 80220, 1980.

3-2 Stumpfel, Charles R.; Weaver, Calvin E.: Measured Carbon Fiber Exposures to Malfunctions for Civilian Electronic Items. ARBRL-MR-02943, 1980.

Section 4

EFFECTS OF FIRE-RELEASED CARBON FIBERS ON POWER AMPLIFIERS

As a part of its study of carbon-fiber effects on electrical and electronic equipment, NASA conducted experiments (ref. 4-2) in which carbon-fiber composites were deliberately consumed by jet-fuel fires. The experiments were performed in the shock-tube facility at the Naval Surface Weapons Center, Dahlgren, Virginia. The Bionetics Corporation supported this series of experiments by providing instrumentation that monitored the exposure rates (section 2.4 of this report), and by exposing power amplifiers to fire-released fibers in these experiments. Identical amplifiers were also subjected to virgin carbon-fiber exposure tests (ref. 4-1) and to fiber-simulator probe tests (section 3.1 of this report). This section discusses the results of the fire-released fiber tests on the amplifiers.

4.1 AMPLIFIER DESCRIPTION

The units tested were two-channel fan-cooled power amplifiers employing silicon semiconductors and conventional printed circuit boards. Figures 3.1-1 and -2 are photographs of one of the several identical amplifiers tested. This device was chosen for testing because it was considered representative of electrical/electronic equipment having greatest vulnerability to damage by carbon fibers. This judgment was based primarily on the type of circuitry and the cooling provisions. The amplifiers employ both unprotected printed circuitry and unfiltered fan cooling. The amplifier cooling fans were operated continuously during the tests rather in their normal thermostat controlled mode to insure maximum internal fiber exposure during tests.

4.2 TEST CONDITIONS

Four tests were conducted in which the power amplifiers were used. The first and second tests were soot tests in which amplifiers were operated in the smoke environment produced by the products of combustion of JP-1 fuel used in small-scale simulations of aircraft crash fires in the shock tube. Two amplifiers were tested in the first test and six amplifiers were tested in the second test. In the third test, carbon-fiber composite material was burned in the test fire, exposing six amplifiers to the carbon fiber, the smoke from the burning fuel, and the effluent from the burning matrix of the composite material. The fourth test exposed six amplifiers to the effluent from a similar test fire in which a glass-fiber composite material was burned. The epoxy matrix material of the glass-fiber composite was similar to that of the

carbon-fiber composite material burned in the third test. The first, second and fourth tests were intended to provide a basis for isolating the effects on the electronics of the fuel and composite resin products of combustion from the effects of the carbon fiber released in the third test. A summary of the amplifier test experience is contained in Table 4-1.

4.3 TESTS AND RESULTS

First soot-exposure test.- Two amplifiers were placed on the test table in the shock tube approximately 170 m downstream from a burning pool of JP-1 fuel. A fan drew the smoke plume through the shock tube and over the equipment under test. The fire lasted for approximately one-and-one-half hours with varying degrees of soot release and a peak temperature of 322 K at the amplifiers.

Both amplifiers were powered during the exposure and their outputs were fed to dummy loads drawing about 50% of the rated power. Both amplifiers operated within test specification throughout the test.

Sticky paper slides and cylinders from various positions on the test table and inside the amplifiers were compared using a light depletion technique. Soot deposition inside the amplifiers was approximately 70% of deposition outside the amplifiers.

Second soot-exposure test.- Six amplifiers were placed on the test table and operated as in the first soot test. The temperature of the airstream near the amplifiers did not exceed 330 K during the test. During the initial twenty minutes of exposure, the voltage of the common oscillator input to the amplifiers dropped 2.8%. Operation of the amplifiers was continued for 2½ hours (through fuel burnout and cool down of the facility), during which time the input oscillator voltage in one amplifier dropped 33% to 1.18 V ac. Examination indicated a fault in one channel of one of the amplifiers.

The failed unit was analyzed for cause of failure. The malfunction was traced to the existence of a negative 71 V dc at the amplifier output and a negative 30.5 V dc at the input with the amplifier energized and no input signal. Visual inspection of the channel A circuit board with a magnifying glass revealed no fiber, soot or other particles which may have caused short circuits. Voltage checks were then made which indicated that the negative dc supply voltage existed throughout the board. Based on voltage drops, the second differential amplifier was indicated as a problem area. A transistor from the second differential amplifier was replaced as were four resistors which had appeared bad in the visual check. After these replacements, the negative dc supply voltage disappeared from the output and input. However, positive dc supply voltage appeared at both output and input.

The board was again checked for voltage levels at pin and node locations. The positive supply voltage appeared to be shorted to the signal path. The board was taken out, cleaned, and brushed. The problem still remained, so the positive voltage line was broken in order to isolate the problem. This left the problem to three components which were removed, but each was found to be in good condition.

The board was then checked with a magnifying glass for particles that could be causing the short. A thin, wirelike piece of metal was found between the collector and base of a transistor. This was removed, correcting the shorting problem, but there was still a small amount of dc voltage on the output. A diode was then found to be shorted. The diode was replaced to correct the problem. The amplifier now performed within specification.

The failure probably resulted from part(s) failure and was probably unrelated to the exposure in the shock tube environment.

Soot is unlikely to have caused the malfunction because soot has generally been found to be nonconductive in the voltage ranges which exist in the amplifier system. Visual inspection did not reveal any short-circuit paths attributable to soot.

Carbon fibers may have caused the failure. Although the shock tube was washed down prior to the test, a few residual carbon fibers from prior testing may have been present during this test. However, the visual microscope inspection gave no indication of a fiber short circuit.

The wirelike piece of metal, which was found during the tracing of the later, positive voltage problem, was basic to that problem but probably not to the original problem. The metal was not found in the original microscope inspection. Also, the nature of the problem created by the wirelike metal was unlike the original problem. The piece of metal was probably introduced accidentally during removal and replacement of parts.

Fire-released carbon-fiber exposure test (test no. 53, ref. 4-2).- Six amplifiers were exposed in this test to the products of combustion of both fuel and carbon-fiber composite material. The duration of the fire was 3½ hours and 10 kg of carbon-fiber composite material were burned in the fire. The amplifiers were mounted approximately eight feet above the mounting elevation used in the soot tests in order to locate the amplifiers in a region of maximum fiber concentration in the shock tube. The ambient temperature during the test was 302 K in the region of the amplifiers. The test set-up and test observation data follow:

The amplifiers were fed by a 0.64-Vrms, 1-kHz input signal from a 10:1 attenuating buffer device driven by a 6.4-V rms, 1-kHz

oscillator. Each of the amplifiers was loaded with two 100-watt light bulbs, one for each channel. A nominal 30-V rms, 1-kHz output signal was obtained from each amplifier channel. Each amplifier channel was monitored by a sensing device which activated an LED display for output voltage changes in excess of 30% of the nominal output. The outputs were also monitored by an oscilloscope and digital multi-meter to indicate deviations in output voltages.

Test observations are contained in Table 4-1. All amplifier channels had failed permanently after 57 minutes of exposure. A few malfunctioned or failed after only 10 minutes of exposure. Sometimes a particular channel revived one or more times after malfunctioning or failing to produce a signal.

The amplifiers were returned to NASA Langley Research Center after the test and were cleaned inside and out by vacuum cleaning. They were then performance checked, using the same equipment and setup used at Dahlgren. All channels performed out of specification limits. The systems and frequency of occurrence of each were:

Malfunction	No. of channels
Positive 7.2 Vrms on output	1
Negative 56-72 V dc on output	7
No output	3
ac ripple on output	6
Low output	1

The amplifiers were repaired and returned to specification level operating condition. No specific pattern of failure was found. However, replacement of several parts was generally required to return the units to operating condition. Replacement parts included fuses, resistors, condensors, diodes and transistors.

Soot/epoxy-matrix exposure test (test no. 54, ref. 4-2).- Six amplifiers were exposed to conditions essentially identical to those in the previous carbon-fiber exposure test except that rather than burning carbon fiber composite material, fiberglass composite material was burned which contained the same type and quantity of matrix as was present in the carbon-fiber test. The test set up, including monitoring instrumentation was identical to that used for the fire-released carbon-fiber-exposure test.

Two amplifier channels were inoperative prior to and during the test. The remaining 10 channels operated within specification limits throughout the test. The output voltage deviated gradually

from nominal for the ten operational channels during the test. The final average deviation, after 200 minutes of test, was 6.2%.

4.4 CONCLUSIONS

The stereo power amplifiers tested had a low-to-negligible vulnerability to damage by soot released by burning JP-1 aircraft fuel and to soot plus the residue from burning epoxy resins such as used as matrix for structural composite materials. However, the amplifiers were vulnerable to damage by carbon fibers released from burning carbon fiber composite material. The exposure levels that caused these amplifiers to malfunction or fail are reported in reference 4-2.

References

4-1 Stumpfel, Charles R.; and Weaver, Calvin E.: Measured Carbon Fiber Exposures to Malfunction for Civilian Electronic Items. ARBRL-MR-02943, U. S. Army Ballistics Research Laboratory, 1980.

4-2 Pride, Richard A.; McHatton, Austin D.; and Musselman, K. A.: Electronic Equipment Vulnerability to Fire Released Carbon Fibers. NASA TM-80219, 1980.

TABLE 4-1 - RESULTS OF FIRE-RELEASED CARBON-FIBER EXPOSURE TEST

	Amplifier output, volts											
Amplifier No.	1		2		3		4		5		6	
Channel	R	L	R	L	R	L	R	L	R	L	R	L
Test time, minutes												
0 (ignition)	√*	√	√	√	√	√	√	√	√	√	√	√
10	√	√	√	√	√	0	√	0	39	39	√	0
15	√	√	√	√	√	0	√	0	0	√	3	3
20	√	√	√	√	√	0	√	0	0	√	√	0
25	√	√	√	√	√	0	√	0	0	√	√	0
30	√	√	√	3	√	0	0	0	0	0	√	0
35	√	√	√	√	0	0	0	0	0	0	√	3
40	√	0	√	√	0	0	0	0	0	0	√	3
45	√	0	√	√	0	0	0	0	0	0	√	3
50	√	0	0	√	√	0	0	0	0	0	√	√
55	√	0	0	5	√	0	0	0	0	0	0	0
57	0	0	0	8	16	0	0	0	0	0	0	0
65	√	0	0	7	12	0	0	0	0	0	0	0
70	√	0	0	6	2	0	0	0	0	0	0	0
75	0	0	0	0	0	0	0	0	0	0	0	0
100	0	0	0	0	0	0	0	0	0	0	0	0
130	All channels inoperative - turned all amplifiers off											
200	Turned all amplifiers on											
205	All channels inoperative - turned all amplifiers off											

*Indicates output voltage within specification limits of 30 ± 9 volts (rms).

Section 5

POST-EXPOSURE FAILURE OF ELECTRONIC EQUIPMENT

Most of the testing of equipment to determine vulnerability to graphite fiber was concerned with only those failures that occurred during or immediately following an exposure. As soon as a test was completed, the test item was cleaned, thus removing any trapped fibers. In an accidental exposure, equipment may not be cleaned thoroughly for years. Thus, trapped fibers could remain dormant in the device, but be dislodged by normal handling, be redisseminated in the chassis and possibly cause future problems. To provide data on this problem, a series of tests were performed in the Langley Research Center carbon-fiber test facility (ref. 5-1).

To simulate long-term use, previously exposed electrical units were subjected to gentle airflow, mechanical jostling and electrostatic forces to induce fiber dissemination. The airflow was produced by a small fan and was intended to simulate the air velocities which are typical of a household fan. The mechanical jostling consisted of sliding the unit back and forth across a table for a distance of about one-third meter, lifting the unit, and then replacing it on the table. The sequence of events for each cycle was:

1. Expose to E = 10^5 f·s/m^3, in the ON or OFF condition.
2. Turn ON if exposed OFF
3. After 2-minute wait, turn OFF
4. Simulate fan-forced airflow
5. After 2-minute wait, jostle device by moving to new tabletop position.
6. Turn ON and repeat cycle 49 times, starting at step 3.

If no failures occurred within fifty such sequences the device was judged to be immune to the fibers trapped inside. Fifty cycles were chosen as the appropriate number by the following reasoning. Each time fibers are redisseminated, some of them will become permanently trapped. Even if the number trapped is small, say 5%, after fifty redisseminations over 90% of the fibers will be permanently trapped. Thus, further testing would be fruitless.

Two items were chosen for these tests. They were:

1. 19" color TV

2. Stereo power amplifier.

Identical amplifiers were subjected to simulated fiber-probe tests (section 3.1 of this report), virgin-fiber exposure tests (ref. 5-2) and fire-released-fiber exposure tests (section 4 of this report.

The test items were exposed to Thornel 300 fibers 4, 8 and 12 mm long in both the "ON" and "OFF" condition. Three replicate tests were conducted for each length and condition. Thus, eighteen tests were conducted on each device. The exposure level of each was approximately 10^5 fiber sec/m^3, an exposure higher than would be expected for household interiors from aircraft accidents of large size and close proximity. The results of these tests are shown in table 5-1.

The amplifier failed three times at the exposure levels indicated in the table. The exposures that caused these failures are consistent with previous test results under the same conditions (ref. 5-2). No post-exposure failures occurred for either device. This indicates that the problem is small for similar household electronics such as televisions, amplifiers and radios.

References

5-1 Newcomb, Arthur L.: Carbon Fiber Exposure Test Facility and Instrumentation. NASA TM-80220, 1980.

5-2 Stumpfel, Charles R.; and Weaver, Calvin E.: Measured Carbon Fiber Exposures to Malfunction for Civilian Electronic Items. ARBRL-MR-02943, U. S. Army Ballistics Research Laboratory, 1980.

TABLE 5-1 POST-EXPOSURE TEST DATA, COLOR TV AND STEREO POWER AMPLIFIER

Fiber length, mm	Exposure, $f \cdot s/m^3$	Condition during exposure	Exposure failures	Post-exposure failures
4	4×10^5	On	None	None
4	3×10^5	On	None	None
4	2×10^5	On	None	None
4	3×10^5	Off	None	None
4	4×10^5	Off	None	None
4	2×10^6	Off	None	None
8	2×10^5	On	None	None
8	2×10^5	On	Amplifier	None*
8	2×10^5	On	None	None
8	1×10^5	Off	None	None
8	4×10^5	Off	None	None
8	4×10^5	Off	None	None
12	4×10^5	On	None	None
12	2×10^5	On	Amplifier	None*
12	2×10^5	On	Amplifier	None*
12	3×10^5	Off	None	None
12	1×10^6	Off	None	None
12	1×10^6	Off	None	None

*Only the TV was post-exposure tested. The amplifier failed during exposure and therefore was not post-exposure tested.

Section 6

VULNERABILITY OF GENERAL AVIATION AVIONICS EQUIPMENT

General aviation avionics equipment was evaluated for its vulnerability to damage from carbon fibers. General aviation encompasses all civil flying except that of the certified scheduled airlines. 99% of all the civil aircraft, 95% of the pilots, 84% of the total hours, even 43% of all instrument approaches are associated with general aviation (ref. 6-1).

Various prior surveys of general aviation owner characteristics (refs. 6-1 and 6-2), and avionics (ref. 6-3) were examined. A unique characteristic of these airplanes is that they are rarely discarded. On occasion, aircraft are cannibalized to maintain other machines. A considerable number of old aircraft are restored each year. Accidents, principally those involving older aircraft, are the primary cause of attrition. Of all registered aircraft, 56% are over 10 years old. Reference 6-2 estimates that 80% of all aircraft in use today are likely to be flying in the year 2000.

As a part of the study, visits were made to airports, maintenance facilities and avionics manufacturing plants to determine generic characteristics of widely used equipment. Equipment was selected for testing to bound the variety of construction and operating techniques. The selected equipment was tested at the Ballistics Research Laboratory (ref. 6-4) and at the NASA Langley Research Center in the carbon fiber test chamber described in reference 6-5.

Current avionics characteristics.- The spectrum of avionics equipment ranges from single-tube radios to complex area navigation (RNAV) inertial equipment superior to that used by the airlines.

Visits to active aircraft indicated a substantial quantity of tube-type equipment was still in use. However, current production airplanes and most existing aircraft use transistorized equipment. The current general aviation avionic gear is differentiated from that used by airlines by being smaller, by generating less transmitted power, by frequently using less-durable components, by having broader tolerances for the same function and by having fewer features. Also important, is the fact that general aviation avionics packages are not physically, and only barely functionally interchangeable, so that almost every feature is varied by all the manufacturers.

One avionics manufacturer coats all the circuit boards during and after assembly, rendering the components on the boards relatively invulnerable. Another manufacturer uses uncoated boards with the

components internally cooled by forced airflow. The features of most other equipment fall somewhere between these extremes. One justification for post-coating a circuit board is to protect it against possible exposure to moisture. Thus, a producer may not coat boards for equipment that is panel mounted but will coat boards for equipment mounted in landing gear bays where exposure to moisture is a direct cause of concern. Because of the present effort to provide a great deal of capability through digital technology in a very small volume, cooling is a very critical problem. Many manufacturers incorporate forced-air cooling to cool their own equipment, rather than depend on the air supplied by the airframe manufacturer. None of the blower-cooled equipment obtained for the test program was equipped with filters.

Avionics component tests.- As part of the NASA carbon fiber study, the United States Army Ballistic Research Laboratory at the Aberdeen Proving Ground exposed a number of general aviation avionics components to carbon fibers. Table 6-1 is a summary of the equipment tested and the average exposure, $\bar{E}$, required to cause malfunction. Failures were noted on all the equipment except for the Distance Measuring Equipment, (DME) and the Combination Navigation-Communications Equipment, (NAV/COM), but at such high exposure rates that the equipment must be considered invulnerable in realistic environments.

Two units currently manufactured and sold in relatively large volume were selected for testing at the NASA Langley Research Center. One was a very commonly used NAV/COM combination of communication transceiver and very-high frequency omni-range (VOR) navigation receiver with a separate VOR course-deviation indicator. This unit was selected because of its wide use and because of the way it was cooled. Cooling air is pumped into the back of the unit at about 0.001 m^3/sec, passed over horizontally layered boards, across the back of the front-panel indicator lamps and out the sides at the front end. A second unit was a remote mounted DME and its panel-mounted indicator. This unit is dependent on the VOR frequency selector in the NAV/COM unit. The remote part of this DME was covered with a coarse filter which might readily admit carbon fibers. This DME was a precision digital instrument.

The tests were conducted by Bionetics in the NASA carbon fiber test chamber. The test procedures and the exposure data collection and analysis were identical to those described in reference 6-6 for commercial aviation avionics.

The avionics devices were subjected to acoustic, maneuver and shock environments at intervals during the carbon fiber exposure test sequence. These environments were intended to simulate the flight operational environments which could affect fiber dissemination within the devices. The simulated flight maneuver and landing shock environments consisted of manual

movement of the devices six inches front to rear four times, then repeating the movement four times in a side to side direction and finally repeating the movement up and down. This movement produced accelerations of .5 to .8 g's. After this movement, the devices were subjected to 100 decibels of pink noise for five minutes to simulate the flight acoustic environment. A shaper, amplifier and mixer were set for a flat response from 40 Hz to 1000 Hz. The sound level was established based on measured noise levels in avionics bays of commercial transport aircraft. This level is above that normally experienced in general aviation aircraft.

The test logic for the devices is shown in figure 6-1. After turning the test device "on" it was exposed to 3×10^7 fiber-seconds/meter^3 ($f \cdot s/m^3$) of selected length fibers and then to an application of the simulated flight environment (FE). The fiber and acoustic exposures were applied a third time unless failure occurred earlier. If no failures occurred before completion of the third exposure, the test unit was declared invulnerable.

If an item failed during this procedure, a more detailed procedure, as outlined in figure 6-1, was followed to quantify the exposure levels at which failures occurred. Exposure to fibers advanced stepwise in increments of ($\sqrt{10}$) times each earlier step. After each such increment, the unit was subjected to acoustic and mechanical accelerations and was checked to see whether failure had occurred. Each instrument was subjected to this sequence four times to establish average values of exposure to failure.

The functions monitored for failure in the tests were:

NAV/COM	DME
Course deviation indicator (CDI) needle deflection	Distance
"To-from" indicator	Velocity
Flags	Transmitter power

The communications transceiver was tested by listening to local airport traffic. A transmission radio check was conducted before and after the acoustic and shock tests.

The results from the exposure tests are indicated in table 6-2. The very-high-frequency omni-range VOR, course-deviation indicator and the DME control and display units were not tested because these items were well sealed and presented no potential problems.

Seven failures were encountered. The four DME failures all occurred at exceptionally high exposure levels, similar to those reported for the DME in reference 6-1. None of the failures occurred during exposure. All occurred after post exposure shock or acoustics environments. The communications systems failed first at very high exposure ($E = 9 \times 10^7$ fiber-sec/m^3) to 1-mm-long fibers. The failure was "poor reception". The unit was cleaned and checked to no avail. It was returned to the manufacturers, who could find no fault. When it was retested at NASA, the unit performed satisfactorily. The subsequent two failures occurred at high exposures (1×10^7 and 1.8×10^7 fiber-sec/m^3) to 10-mm-long fibers. Examination of the unit showed that the circuit boards were stacked as parallel planes somewhat less than 10 mm apart. The offending fibers bridged gaps between the boards. Such fibers were easily removed by vacuum cleaning. One failure was traced directly to the 10-mm fibers getting into the relatively open volume and squelch control pots. These pots had to be replaced to restore the equipment to operating condition.

Although this assortment of failures was observed, the exposures and fiber lengths required to cause them were orders of magnitude higher than exposures expected from aircraft fires. Thus, the general aviation avionics equipment tested was judged to be essentially invulnerable to accidentally released carbon fibers.

References

6-1 Aircraft Owners and Pilots Association: Profile of Flying and Buying. AOPA, Washington, DC 1978.

6-2 Optimum Computer Systems, Inc.: A Study of Attrition in the Domestic General Aviation Fleet, FAA. AVP-75-14, April 1976.

6-3 Vohovich, Stephen G.: General Aviation: Hours Flown and Avionics Purchase Decisions, FAA-AVP-78-9, May 1978.

6-4 Morrissey, John A.; Taylor, Clifford; Brannan, William I.; Patrick, James H.: Measurement of Carbon Fiber Exposures to Failure for Certain Aviation Components. ARBRL-MR-02944, January 1980.

6-5 Newcomb, Arthur: Carbon Fiber Exposure Test Facility and Instrumentation. NASA TM 80220, 1980.

6-6 Meyers, Jerome A.; Salmirs, Seymour: The Vulnerability of Commercial Aircraft Avionics to Carbon Fibers (The Bionetics Corporation, NASA Contract NAS1-15238) NASA CR-159213, 1980.

TABLE 6-1

RESULTS OF CARBON-FIBER EXPOSURE TESTS AT BRL

Equipment	Fiber length, mm	No. of tests	No. of failures	Average exposure, $f \cdot s/m^3$
Communications (from 4 different manufacturers)	3.5	6	1	10^8
	3.5	5	2	10^8
	3.5	7	4	10^8
	3.5	7	3	10^8
NAV/COM (a)	3.5	4	0	10^8
DME (b)	1	2	0	6×10^7
	3.5	3	0	6×10^7
	7	2	0	6×10^7
Transponder	3.5	12	3	10^8
	7	12	2	10^8
	15	12	1	10^8

a) Navigation Receiver and Communications Transceiver Packages.

b) Distance Measuring Equipment.

TABLE 6-2

RESULTS OF CARBON-FIBER EXPOSURE TESTS AT NASA

Fiber length	Exposure, $f \cdot s/m^3$	NAV/COM	DME
1 mm	9×10^7	Failure after vibration	Failure after vibration
3 mm	6×10^7	No failure	Failure after vibration
	9×10^7	No failure	Failure after vibration
	6×10^7	No failure	No failure
10 mm	1×10^7	Failure	No failure
	9×10^7	No failure	Failure after acoustic exposure
	1.8×10^7	Failure	No failure

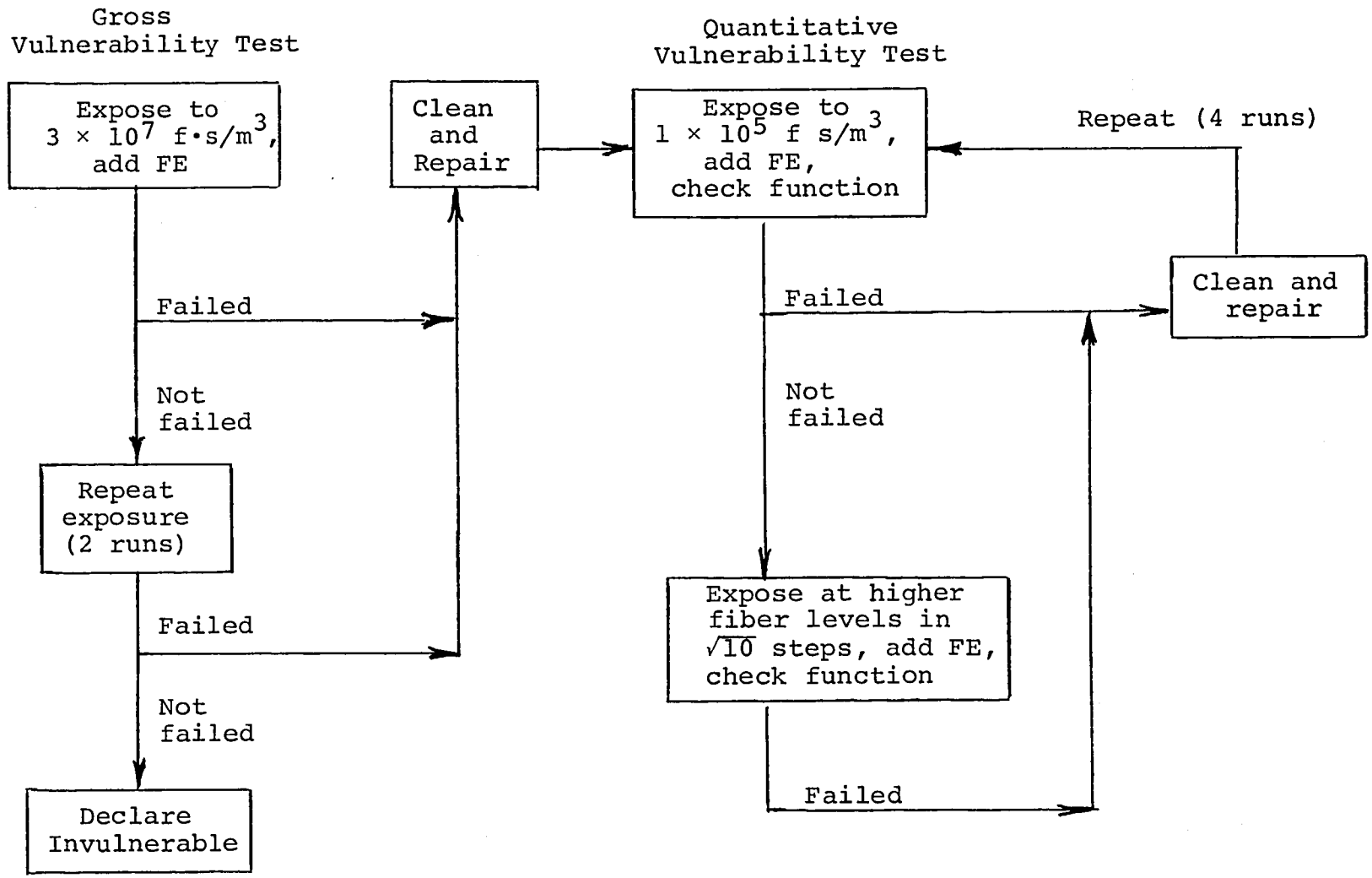

Figure 6-1 - Avionics Test Logic

Section 7

ATTENUATION EFFECTS OF CARBON FIBERS ON AIRCRAFT LANDING AIDS

The possible degradation in performance of instrument landing systems by carbon fibers released from a fire involving carbon fiber composite material was evaluated analytically. This analysis considered only the attenuation of electromagnetic energy in the transmission through a radome with carbon fiber deposits on it, or through a cloud of airborne carbon fibers. The basis of the study is the theoretical formulation of the absorption and scattering cross section of resistive cylinders given by Renau (ref. 7-1). These formulations are valid only when the cylinder is short relative to a half wavelength of the radiated energy. For cylinders with large length-to-diameter ratios (ℓ/d), the mean (over all incidence angles) absorption and scattering cross sections (σ_a and σ_s respectively) from Renau may be written in the following form:

If $\ell/d >> 1$

$$\sigma_a = \left(\frac{Z_o}{3}\right)\left(\frac{V}{r}\right)\left[\frac{1}{1+\left(\frac{\omega_o}{\omega}\right)^2}\right] \qquad (1)$$

$$\sigma_s = \left(\frac{\mu_v^2}{24\pi}\right)\left(\frac{V}{r}\right)^2\left[\frac{\omega^2}{1+\left(\frac{\omega_o}{\omega}\right)^2}\right] \qquad (2)$$

where ω is the frequency, μ_v and Z_o are the permeability and characteristic impedance of free space and V and r are the volume and bulk resistivity of the cylinder. The constant ω_o is a function of the length-to-diameter ratio, ℓ/d, and resistivity, r, of the cylinder as follows:

$$\omega_o = \left(\frac{1}{r\,\varepsilon_v}\right)\left(\frac{d}{\ell}\right)^2\left[\ell n\left(\frac{2\ell}{d}\right) - 1\right] \qquad (3)$$

where ε_v is the permittivity of free space. Figure 7-1 shows the absorption and scattering cross sections of cylinders with dimensions and resistivity typical of fire-released carbon fibers. It can be seen that the scattering cross section is at least 3 orders of magnitude smaller than the absorption cross section for the frequencies of interest.

To determine the attenuation of a plane wave passing through a plane surface, such as a radome, with a uniform deposition, D,

of carbon fibers, the power density of the field exiting from the surface, p_1, relative to the power density incident on the surface, p_o, is

$$p_1 = p_o\ (1-D\sigma_a-D\sigma_s)$$

$$\frac{p_1}{p_o} = 1-D\ (\sigma_a + \sigma_s)$$

As can be seen from figure 1, σ_s is much smaller than σ_a and may be neglected, resulting in an attenuation, A_s, in db as follows:

$$A_s = 10\ \log\ (1-D\sigma_a) \qquad (4)$$

To determine the attenuation of a plane wave (ideal) propagating through a volume with a uniform concentration, C, of fibers, it is necessary to consider the reduction in field power density occurring as each fiber is intercepted. Assuming the power density, after intercepting a fiber, is uniformly reduced over a unit area, and again neglecting σ_s,

$$p_1 = p_o\ (1-\sigma_a)$$

where p_o is the power density prior to, and p_1 is the power density after, intercepting the first fiber. The power density (p_n) after intercepting n fibers is

$$p_n = p_o\ (1-\sigma_a)^n$$

The attenuation, A_v, in db is

$$A_v = 10\ n\ \log\ (1-\sigma_a)$$

Since the number of fibers intercepted in a unit volume is the fiber concentration, C, the attenuation per unit path length is,

$$A_v = 10\ C\ \log\ (1-\sigma_a) \qquad (5)$$

Approximation of the attenuations, A_s and A_v, relating them to the mass of carbon fiber material, M_f, follow:

$$A_s = 10\ \log \left[1-\ \frac{M_s\ Z_o\ F(\omega)}{3\rho r}\right]$$

$$A_v = 10\ C\ \log\left[1 - \frac{M_f\ Z_o\ F(\omega)}{3\rho r}\right]$$

$$F(\omega) = \frac{1}{1 + \left(\frac{\omega_o}{\omega}\right)^2}$$

$$v = \frac{M_f}{\rho}$$

$$M_s = D\ M_f$$

$$M_v = C\ M_f$$

where ρ is the density of carbon fiber, M_f is the mass of a single fiber, M_s is the mass of carbon fiber per unit surface area and M_v is the mass of carbon fiber per unit volume in a cloud. For carbon fiber,

$$\rho = 1.8\ Mg/m^3$$

$$r = 2.10^{-5}\ \Omega\ m$$

$$\frac{Z_o\ F(\omega)}{3\rho r} < 3.5\ m^2/g$$

If the mass of carbon fiber deposited per square meter, M_s, and the mass of a single fiber is limited, a further simplification of equations (4) and (5) follows.

If $M_s \leq 10^2$ mg/m^2 and $M_f \leq 10^2$ mg

$$1 - \frac{M_s\ Z_o\ F(\omega)}{3\rho r} \simeq \left[1 - \frac{Z_o\ F(\omega)}{3\rho r}\right]^{M_s}$$

$$1 - \frac{M_f\ Z_o\ F(\omega)}{3\rho r} \simeq \left[1 - \frac{Z_o\ F(\omega)}{3\rho r}\right]^{M_f}$$

$$\frac{A_s}{M_s} = 10\ \log\left[1 - \frac{Z_o\ F(\omega)}{3\rho r}\right] \qquad (6)$$

$$\frac{A_v}{M_v} = 10\ \log\left[1 - \frac{Z_o\ F(\omega)}{3\rho r}\right] \qquad (7)$$

Equations (6) and (7) provide a good estimate of the attenuation of carbon fiber as a function of the length-to-diameter ratio and the mass of material. These normalized attenuation factors are shown in figure 7-2.

Table 7-1 is a summary of the maximum levels of attenuation that can be expected at the upper I.L.S. and M.L.S. frequencies. These numbers were derived assuming a single fiber mass of 2.10^{-4} mg, maximum concentrations of 10^3 fibers/m^3 and maximum depositions of 10^4 fibers/m^2. At these levels, the individual fiber spacing should be such that no significant electrical coupling between fibers exists. Attenuation values are given for length-to-diameter ratios of up to 1000 as an upper value even though these ratios are unlikely. The attenuation appears to be negligible except in the MLS case with a fiber length-to-diameter ratio of 1000. In this case, if the fiber cloud (fire plume) is oriented directly along the transmission path to an approaching aircraft and is several kilometers long, the attenuation may be enough to reduce the operating range by 30%, however no bias errors would result.

Reference

7-1 Renau, Jacques: Theory and Applications of Absorbing Chaff Clouds at Radar Frequencies. SAMSO-TR-76-9, 1975.

TABLE 7-1 - SUMMARY OF MAXIMUM ESTIMATED ATTENUATION FOR I.L.S. AND M.L.S. NAVIGATION AIDS

	(ℓ/d)	Path Atten. per Km ($C = 10^3$ f/m^3)	Radome Atten. ($D = 10^4$ f/m^2)
I.L.S. (300 MHz)	200	2×10^{-5} db	2×10^{-6} db
	1000	6×10^{-3} db	6×10^{-4} db
M.L.S. (5 GHz)	200	6×10^{-3} db	6×10^{-4} db
	1000	1 db	1×10^{-1} db

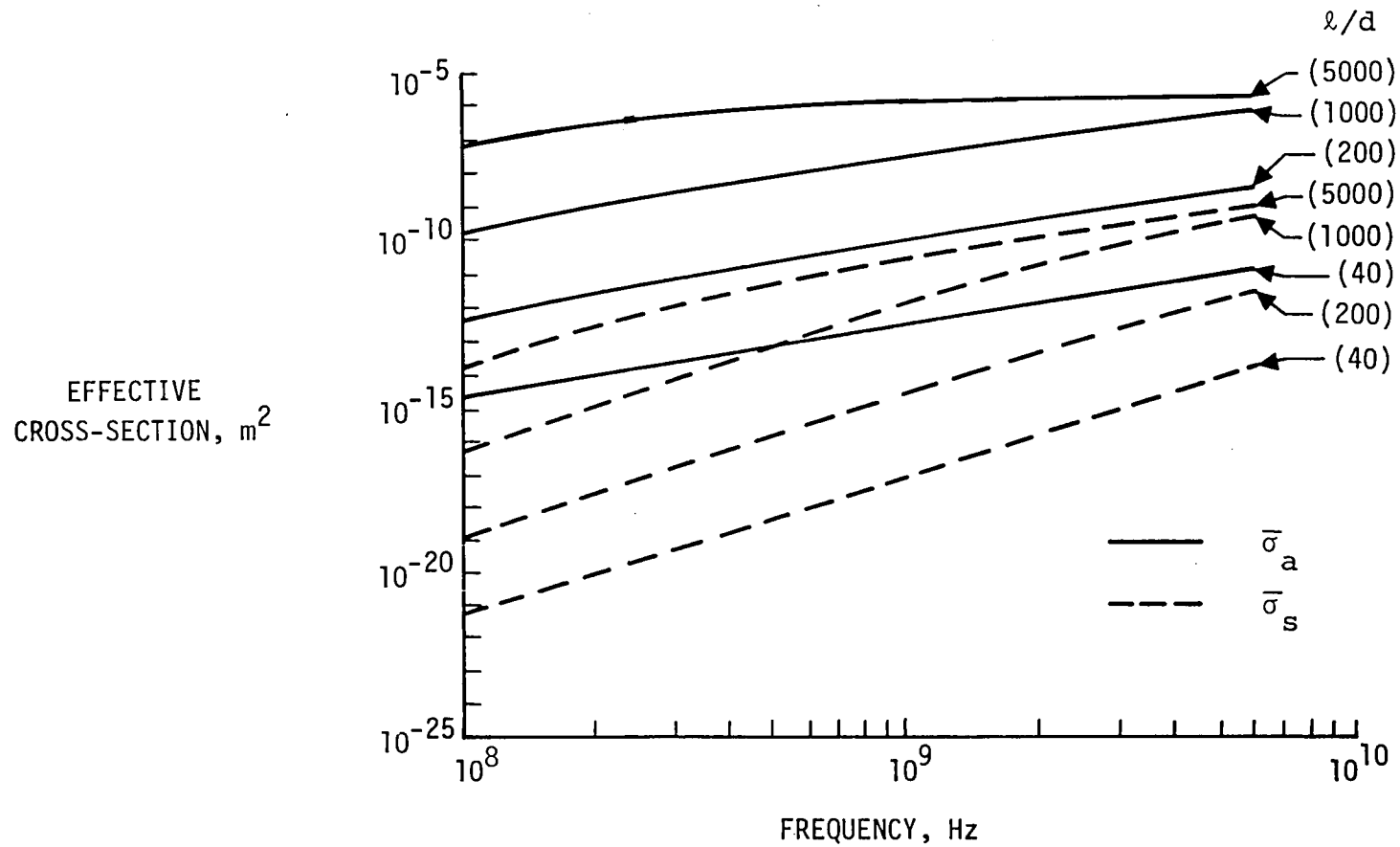

Figure 7-1 Absorption and scattering cross-sections of a single carbon fiber for various length-to-diameter ratios (assumes fiber volume = 10^{-13} m^3, bulk resistivity = 2×10^{-5} Ωm, fiber length $<<\lambda/2$)

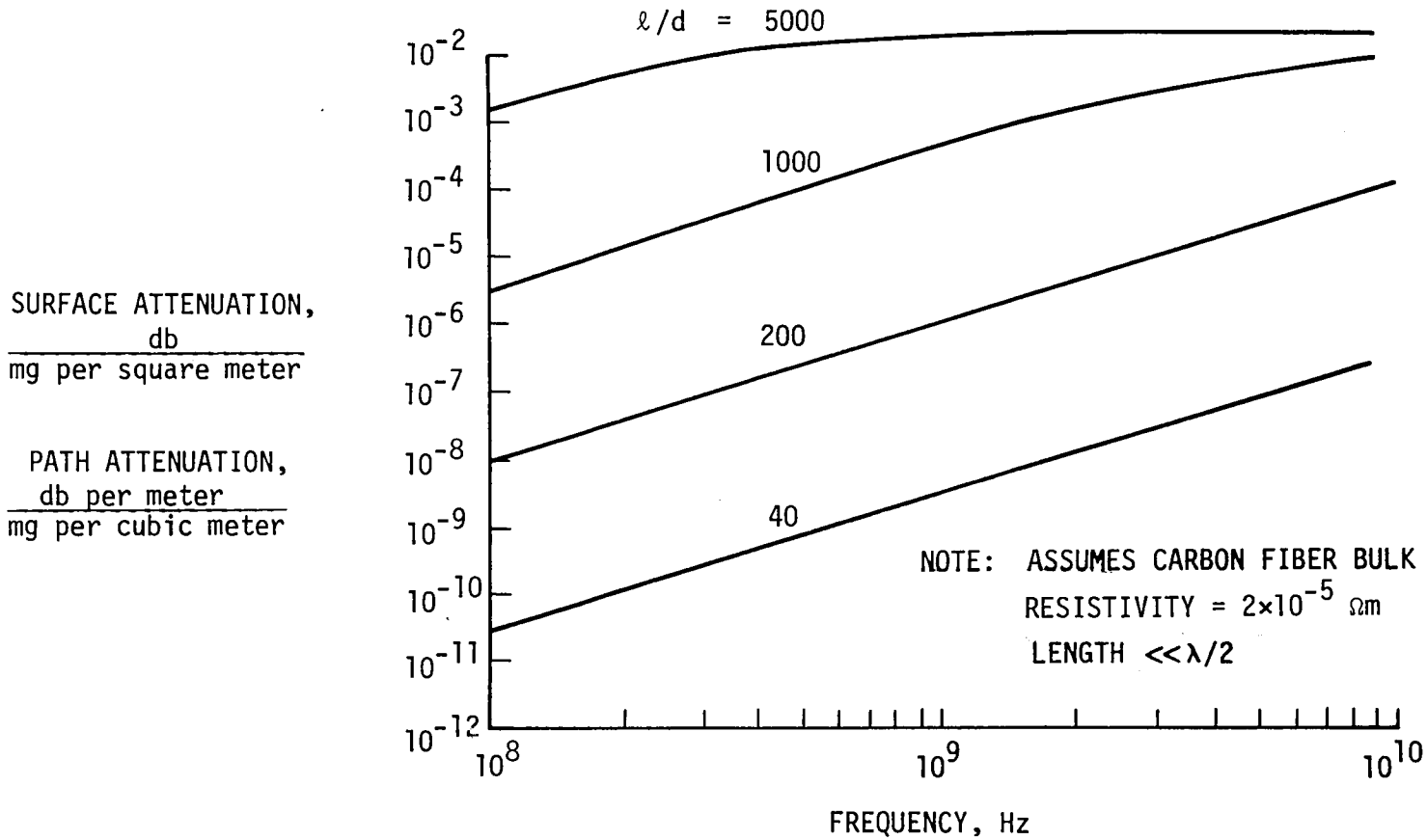

Figure 7-2 Normalized attenuation factors for various length-to-diameter ratios

Section 8

VULNERABILITY SURVEYS OF INDUSTRIAL FACILITIES AND EQUIPMENT

A major consideration in assessing the economic impact resulting from the release of carbon fibers from crash-fire accidents of civil aircraft was the effect of the fibers on industrial, commercial and public facilities. Evaluation of the economic impact of facility exposure required estimates of the vulnerability of equipment and effectiveness of filters in restricting the passage of carbon fibers. Vulnerability estimates were based on the results of exposure tests reported in reference 8-1. In addition, Bionetics performed qualitative evaluations of the vulnerability of industrial control elements and of the effectiveness of electrical equipment enclosures in restricting the passage of carbon fibers. Carbon fiber transmission tests of industrial filters were performed by Bionetics and the Ballistics Research Laboratory. Correlations between ASHRAE established dust spot efficiency ratings and carbon fiber transmission were made by Bionetics based on the test results.

Four industrial facilities were selected for surveys by a NASA-Bionetics Corporation technical team to gather data required for economic impact studies. Analysis of the data provided estimates of the equipment failure and cost effects of several levels of carbon fiber exposure. The results of these surveys and analyses were combined with the results of approximately 60 surveys and analyses performed by Bionetics and other participants in the carbon fiber risk assessment program to provide the basic data for the national economic impact estimates.

These subjects are discussed in the following sections.

8.1 TRANSFER FUNCTION ASSESSMENT

Transfer functions play a prominent role in establishing the likelihood of failures of specific items of equipment and the potential cost risks accompanying such failures. To establish the appropriate transfer function for potentially vulnerable equipment items, each manufacturing facility was inspected to determine the wiring standards employed, the effectiveness of filters included in the plant ventilation systems and in the enclosures for each item of electrical or electronic equipment that might be vulnerable.

Many electrical and electronic components are enclosed in standardized boxes for a variety of reasons, ranging from assuring that personnel do not contact live circuits accidentally to assuring

that circuitry is not adversely affected even when the electrical device is submerged or subjected to sprays, explosive gases or contaminants. Standards established by the National Electrical Manufacturers Association, NEMA, are almost universally employed in designing the electrical wiring systems for industrial facilities. Even though these standards are not specifically designed to prevent intrusion by carbon fibers, the NEMA standard enclosures that assure safe operations in hostile environments are also certain to preclude ingestion of carbon fibers. In addition, much industrial wiring is enclosed in conduits attached to terminal boxes with pipe or other essentially sealed fittings. All such installations would also be fiber-proof.

NEMA also has standards for spacings between conductor terminals in or on the less well-protected enclosures. Barriers are frequently prescribed between contacts to create a longer path for flash-overs if the terminal board were to become contaminated. Such spacings and barriers have been established by experience and serve to protect circuitry against malfunction because of exposures to carbon fibers. The effectiveness of these spacings and barriers are examined in section 9 of this report. These and other features of electrical circuitry were noted in the industrial surveys conducted and were accounted for in assessing the transfer function for a given installation.

Industrial filters are generally rated according to an "ASHRAE Dust Spot" number by the American Society of Heating, Refrigeration and Air-Conditioning Engineers. These numbers are assigned from tests with reasonably spherical particles normally found in industrial environments. Because the effectiveness of filters was expected to differ for fiber particles, a systematic evaluation of filters with known ASHRAE ratings was performed with carbon fibers of known length by the Army Ballistic Research Laboratory (ref. 8-2). The results were plotted as indicated in figure 8-1 and a curve was fitted to the data. This curve was used in the Bionetics analysis to develop filter factors for individual units of electrical and electronic equipment in the factories surveyed.

Generally, the filters were more effective in trapping fibers than spherical particles of equal diameter and more effective in trapping long fibers than short ones. Thus, the actual exposure inside an electrical device was expected to have relatively fewer long fibers than were present in the originally released fiber cloud. This effect was ignored in the analysis; consequently, the estimates of transfer functions are expected to be more severe than would be experienced for a given incident.

8.2 SURVEYS OF INDUSTRIAL FACILITIES

The following four industrial facilities were selected for the surveys.

An automotive electronics and electromechanical components manufacturing plant.

A television receiver assembly plant.

A light truck assembly plant.

A textile fiber production plant.

Some of the characteristics of the facilities are summarized in table 8-1.

The surveys determined the types of equipment used, the effect of equipment failures on plant operations, the types of ventilation systems employed and the equipment features which would be effective in protecting against carbon fibers. This information provided the basis for estimating the potential for entry of carbon fibers into the plants, the extent of equipment and product failures which would result from carbon fiber exposure and the economic impact of those failures. The analysis consisted of the following six steps:

1. A product flow diagram was developed for each factory which described the principal features of the electrical power supply system, identified the potentially vulnerable equipment, and indicated the normal protections for the equipment.

2. A modified fault-tree technique was employed to define the effects of carbon-fiber-induced failures in terms of spoiled product, lost production time and materials and manpower required for equipment repair.

3. A cost for each failure was developed based upon estimates of labor rates, material costs, value of the product and repairs.

4. Transfer functions were developed for the factory and the equipment enclosures based on the effectiveness of the ventilation, system, filters and equipment enclosures in restricting fiber entry.

5. The number of failures were estimated based upon a linear failure prediction model for outdoor exposures of $E = 10^5$ fiber seconds/meter^3. These calculations utilized an estimated value of $\bar{E}$ for equipment items that had not been tested specifically, but which were generically similar to others for which test data were available.

6. Cost risk was calculated as the cost of a failure times the number of failures predicted from outside exposures of $E = 10^5$ fiber seconds/meter^3. To a very good first approximation, the costs for other exposure levels are expected to be in linear proportion to those reported. For example, costs for $E = 10^3$

fiber seconds/meter^3 are expected to be .01 times the values given. For reference, an E of 10^5 fiber seconds/meter^3 is very unlikely to be experienced in fiber-release incidents from civil aircraft crashes even close to the incident (ref. 8-3).

Because the exposures, E, predicted were usually several orders of magnitude less severe than the mean exposure $\bar{E}$ required to produce a failure, a probability approach was required to assess the likelihood of failure. The relation $P_f \simeq E/\bar{E}$ was used to approximate the true probability $P_f = 1 - e^{-E/\bar{E}}$. This approximation is valid whenever $E << \bar{E}$.

Tables 8-2 through 8-5 present summaries of the risk assessments for each of the four manufacturing plants if they were subjected to an outdoor exposure of E = 10^5 fiber seconds/meter^3.

The plant manufacturing automotive components (table 8-2) has four separate production lines, one for an electronic control for a fuel injector, one for the injector, one for an electronic brake control and the fourth for emission-control air pumps. Each line is fed by a separate 480-volt transformer through a master switch. Failures of the transformer switches were found to be the costliest potential failures, because an entire production line would be stalled. A recent incident in which such a switch failed for another reason gave specific cost information for such an incident. Items 2 through 8 in table 8-2 list probable costs for failures in each of several portions of the electronic control production lines. Although each item is critical to successful operation, the combinations of low transfer function, low individual costs, and high values of $\bar{E}$ resulted in very small potential losses for a fiber incident. A bake-out step (item B) and the heat-treatment of injectors (item 10) would incur very high costs, but failure at these stations was very unlikely because of the very high exposure required to cause a failure. Loss of control of the ph in waste water from etching processes could result in significant cost penalties or fines levied by the local sanitation district (item 11); however, the required $\bar{E}$ was also high for this failure mode.

The plant assembling television receivers (table 8-3) uses a relatively large amount of electrical power (12,000 kW), for plastic processing, for circuit testing, burn-in and life testing. The plant is fed by 16 oil-cooled 440-V transformers, each rated at 750 kVA. Failure of such a transformer or its switch (item 8) is the costliest single potential failure, but the failure is highly unlikely ($\bar{E}$ = 10^8 fiber seconds/meter^3). The entire plant is critically dependent on a single master oscillator (item 1) that furnishes power at a set of standard frequencies against which to tune the electronic circuitry. This item carries the highest cost risk in this factory. The parts of the factory that

deal with processing plastic parts for cabinets and instrument panels (items 5, 6, 10, 11) would incur significant costs if failed, but the exposures required to cause such failures make the risk of such failures a modest concern.

Because the truck assembly plant (table 8-4), is characterized by a single production line, the failure of a single critical element, requiring a significant time to correct, could idle the entire plant. Consequently, failure of the main transformer switch (item 3), the 440-V distribution system (item 1) overhead trolley system (item 2) and the robotic welder (item 8) could each cause major costs. However, the $\bar{E}$ values required to cause such failures are quite high. On the other hand, spot welders (item 7) and a 440-V compressor drive (item 6) have relatively high transfer functions, and, therefore, the highest cost risks. Some equipment, such as welder controls were recognized as being vulnerable to a variety of normally encountered failures. Consequently, replacement spares were kept available and repairs would be accomplished expeditiously with reasonable cost and minimal impact on productivity.

The plant manufacturing synthetic fibers (table 8-5) operated by continuous flow in four separate lines. Disruption of power or loss of control at any one of these lines would be extremely costly because of the clean-up required. Most electrical switch gear and sensitive controls had high $\bar{E}$ values or were protected in cabinets with low transfer functions, so that the cost risks for components of this plant were generally low.

References

8-1 Assessment of Carbon Fiber Electrical Effects. NASA CP-2119, 1979.

8-2 Paszek, John T.; Davis, Dudley D.; Patrick, James H.: Carbon Fiber Transfer Function Through Filters and Enclosures, ARBRL-MR-02946, U. S. Army Ballistics Research Laboratory, 1980.

8-3 Daniledes, James; and Koch, John R.: Carbon/Graphite Fiber Risk Analysis and Assessment Study. Assessment of Risk to the Lockheed Model L-1011 Commercial Transport Aircraft, Lockheed-California Company, NASA CR-159201, 1980

TABLE 8-1 FACILITY CHARACTERISTICS

Characteristic \ Facility	Automotive Components Manufacture	TV Receiver Assembly	Truck Assembly	Textile Fiber Production
Electrical Equipment	Main power Mat'ls. handling Automated ops Functional test Heat treating	Main power Mat'ls. handling Master oscillator Burn-in Functional test	Main power Mat'ls. handling Automated welding Harness test Electrostatic paint	Main power Mat'ls. handling Process control Variable freq. drive
Product	Fuel injectors Injector controls Air pumps	Color TV Black & white TV	Pick-up trucks	Synthetic fibers Yarn
Mode of Operation	4 lines 3 products	7 lines 7 models	1 line 1 product with variations	Continuous process 10 lines 3 products
Ventilation	Air conditioned Clean rooms	Air conditioned	Windows	Open Lint shields
Age	< 10 yr.	∿10 yr.	> 40 yr.	∿20 yr.
Distance from airport	1.6 km	24 km	8 km	13 km
Shifts	2 @ 8 hr.	1 @ 8 hr.	2 @ 10 hr.	3 @ 8 hr.
Work force personnel	750	1700	1900	600

TABLE 8-2 ASSESSMENT OF POTENTIAL LOSSES

Manufacturer of Automotive Components

Vulnerable Element	Transfer Function	$\bar{E}$, $f \cdot s/m^3$	Max. Cost of Failure	Risk if $E = 10^5$ $f \cdot s/m^3$
Main Transformer Switch	1.6×10^{-2}	10^6	$65,800	$420.00
Fab. Circuit Boards	4.1×10^{-5}	10^6	2,842	.01
Laser Trim Resistors	5.0×10^{-4}	10^6	528	.03
Integrator & Populator	3.0×10^{-4}	10^6	490	.06
Operational Test	3.0×10^{-4}	10^6	478	.06
Circuit Test	2.3×10^{-5}	10^6	529	.007
Burn-in	6.2×10^{-4}	10^6	252	.01
Bake-out	6.2×10^{-4}	10^7	52,700	.35
Incoming Inspection	7.6×10^{-4}	10^6	314	.10
Injector Heat Treat	2.2×10^{-3}	10^7	9,920	.65
Waste Water Processing	2.2×10^{-3}	10^7	5,037	.11

TABLE 8-3 ASSESSMENT OF POTENTIAL LOSSES

Plant Assembling Television Receivers

Vulnerable Element	Transfer Function	$\bar{E}$, $f \cdot s/m^3$	Max. Cost of Failure	No. of Units	Risk if $E = 10^5$ $f \cdot s/m^3$
Master Oscillator	7.3×10^{-3}	10^5	$16,400	1	$119.00
Incoming Inspection	7.3×10^{-3}	10^6	6,340	3	9.70
Populator & Integrator	8.4×10^{-3}	10^6	940	2	1.58
Signal Interconnect	4.0×10^{-2}	10^7	34	14	.18
Plastic Press	2.5×10^{-2}	10^7	1,800	20	8.87
Embossing Press	5.5×10^{-4}	10^7	228	20	.02
Encapsulator	2.2×10^{-3}	10^5	1,040	1	2.25
Transformer Switch	5.5×10^{-5}	10^8	26,200	16	.23
440-V Distribution	6.6×10^{-3}	10^6	2,720	6	10.73
Plastic Contamination	4.9×10^{-2}	10^6	2,420	1	.30
Spray Paint	7.9×10^{-2}	10^6	3,760	1	.73
Tuning and Alinement	4.0×10^{-3}	10^5	1.10	3500	16.00
Burn-in	4.0×10^{-3}	10^5	0.75	3500	9.00
Life Test	3.1×10^{-3}	10^6	2.50	100	.13

TABLE 8-4 ASSESSMENT OF POTENTIAL LOSSES

Truck Assembly

Vulnerable Element	Transfer Function	$\bar{E}$, $f \cdot s/m^3$	Max. Cost of Failure	No. of Units	Risk if $E = 10^5$ $f \cdot s/m^3$
440-Volt Bus	1×10^{-2}	10^6	$84,000	1	$84.00
Overhead Trolleys	2×10^{-3}	10^6	41,500	6	45.00
Transformer Switch	1×10^{-3}	10^7	435,000	9	39.00
13.2-kV Circuit Breaker	1×10^{-4}	10^7	41,500	9	0.37
110-V Aux. Transformer	5×10^{-3}	10^6	6,750	12	40.00
440-V Compressor Drive	5×10^{-2}	10^7	23,400	4	460.00
Spot Welder	2.5×10^{-1}	10^6	1,700	50	2,200.00
Robotic Welder	2×10^{-5}	10^7	41,900	2	0.01
Stud Welder	2×10^{-2}	10^6	1,850	2	7.40
Teletype Printer	2×10^{-5}	10^7	900	15	0.002
Electrical Harness Test	1×10^{-2}	10^7	1,670	1	0.16
Electrostatic Paint Spray	1×10^{-4}	10^7	1,700	8	0.01

TABLE 8-5 ASSESSMENT OF POTENTIAL LOSSES

Textile Fiber Manufacturer

Vulnerable Element	Transfer Function	$\bar{E}$, $f \cdot s/m^3$	Max. Cost of Failure	No. of Units	Risk if $E = 10^5$ $f\ s/m^3$
13.2-kV Transformer Switch	1×10^{-3}	10^7	$93,000	6	$5.57
440-V Var. Frequency Drive	1×10^{-3}	10^6	15,000	6	9.10
Chemical Supply	1×10^{-3}	10^7	28,000	24	6.81
Hydraulic Power	5×10^{-4}	10^6	6,600	6	1.97
Temperature Control	5×10^{-4}	10^7	3,400	60	1.01
Temperature Reference	5×10^{-5}	10^7	6,700	24	0.08
Bath Control Acrylic Yarn Line	5×10^{-4}	10^7	5,300	36	0.96
13.2-kV Transformer Switch Nylon Coating Line	1×10^{-3}	10^7	98,000	1	0.98
13.2-kV Transformer Switch	1×10^{-3}	10^7	41,000	1	0.41
Speed Control	5×10^{-4}	10^6	1,700	2	0.17

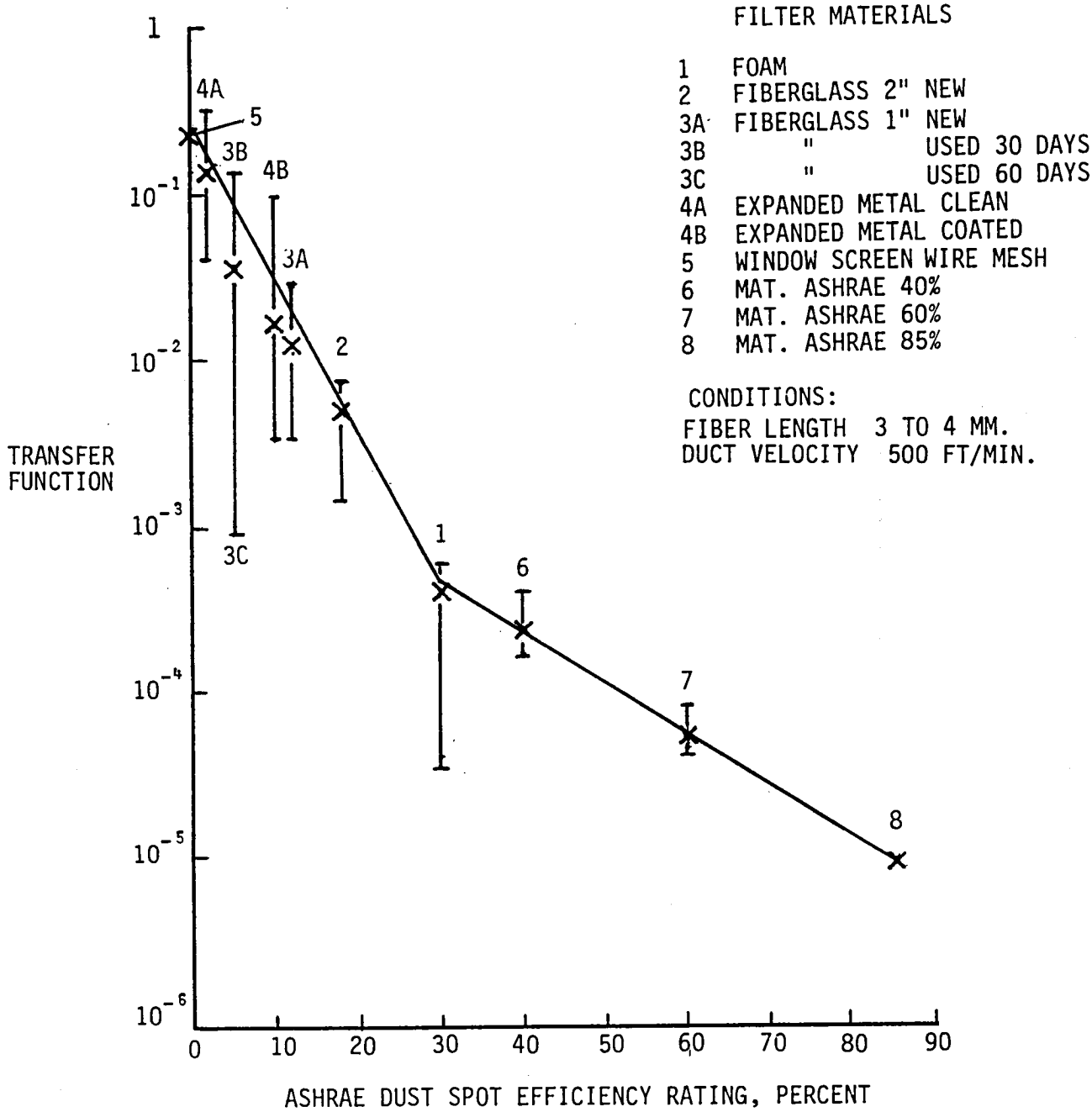

Figure 8-1 - Transfer functions for air filters compared to ASHRAE dust spot efficiency ratings

Section 9

CARBON FIBER INDUCED ARCS

Tests were conducted to observe the effects of exposure to carbon fibers on 460-volt, 60-hertz industrial equipment and to investigate the occurrence of arcs resulting from the exposure.

The NEMA standards and MIL specifications were examined to find the minimum spacings allowable between energized parts in industrial applications and the type of enclosures that would be most likely to be penetrated by fibers. Exposed buses, wires and terminals were determined to be the most vulnerable points of an electrical installation.

Representative components were exposed to carbon fibers to determine whether or not a sustained arc could be produced in such components, and, secondly, to determine the average exposure to create an arc.

9.1 TEST EQUIPMENT AND GENERAL PROCEDURES

Two power sources were used:

A 1500-kw, 460-volt, 60-hertz, 3-phase transformer with a 6900-volt primary. This unit was part of the NASA Langley Research Center electrical power distribution system.

A 60-kw, 416-volt, 60-hertz, 3-phase diesel-driven generator. This generator was a portable emergency power supply used at the NASA Langley Research Center. The voltage was adjusted to 460 volts phase to phase.

Three representative electrical installations were evaluated:

Copper bus bars
Bare copper wires
Terminal boards (MIL-T-Spec 55164, Types TB38 and TB39).

Three characteristic measurements were made:

Current and voltage accompanying arcing.
Arc duration (cycles)
Exposure level (large chamber only).

Three methods of producing an arc were employed:

A carbon fiber was placed across conductors before energizing the circuit.

A carbon fiber was placed across conductors after energizing the circuit.

Airborne carbon fibers (1, 3 or 10 mm long) were disseminated after energizing the circuit.

A small test chamber was used to conduct qualitative tests for sustained arcs across pairs of wires and terminal boards. This chamber was a 1 m by 1 m by 1 m box with a removable side and several penetrations. Carbon fibers in the box were distributed by an air jet for the airborne carbon fiber arc tests. Exposures were not monitored.

The NASA vulnerability exposure test chamber (ref. 9-1) was used to conduct the tests for sustained arcs between bus bars and to measure the exposure level required to create an arc across pairs of wires and terminal boards. This chamber was approximately 2.5 m wide by 2.5 m long by 2.75 m high. Fibers of the specified length were blown into the chamber from a chopper. Fiber exposure was monitored by ball detectors described in section 2.1.

The maximum current available in each test was limited by the line resistance (approximately 0.23 Ω per phase). A nichrome wire variable resistor was used in some tests to further limit the current. All tests were conducted with no load connected to the test components. The lines were fused to protect against damage from prolonged arcs.

Figure 9-1 is a diagram of the measurement circuitry employed. Current was sensed by a clamp-on current transformer and voltage was sensed across only one pair of lines through a 1-megohm loading resistor and a voltage divider, as shown.

9.2 TEST CONDITIONS AND RESULTS

The test conditions and results are summarized in Table 9-1.

Bus-bar tests.- Bare copper bus bars (test 1) were exposed to carbon fibers in the arrangement shown in figure 9-2. The bars were 6 mm thick, 16 mm wide and 153 mm long. Four pairs of bars were spaced 12.7, 19.0, 25.4 and 31.7 mm apart. Single-phase power was fed simultaneously to each pair of bars, but no loads were connected. Flashovers were noted for pairs of bars spaced at 12.7 and 19 mm, but not for those spaced further apart. Flashovers did not persist more than ½ cycle. Only single-phase tests were conducted and no attempt was made to establish the exposure levels required to cause arcs.

Bare-wire tests.- In tests 2 through 4, copper wires, 2 mm in diameter, were clamped between insulated blocks with their axes parallel and in a horizontal plane (fig. 9-3). For single-phase

tests (tests 2 and 3), two wires were side-by-side and spaced 1.5 mm to 38.1 mm apart. The insulation was stripped from the ends of the wires to expose 10 to 15 mm of bare copper. In some tests, fibers were laid across the wires before the 460-volt power was turned on. However, the characteristics of flashovers produced with this technique and those produced by airborne fibers were identical.

Arcs produced in single-phase tests fed by the transformer (test 2) were not sustained beyond the first ½ cycle even for wire spacings as small as 1.5 mm. The oscillograms in figure 9-4 were recorded in two identical tests except that the fuse ratings were different (30A and 60A). Oscillogram A shows that the fuse opened when the first flashover occurred. Oscillogram B shows that the fuse survived three flashovers. The traces indicate that the voltage was reduced to zero instantaneously when an arc formed. This loss of power allowed the ionized environment to cool so that the arc was not sustained. Voltage built back to its normal level until the next fiber made contact and the process was repeated.

Arcs formed in single-phase tests fed by the generator (test 3) were sustained even with wire spacings up to 38.1 mm. The oscillograms in figure 9-5 show that, when current flowed in the arc, the voltage led the open-circuit voltage by as much as 30^{o}, and was 180^{o} out of phase with the current. Although the voltage and current reached zero at the same instant, a sustaining voltage was available to reinitiate the arc before it was cooled completely. Thus, the arc was sustained for from 2 to 3 cycles, depending on the arc length. The observed phase shifts were attributed to the inductive character of the generator power source.

For tests of copper wires in three-phase transformer-powered circuits (test 4), the third wire was mounted below the first two, so that the three free ends formed an equilateral triangle 9.5 mm on each side (fig. 9-6). A sustained arc was formed, probably because the arc across at least one phase was active at any instant and, thus, preserved an ionized environment that sustained other arcs when 1000 amperes were available. The arcs did not persist if the circuit was limited to 285 amperes. Figure 9-7 is an oscillogram of current and voltage in one phase of such a test. The arc persisted for 2.5 cycles, when the fuse failed in one of the other phases. No three-phase tests were performed with the generator-power-supply because that configuration was deemed certain to sustain arcs.

Terminal-board tests.- Terminal boards of two types (38 TB and 39 TB) described in MIL-T-55164 were tested in single and three-phase circuits powered by the transformer (tests 5 through 10). The two terminal boards were similar in design, but the spacing between terminals was different (5.1 and 7.1 mm). The rated current capacities were 20 and 30 amperes, respectively. Two or

three conductors were connected to consecutive terminals with standard insulated lug connectors (fig. 9-8). No load was connected to the other side of the terminals and seven other terminals were inactive.

In single-phase circuits, arcs were formed, but were not sustained for more than one half-cycle. In three-phase circuits, arcs were sustained only if more than 285 amperes of current were available. The arcs over the 38 TB and the 39 TB terminal boards behaved identically.

Exposure levels to sustain continuous arcs were established by testing additional terminal boards in environments where the exposure was monitored by ball sensors and chopped fibers were blown into the chamber in a controlled manner. Four circuit boards were exposed simultaneously in the arrangement shown in figure 9-8. One of each type of board was oriented vertically and the other was oriented horizontally. Results are given in Table 9-2 and are plotted in figure 9-9. No sustained arcs were formed with fibers 1 mm long because several fibers would be needed to bridge a given terminal spacing. (A higher exposure, $\overline{E}$, was required with 3-mm-long fibers then with 10-mm-long fibers because of the higher likelihood that two or more long fibers would be deposited to bridge the distance over the barriers between terminals). The required exposure to sustain arcs on vertically mounted boards was approximately 4 times as great as that for horizontally mounted boards.

Damage caused by arcs.- Figures 9-10 and 9-11 are photographs of damage caused by the arcs produced in this study. The copper wires (figure 9-10) were melted down to their clamping blocks and the micarta clamping block was severely scorched. The damage to terminal boards, 38 TB, was severe, but was limited to the affected terminals (fig. 9-11).

Reference

9-1 Newcomb, Arthur L.: Carbon Fiber Exposure Test Facility and Instrumentation. NASA TM 80220, 1980.

TABLE 9-1 - SUSTAINED ARC TESTS

Test #	Test Specimen	Specimen Spacing, mm	Phase	Power Source	Chamber	Amperes, Rms	Results
1	Copper Bus Bar - 6.3 mm × 16 mm	12.7 - 19	1	Transformer	Large	1000	Flashover - 1/2 cycle
2	Copper Wire	1.52	1	Transformer	Small	100<I<1000	Flashover - 1/2 cycle
3	Copper Wire	12.7 - 38.1	1	Generator	Small	425	Sustained Arc
4	Copper Wire	9.5	3	Transformer	Small	285<I<1000	Sustained Arc
5	38 TB Terminals	5.1	1	Transformer	Small	100<I<1000	Flashover - 1/2 cycle
6	38 TB Terminals	5.1	3	Transformer	Small	<100	Flashover - 1/2 cycle
7	38 TB Terminals	5.1	3	Transformer	Small	285<I<1000	Sustained Arc
8	39 TB Terminals	7.1	1	Transformer	Small	100<I<1000	Flashover - 1/2 cycle
9	39 TB Terminals	7.1	3	Transformer	Small	285	Flashover - 1/2 cycle
10	39 TB Terminals	7.1	3	Transformer	Small	1000	Sustained Arc

TABLE 9-2 - EXPOSURES FOR SUSTAINED ARCS FOR TERMINAL BOARDS
INDUSTRIAL POWER AT 460 VOLTS, 60 HERTZ, 3 PHASE

	$\bar{E}$ - AVERAGE EXPOSURE TO ARC, FIBERS SECS/METER^3			
Terminal Board	39 TB (a)	38 TB (a)	39 TB (a)	38 TB (a)
Axis / Fiber Length	Vertical	Vertical	Horizontal	Horizontal
1 mm	$> 10^8$	$> 10^8$	$> 10^8$	$> 10^8$
3 mm	8.4×10^7	8.7×10^7	1.96×10^7	1.37×10^7
10 mm	1.27×10^6	1.67×10^6	3.45×10^5	7.48×10^5

(a) From MIL-T-54164

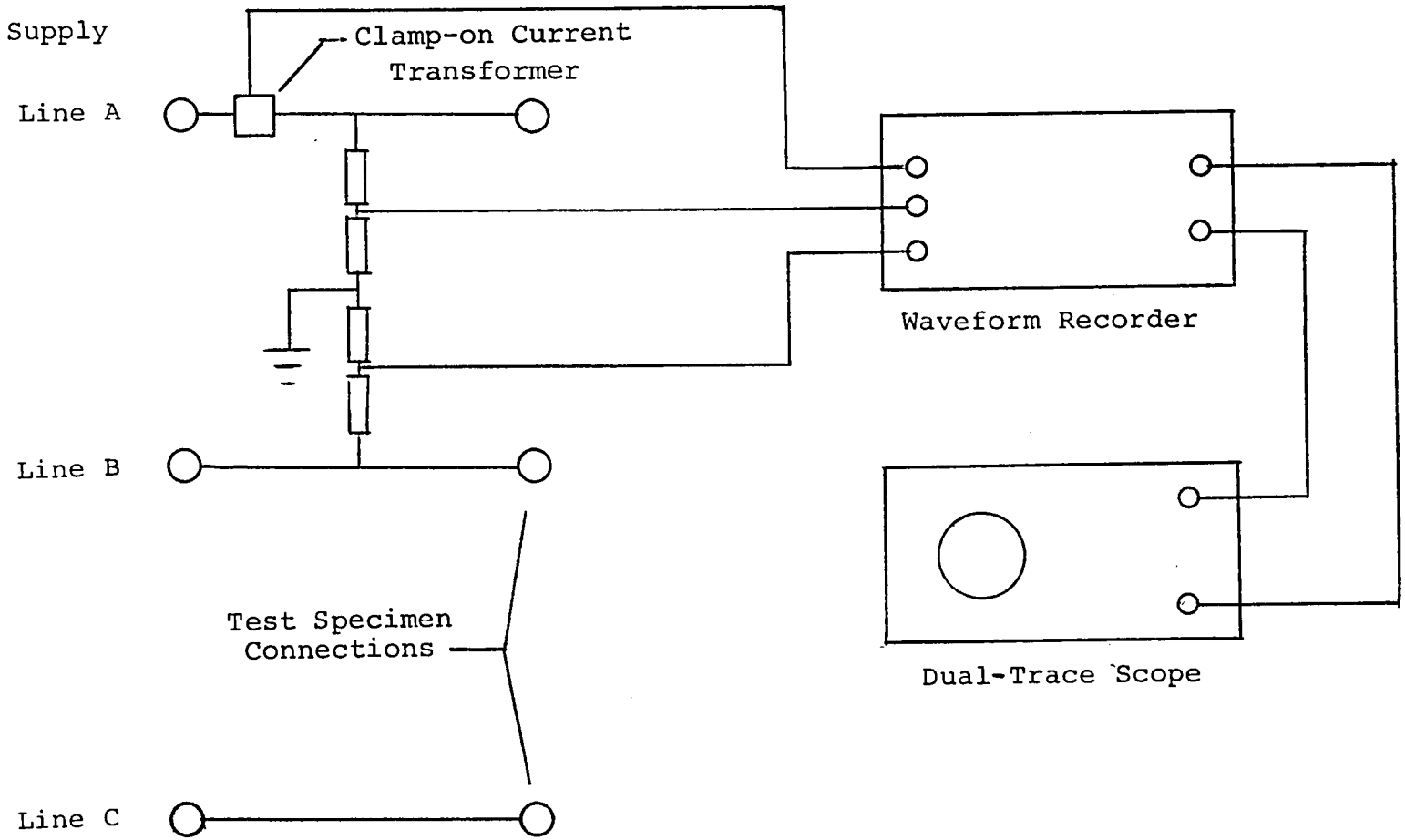

Figure 9-1 Electrical Circuit for Measuring Voltage and Current. (Line C was deleted for Single-Phase Experiments).

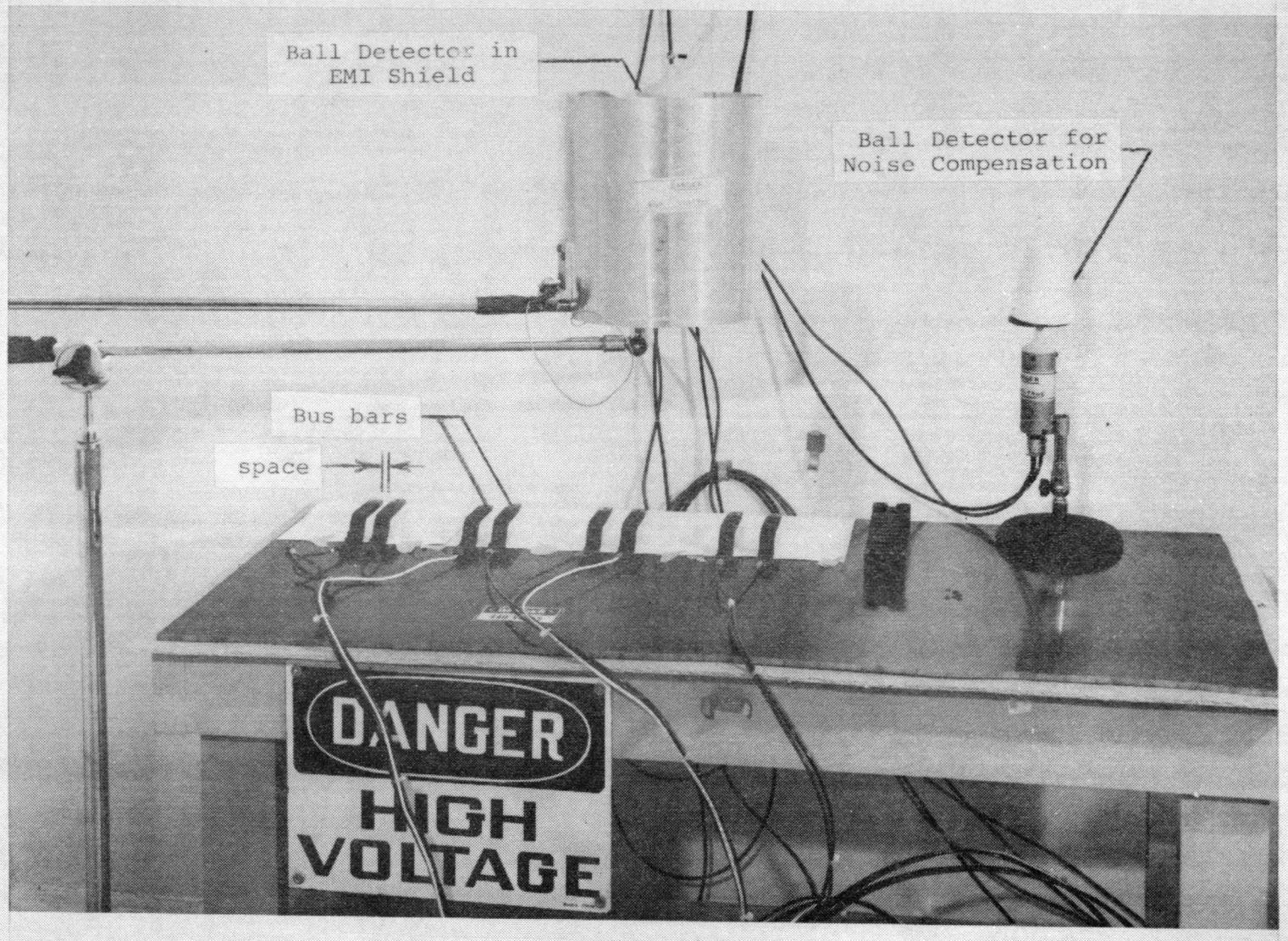

Figure 9-2 Bus-Bar Test Configuration.

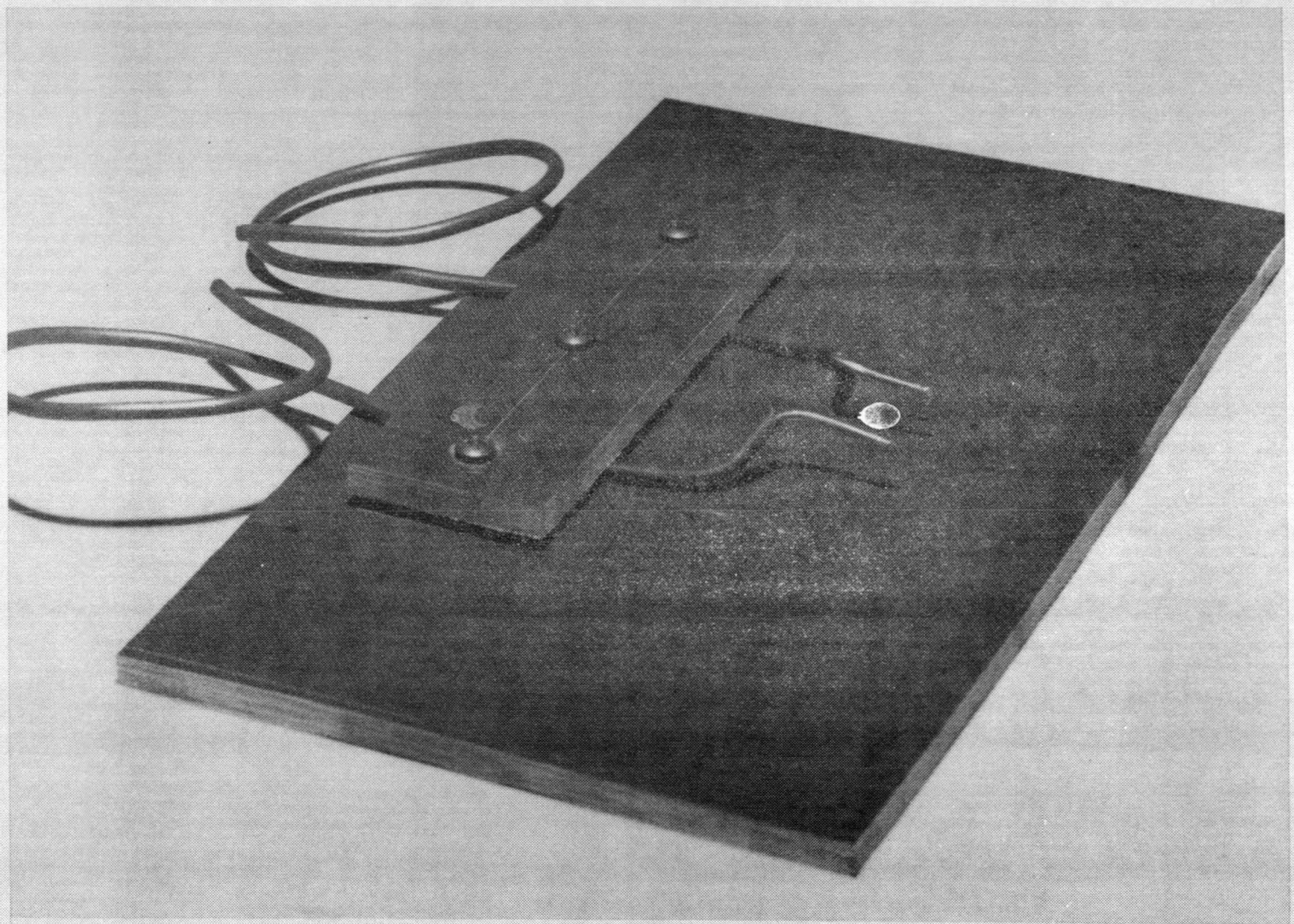

Figure 9-3 Configuration for Single-Phase Tests of Copper Wires.

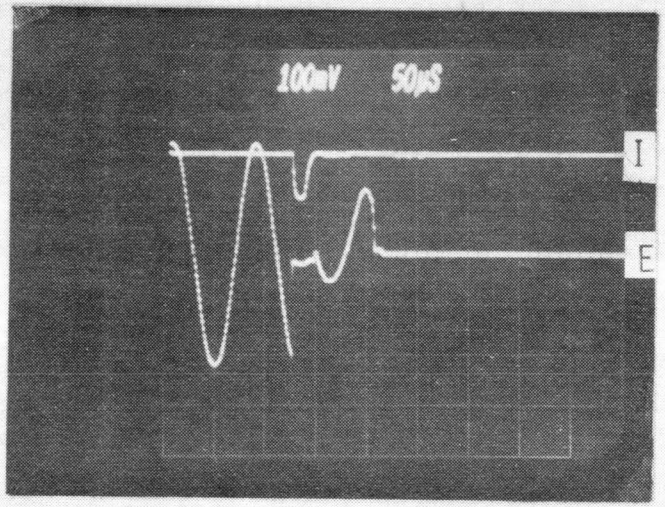

a. Wire spacing - 1.52 mm
Peak current - 1400 A
30-A fuse opened when
flashover occurred.

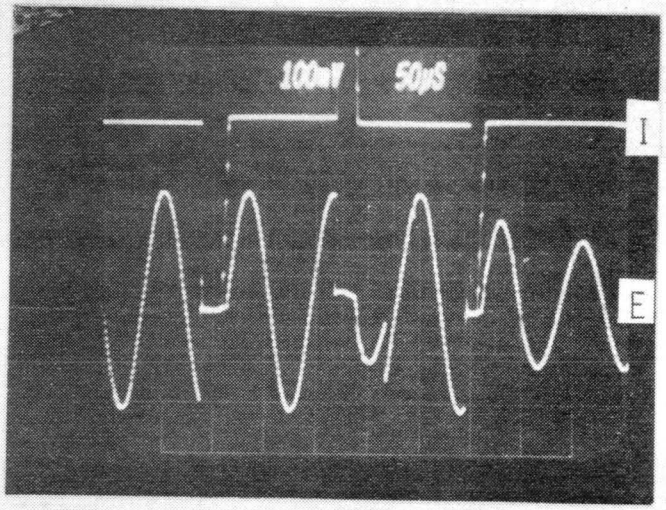

b. Wire spacing - 1.52 mm
Peak current - 1400 A
60-A fuse opened after
several flashovers.
Arcs were not sustained.

Figure 9-4 Current-Voltage Traces

for Single-Phase Tests on Wires Fed by a Transformer.

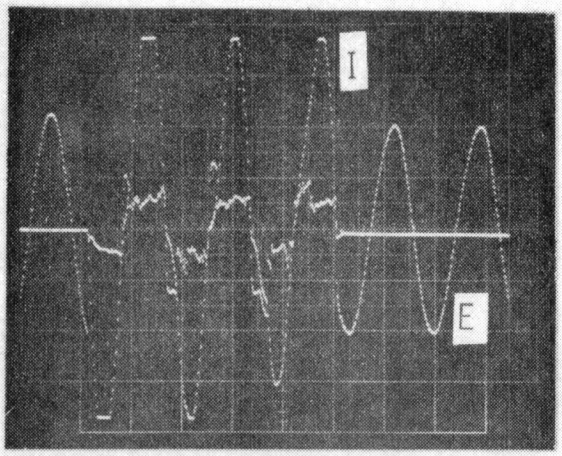

a. Wire Spacing - 12.7 mm

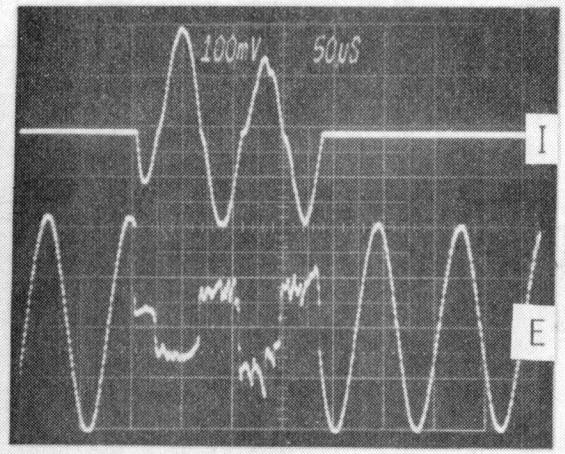

b. Wire Spacing - 19 mm

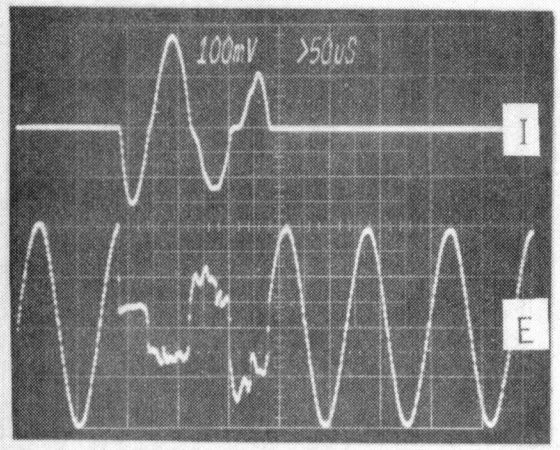

c. Wire Spacing - 25.4 mm

Figure 9-5 Current and Voltage Traces for Single-Phase Generator-Powered Tests of Bare Wires.

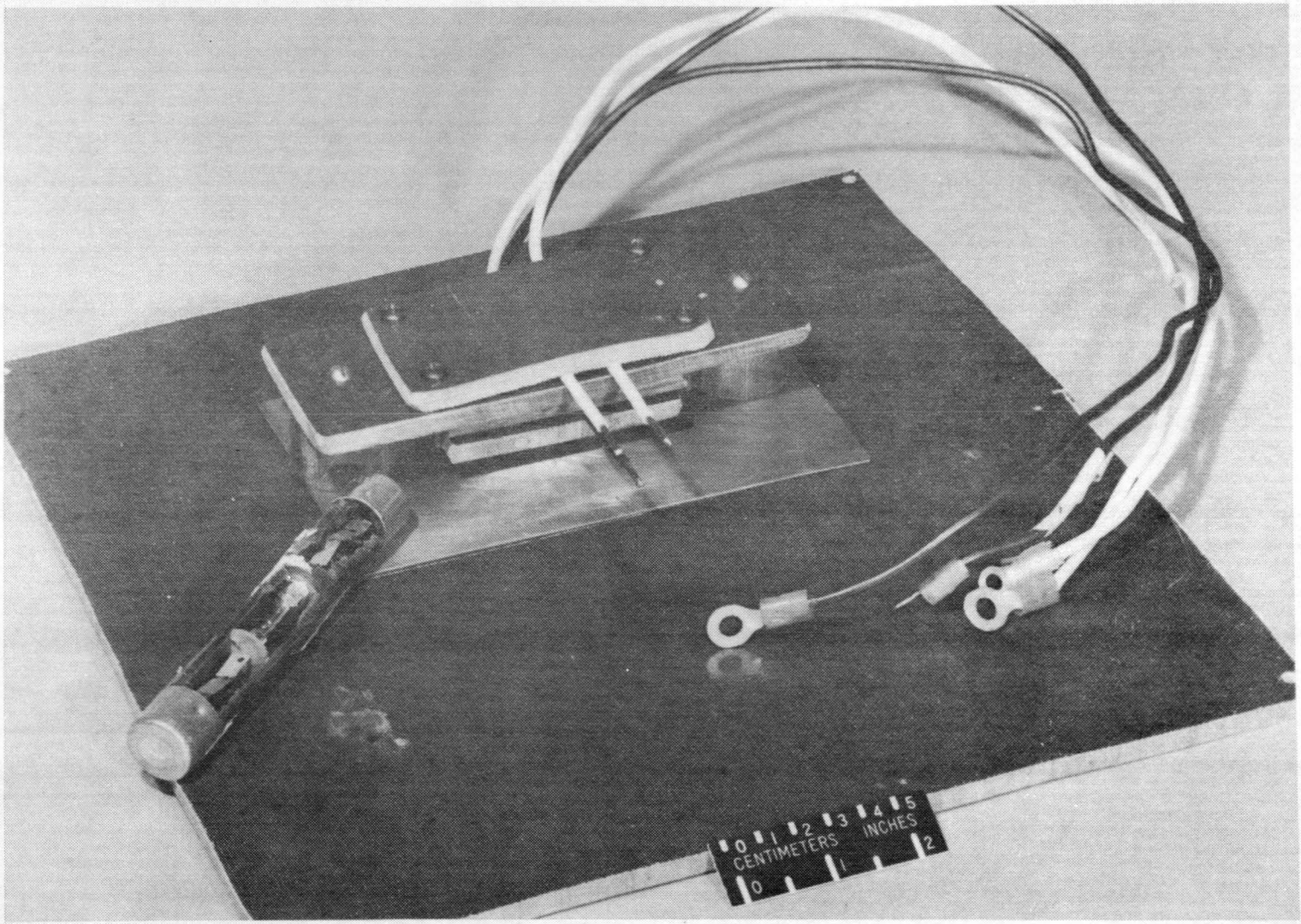

Figure 9-6 Configuration for Three-Phase Tests on Copper Wires.

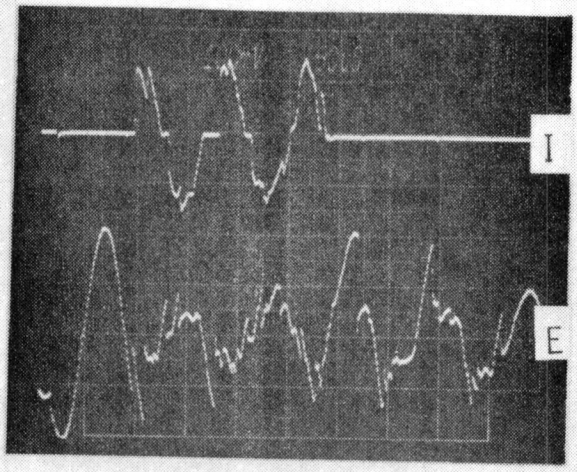

a.
Copper wires spaced 9.5 mm
Peak current 400 A
60-A fuse opened
after 2.5 cycles

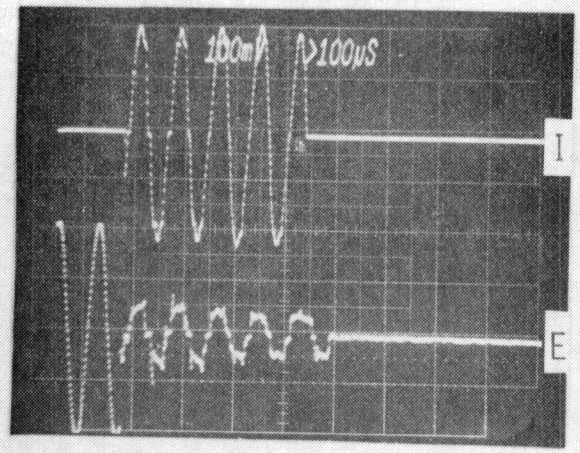

b.
Terminal board TB 38
Peak current 1400 A
75-A fuse opened
after 4.5 cycles

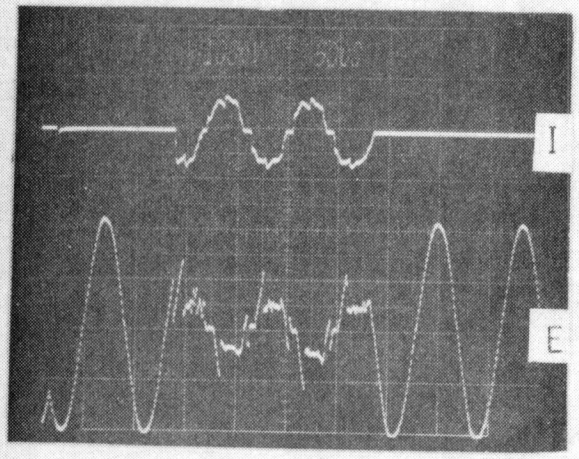

c.
Terminal board TB 38
Peak current - 400 A
60-A fuse did not open.
Arc was sustained
2.5 cycles

Figure 9-7. Current and Voltage Traces, 3-Phase Tests

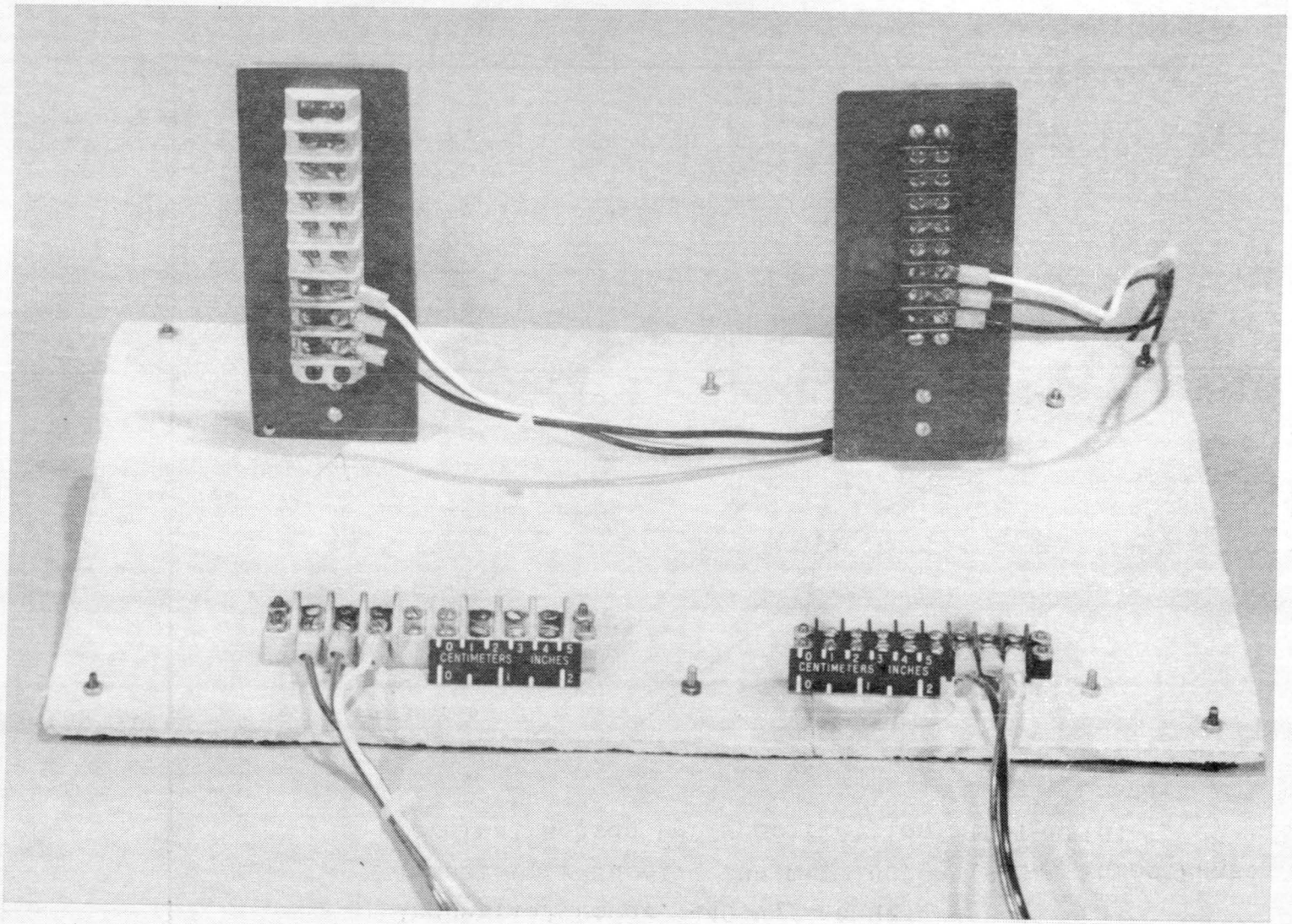

Figure 9-8 Arrangement of Terminal Boards in Tests to Establish Mean Exposure for Sustaining Arcs.

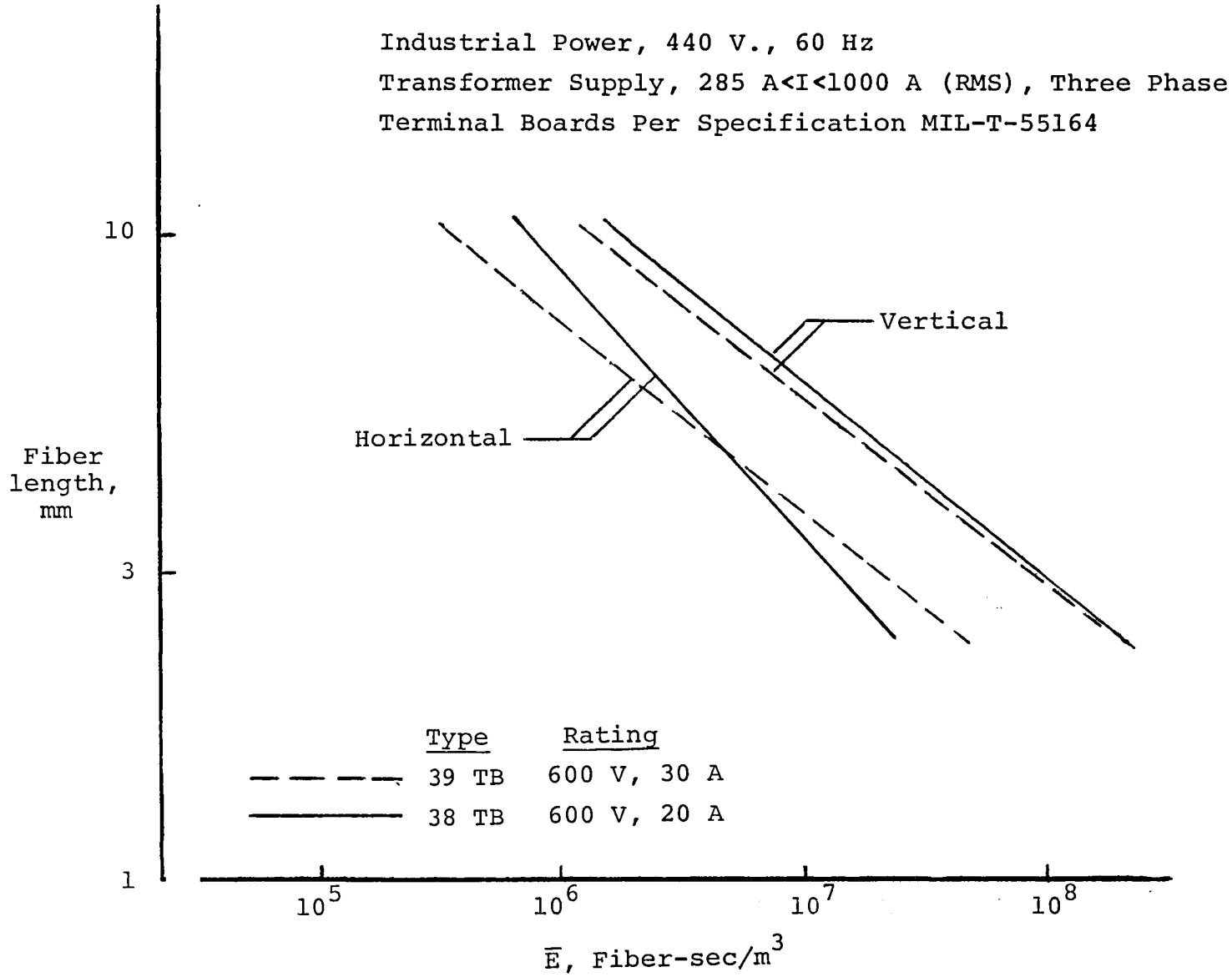

Figure 9-9 - Average exposures to sustain arcs on terminal boards

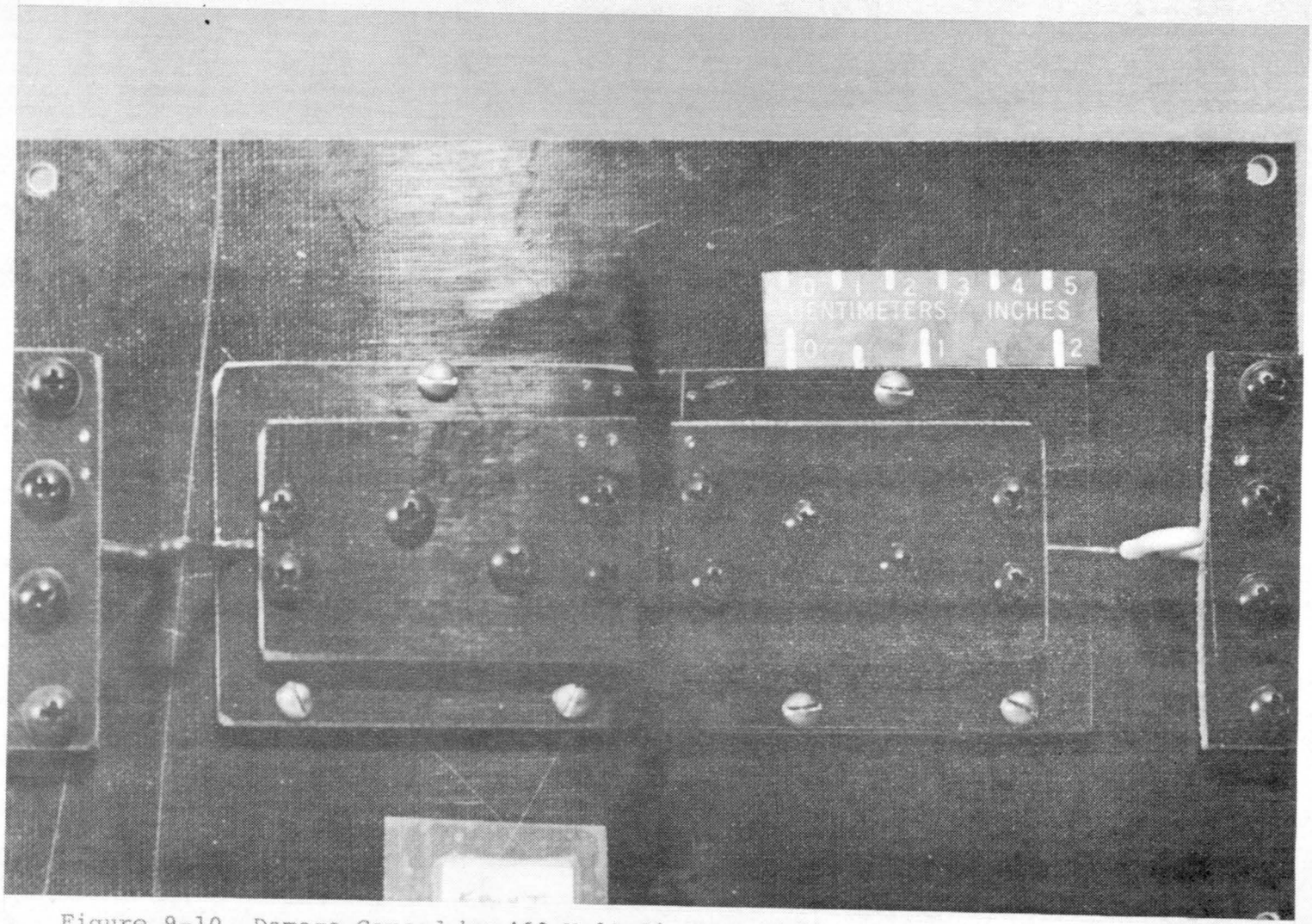

Figure 9-10 Damage Caused by 460-Volt Single-Phase Arcs in Tests of Copper Wires Mounted 1.5 mm Apart.

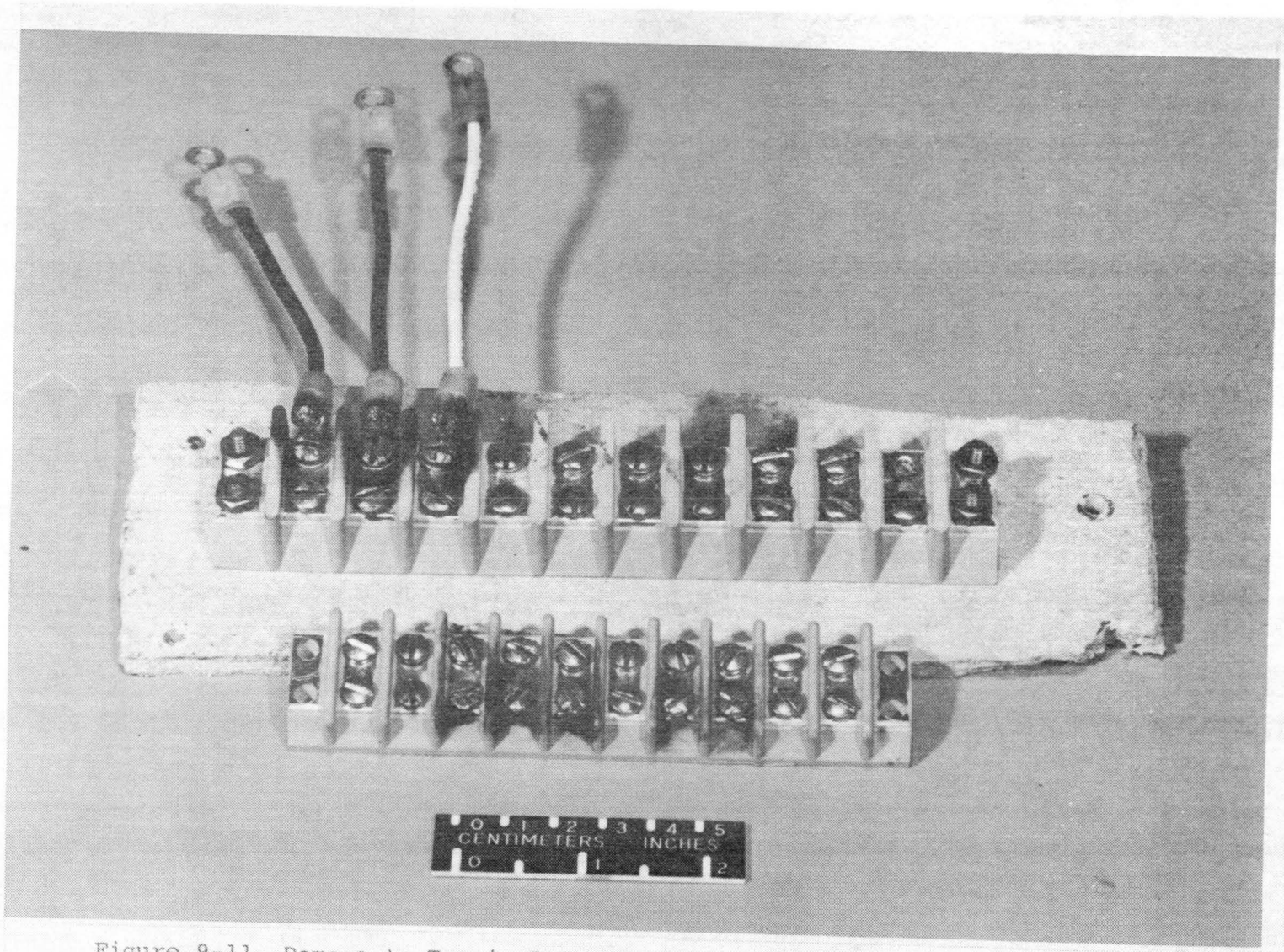

Figure 9-11 Damage to Terminal Boards, Caused by 460-Volt 3-Phase Arcs.

Section 10

INVESTIGATIONS OF ARCING INCIDENTS

Two cases of anomalous electrical behavior occurred at NASA, Langley Research Center during this investigation. One was in a power distribution panel in a manufacturing area for carbon-fiber composites, and the other in wall receptacles in the carbon fiber exposure test chamber. The investigations of these occurrences are reported herein.

10.1 DISTRIBUTION PANEL

An electrical fault occurred in a 3-phase 480-volt ac power panel located in a carbon-fiber composite fabrication shop at NASA Langley Research Center. Witnesses stated that a loud sharp noise was heard and the panel door was blown open at the time of the fault. The 400-ampere main breaker within the panel and the substation breaker located outside the building were tripped. The substation breaker had a 600-ampere frame and the over-current relay was set at 325 amperes. The bus bars or their connectors to the load breakers were burned. This indicated a phase-to-phase fault on all 3 phases, but no visible evidence of a fault to ground.

The damage done inside the panel enclosure was small. It consisted only of copper spattering on the parts involved in the fault. The protective circuit breakers operated quickly enough to prevent further damage.

After the fault, the panel enclosure cover was removed and all of the load circuit breakers were removed in an effort to find a foreign object (such as a bolt or wire) which could have initiated the arcing. No such object was found. After smoothing the affected parts of the bus with a file, the panel was checked electrically at 500 volts dc and was found to have open circuits from phase to phase and from phase to ground. The load breakers were reinstalled and the panel was again energized. Everything appeared normal.

This incident occurred in a room where carbon fibers are "prepregged." Bare carbon fibers are taken directly from a spool, are passed through a bath that wets the fibers with matrix resin and are wound on a drum where the composite is partially cured. A hood collects fumes from the binder and loose fibers emitted from the operation. The hood exhausts to the roof of the building. Several fibers, approximately 10 to 30 mm long, were found inside the electrical panel, which was within 2 meters of the prepreg machine. The inside of the hood over the fabricating machine had many (thousands) of carbon fibers adhering to the metal. A filter

in the exhaust pipe to the roof was heavily coated with fibers and fibers were found on the louvres at the exhaust vent on the roof.

The cost impact of this incident was minimal as the machine was not in use at the time. Less than 25 manhours were spent to inspect the electrical panel after the incident, to dress the damage, and to reenergize the panel.

The carbon-fiber environment in the room was monitored by sticky cylinders such as those described in Section 2.3 of this report. Eleven cylinders were exposed at various points in the room for one week at a time during five successive weeks. None of the samplers were installed inside the electrical panel. No important differences were noted among the eleven samples taken in a given week, the data were averaged for each week and are displayed in Figure 10-1. By far, most of the fibers captured were less than 1 mm long. These short fibers were not expected to constitute a threat to the electrical panel that failed. Conceivably, the total accumulation of longer fibers inside the panel during the four years the prepregging facility was in operation could have been sufficient to cause a flashover (Section 9 of this report). However, the cause of this fault was not positively identified.

10.2 WALL RECEPTACLES

While electrical equipment was being tested in the NASA Langley Research Center exposure chamber (ref. 10-1), arcing was observed at a 4-socket, 3-wire, 110-volt receptacle mounted on a wall in the chamber. Sparks were apparently caused by carbon fibers that bridged the conductors in the receptacle. Fibers had to penetrate about 6 mm into the socket holes to reach conductors and then join with other fibers on the receptacle surface to establish a connection. The arcing occurred frequently during chamber testing with fiber lengths from 3 to 16 mm and at moderate exposures of 10^4 fiber-seconds per meter^3. The chamber was normally vacuum cleaned between tests; however, some fibers probably accumulated in the receptacles as evidenced by the following.

On one occasion, a piece of insulating tape was placed over the receptacles in the chamber prior to a test to prevent arcing during the test. However, the tape began to smolder when it was pressed to the surface. Apparently, fibers were lodged in the holes during earlier tests and were disturbed by the application of the tape making contact across the conductors. On another occasion, after an exposure of 3×10^7 fiber seconds per meter^3, a quasi-sustained arcing was observed. The reaction lasted about 15 seconds, was about 1/4 inch in diameter and resulted in slight charring of the socket.

Tests were conducted to determine whether the electrical potential at the wall receptacle was effective in attracting or repelling fibers. A test jig was made consisting of two receptacle pairs (four sockets). Only one pair of receptacles was powered. The receptacles were exposed to 3-, 7- and 16-mm-long fibers at exposures of approximately 10^8 fiber-seconds/meter^3. Fiber burnouts were seen at the connected receptacles at intervals during the tests. After each run, the receptacles were inspected and the fibers in the holes counted under a microscope. Results are shown in Table 10-1.

The test data do not indicate any significant attraction of fibers by the electrical field of the 110-volt receptacle; however, burnout of fibers on the energized receptacle may have biased the test results. Except during the operational cases cited previously, no presistent arcs were observed. The arcing was self-limiting when the fibers burned, even at the very high exposures deliberately used during the receptacle tests. The flashover arcing observed would be of no importance to most adjacent electrical equipment; however, a small amount of radiated electrical noise could affect neighboring sensitive apparatus.

Reference

10-1 Newcomb, A. L.: Carbon Fiber Exposure Test Facility and Instrumentation. NASA TM-80220, 1980.

TABLE 10-1 NUMBER OF FIBERS COLLECTED IN A 4-SOCKET 110-VOLT WALL RECEPTACLE

Socket	Energized	Exposure f·s/m^3	Fiber length, mm	Pin A (a)	Pin B (a)	Pin C (a)
1	Yes	3×10^8	3	50	20	10
2	Yes			60	70	10
3	No			100	80	10
4	No			400	--	10
1	Yes	8×10^7	7	7	4	4
2	Yes			15	25	4
3	No			3	20	0
4	No			5	4	0
1	Yes	4×10^8	16	100	30	18
2	Yes			20	16	1
3	No			15	26	3
4	No			10	16	15(b)

a) Pin A at 110 volts, Pin B ground return, Pin C ground.

b) One clump of 15 fibers

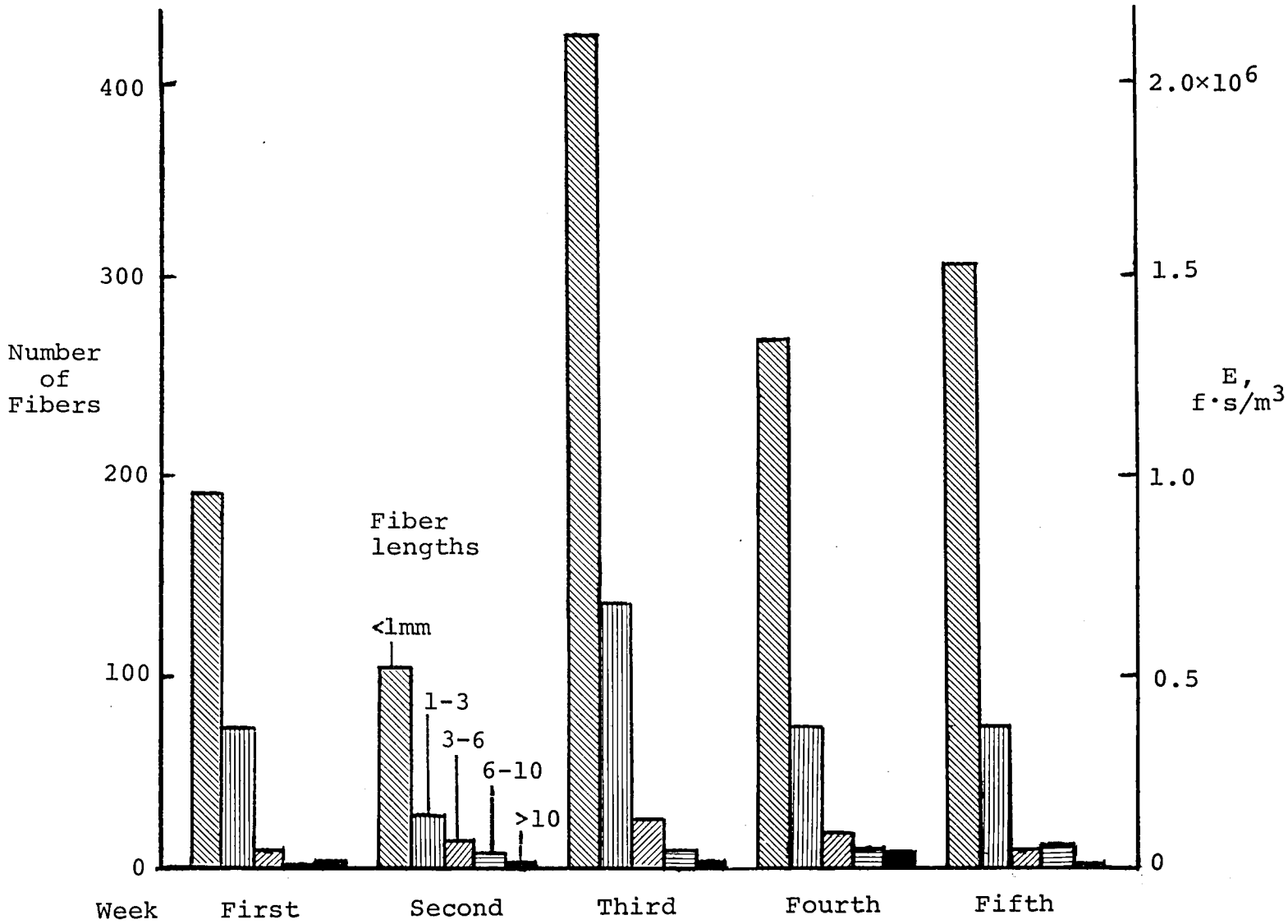

Figure 10.1. Fibers Captured by Sticky Cylinders in Carbon-Fiber Composite Fabrication Shop in Five Successive Weeks.

Section 11

ESTIMATING DAMAGE FROM AIRBORNE CARBON FIBERS

A detailed cost analysis of electrical failures caused by a carbon-fiber incident is a tedious process involving many steps (ref. 11-1), and extensive catalogs of data on specific aspects of the problem. An approximate method suitable for making estimates "on the back of an envelope" was considered desirable and was developed. Necessarily, approximations have been made in the interest of simplicity, but results have been in excellent agreement with many of those derived by more deliberate methods. The method is described herein.

The following assumptions were made:

- The total number, N, of fibers released is known. This number is readily calculated from the mass of fiber involved in a fire, from knowledge that only one percent of the available fiber is released in lengths of interest, and from the fact that 1 kg of fiber is equivalent to 5×10^9 fibers with an average length of 3 mm.

- These fibers are distributed uniformly in a static cloud whose height is h (in m) and whose area is A (in m^2).

- The fall velocity, u (in m/s), is known and atmospheric turbulence is such that the fiber-fall velocity is uniform and equal to the free-fall velocity at ground level. Free-fall velocity for single fibers 7 μm in diameter is 0.02 m/s.

- Objects on the ground are exposed to a uniform concentration, C, of fibers per unit volume in the cloud, or $\frac{N}{hA}$.

- The exposure time, t, is equal to the height, h, of the cloud divided by the fall velocity, u.

- Therefore, the exposure E (in fiber seconds/$meter^3$) is $\frac{N}{hA} \times \frac{h}{u}$ or $\frac{N}{Au}$.

- The effect of wind speed is to increase the affected area, A, and to reduce the corresponding exposure level, E, at the same linear rate.

- The distribution of potentially vulnerable electrical equipment is uniform over the area, A, with a density D (per m^2) estimated for the locality.

- The mean exposure, $\bar{E}$, required to fail typical electronic

devices is known.

• The cost, R, per electrical failure is known. For example, household equipment is generally not vulnerable except for television receivers and similar electronic instruments, whose repair may cost $100 per failure.

Given the foregoing assumptions and estimates of the parameters in the problem, the probable cost of an incident may be estimated as follows.

If E is less than 0.1 $\bar{E}$ the probability P_f of having an electrical failure is

$$P_f = \frac{E}{\bar{E}} = \frac{N}{A\ u\ \bar{E}}$$

and the probable total cost of an incident is

$$\text{Total cost} = P_f\ D\ A\ R = \frac{N\ D\ R}{u\ \bar{E}}$$

As a numerical example, let

$\bar{E} = 10^6$ fiber-seconds/meter^3

D = 4000 devices per km^2 (4×10^{-3}/m^2)

$N = 10^9$ fibers released

u = 0.02 m/s

R = $100 per failure

The total cost of this accident is $20,000. However, this cost is for devices exposed out-of-doors. Most devices are housed in buildings having transfer functions of one percent or less. Therefore, the corresponding total cost is more likely to be $200.

Substitution of values in this simple linear relation serve to demonstrate the effects of the various parameters in this complex problem. Further, because the calculation starts with an estimate of the total number of fibers released in an incident, the total consequence is estimated in each application. Estimates made by this simple relation usually have agreed within a factor of two with those made by more elaborate schemes.

References

11-1 Kalelkar, Ashok S.; Fiksel, Joseph; Rosenfield, Donald; Richardson, David L.; and Hagopian, John: An Assessment of the Risk Arising From Electrical Effects Associated with Carbon Fibers Released From Commercial Aircraft Fires. Arthur D. Little, Inc., Cambridge, MA, NASA CR 159205, 1980.

1. Report No.	2. Government Accession No.	3. Recipient's Catalog No.
NASA CR-159214		

4. Title and Subtitle	5. Report Date
Experimental and Analytical Studies for the NASA Carbon Fiber Risk Assessment	August 1980
	6. Performing Organization Code

7. Author(s)	8. Performing Organization Report No.
Anon	
	10. Work Unit No. 534-03-23

9. Performing Organization Name and Address	11. Contract or Grant No.
Bionetics Corporation 18 Research Drive Hampton, VA 23666	NAS1-15238
	13. Type of Report and Period Covered
12. Sponsoring Agency Name and Address	Contractor Report
National Aeronautics and Space Administration Washington, DC 20546	14. Sponsoring Agency Code

15. Supplementary Notes

Program Manager, Robert J. Huston; contract managers, Vernon L. Bell, and Arthur L. Newcomb, Jr., NASA/Langley Research Center, Hampton, Virginia

16. Abstract

This report describes various experimental and analytical studies performed for the NASA carbon fiber risk assessment program. Contained in this report are data and analysis on carbon fiber characteristics, sensitivity of electrical equipment and components to shorting or arcing by carbon fibers, attenuation effect of carbon fibers on aircraft landing aids, impact of carbon fibers on industrial facilities, and a simple method of estimating damage from airborne carbon fibers.

17. Key Words (Suggested by Author(s))		18. Distribution Statement
Carbon fibers	Instrumentation	Unclassified - Unlimited
Electrical hazards	Risk assessment	
Household equipment		Subject category 24
Avionics	Composites	
Landing aids		

19. Security Classif. (of this report)	20. Security Classif. (of this page)	21. No. of Pages	22. Price*
Unclassified	Unclassified	136	A07

For sale by the National Technical Information Service, Springfield, Virginia 22161